THE ROLE OF MIR-590-3P IN REGULATING HUMAN EPITHELIAL OVARIAN CANCER DEVELOPMENT

MOHAMED SALEM

A DISSERTATION SUBMITTED TO
THE FACULTY OF GRADUATE STUDIES
IN PARTIAL FULFILLMENT OF THE REQUIREMENTS
FOR THE DEGREE OF

DOCTOR OF PHILOSOPHY

GRADUATE PROGRAM IN BIOLOGY
YORK UNIVERSITY
TORONTO, ONTARIO

December 2018

ABSTRACT

Epithelial ovarian cancer (EOC) has the highest mortality rate among all gynecological malignancies. Early detection and intervention remain key to patient prognosis fueling the search for reliable biomarkers. MicroRNAs (miRNAs) are small non-coding RNAs that play a crucial regulatory role within the cell and their dysregulation is associated with many diseases including cancer. In this study, using several well-characterized human EOC cells lines, EOC patient tissue and serum samples, and an *in vivo* mouse model we investigated the role and mechanism of miR-590-3p in promoting ovarian cancer. Our findings indicate that miR-590-3p levels were elevated in both clinical ovarian tumor samples, as well as in the blood serum of the same patients than in subjects with benign gynecological disorders. Overexpression of miR-590-3p in multiple EOC cells led to an increase in cell proliferation, migration, invasion, colony formation, and spheroid formation. In addition, injection of cells overexpressing mir-590 precursor into nude mice increased the dissemination of the tumor nodules, and formed larger tumors compared to control groups. cDNA microarray for cells overexpressing mir-590 revealed Forkhead box A2 (FOXA2) and Versican (VCAN) as one of the top downregulated and upregulated genes, respectively. Interestingly, ChIP-qPCR revealed that FOXA2 binds to *VCAN* promoter, and overexpression of *FOXA2* reduced, while knockout of *FOXA2* increased, VCAN mRNA and protein levels. Moreover, luciferase assay confirmed that miR-590-3p is directly targeting the 3'UTR of FOXA2 and cyclin G2 (CCNG2) to suppress their expressions. In addition, silencing of *CCNG2* mimicked the effect of miR-590-3p and induced cell proliferation, migration and invasion, while CCNG2 overexpression reversed this phenotype. In addition, mir-590 precursor increased the β-catenin activity in TOPflash assays, whereas, knockdown of β-catenin blocks the effect of mir-590 on spheroid formation. Altogether, our results demonstrate that miR-590-3p has tumor-promoting effects in EOCs via targeting FOXA2 and CCNG2 which leads to induction of VCAN and β-catenin signaling.

ACKNOWLEDGEMENTS

First and foremost I would like to thank my mother, **Honey Gawdat**. Mom, you have always been there for me. Thank you for your unconditional love, your kindness and above all, for being my best friend. Without your constant support and prayers, this would not have been possible.

I would like to thank all my family members, my father (**Youssry Salem**), my sister (**Lamis**) and my two brothers (**Haytham** and **Loay**), thank you for your love and support throughout my life. You are the best family anyone can ever have.

I would like to express my warm and sincere gratitude to my supervisor **Dr. Chun Peng** for giving me the opportunity to work in her lab. Thank you for your continued guidance, advice and support. In your lab, I learned countless skills, training and priceless knowledge.

I would like to thank my advisory committee **Dr. Terrance Kubiseski** and **Dr. Michael Scheid.** Your constructive advice, discussions, suggestions and critique were always a great help to improve and develop the project. Thank you for your support.

To all my friends that I had (and will continue to have) countless memories throughout my academic years (Ah, they were sooo long!), I thank you for all the joyful times we've had together.

Jelena Brkic, thank you for your endless support and for being one of my greatest friends. You are very special (in a good way), a problem solver, a fantastic listener and an amazing role model.

Stefanie Bernaudo, you were my mentor and my mini PI throughout this journey. Thank you for all of your guidance. Your dedication to science, your organized and clear mind showed me how a real researcher should be like.

Yara Zayed, I can't describe how thankful I am to have you as a friend. You were always there to help me. Thank you for being my best friend, and for the countless laughs we shared through the years.

Heyam Hayder, the lab angel. Your extraordinary kindness and pure sole are defiantly out of this world. You are always there to listen and offer help, even before anyone asks for it. Thank you truly.

Uzma Nadeem, you have been an amazing friend. Thank you for your encouragement and for being an awesome desk neighbour.

Jake O'Brien, Thank you for your friendship, support, bright ideas and for all those philosophical conversations that neither you nor I have any idea what they mean.

Gang Ye, I can't even count how many things I learned from you. From day 1 you trained me and were my source of knowledge. Gang, I highly value you as my friend and my constant human calculator.

Loan Nguyen, (Vu Hong sometimes) your constant smile, kind heart and cheerful attitude was definably an additive to our lab. Thank you for your friendship and for keeping smiling.

Saviz Ehyai, My best friend and gym buddy. Thank you for your companionship throughout this journey and I am grateful for all your advice and support.

Marlee Ng, the other night raider. Thank you for your company on those long nights we had to stay late in the lab. Too many joyful times and laughs to list. Thank you for the amazing memories and for your friendship.

Dayana D'amoura, We started this degree together, and right from the beginning, we became close friends. Thank you for being a dear friend to me and for all the fun time we spent in the lab.

Hossein Davari Nejad, Thank you for always lending a hand and for your superior electronic skills and for sure, your friendship.

Jyotsna Vinayak, one of the few wise friends that I have. Thanks for all your help and for your friendship.

In alphabetical order, I would also like to thank my wonderful friends: **Anna**, **Gaby**, **Helen,** **Joon**, Marjan and **Vikie**. Thank you, for all the fun time, laughs and memories.

TABLE OF CONTENTS

LIST OF TABLES

Chapter 1

Chapter 2

LIST OF FIGURES

Chapter 1

Chapter 2

Chapter 3

Chapter 4

LIST OF ABBREVIATIONS

Abbreviation	Full name
3'UTR	3′ Untranslated Region
Ago	Argonaute protein
APC	Adenomatous polyposis coli
BCDIN3D	RNA methyltransferase
BCL2	B cell lymphoma 2
CCC	Clear Cell Carcinoma
CCNG2/CG2	Cyclin G2
CDK	Cyclin dependent kinase
ChIP	Chromatin immunoprecipitation
CdkI	Cyclin-dependent kinase inhibitor
CKI	Casein kinase I
CS	Chondroitin sulfate
CTD	Carboxyl-Terminal Domain
DAPI	4',6-Diamidino-2-Phenylindole, Dilactate
Dcr	Dicer
DGCR8	DiGeorge syndrome Critical Region 8
DKK-1	Dickkopf-1
DTT	Dithiothreitol
Dvl	Disheveled
EC	Endometrioid Carcinoma
ECM	Extracellular Matrix
EGF	Epidermal growth factor
eIF4H	Eukaryotic Translation Initiation Factor 4H
EMT	Epithelial–Mesenchymal transition
EOC	Epithelial Ovarian Cancer
ERα	Estrogen receptor α
FAP	Familiar Adenomatous Polyposis
FBS	Fetal Bovine Serum
FHD	Forkhead domain
FIGO	Fédération Internationale de Gynécologie et d'Obstétrique
fkh	Forkhead gene
FOX	The Forkhead Box
FOXA2	Forkhead box A2
FTE	Fallopian Tube Epithelium
Fz	Frizzled
G1	Globular domain
GAG domain	Glycosaminoglycan-domain
GAPDH	Glyceraldehyde 3-phosphate dehydrogenase
GSK	Glycogen synthase kinase 3
HA	Hyaluronan

HGSC	High-Grade Serous Carcinoma
HNF3β	Hepatocyte Nuclear Factor 3β
HRT	Hormone replacement therapy
IF	Immunofluorescence
IPEX	Immune Dysregulation/Polyendocrinopathy/Enteropathy/X-linked syndrome
LEF	lymphoid enhancer-binding factor
Lef-1	Lymphoid enhancer-binding factor 1
LGSC	Low-Grade Serous Carcinoma
LH	Luteinizing hormone
LMP	Low malignancy potential
LRP5/6	Lipoprotein receptor-related protein-5/6
MC	Mucinous carcinoma
miR-590-3p	MicroRNA-590-3p
miRISC	microRNA RISC
miRNAs or miRs	microRNAs
MRE	miRNA response element
mRNAs	Messenger Ribonucleic Acid
NLS	Nuclear localization sequences
NTD	Amino-Terminal Domain
OMIM	Online Mendelian Inheritance in Man
OSE	Ovarian Surface Epithelium
PAPL	Poxvirus-encoded VP55
PDGF	Platelet-derived growth factor
PI3K	Phosphoinositide 3-kinase
pre-miRNAs	Precursors miRNA
pri-miRNA	Primary miRNA
qRT-PCR	Quantitative Real-Time PCR
RISC	RNA-induced silencing complex
SBTs	Serous Borderline Tumors
Ser	Serine
SNPs	Single Nucleotide Polymorphisms
STICs	Serous Tubal Intraepithelial Carcinomas
TAD	Transcription Activation Domain
TCF	T-cell specific factor
TCGA	The Cancer Genome Atlas
TF	Transcription factor
TGFβ	Transforming growth factor-β
Thr	Threonine
TME	The extremely heterogeneous tumor microenvironment
VCAN	Versican
Wnt	Wingless/integrated
Xpo5	Exportin 5 enzyme
β-TrCP	β-transduction repeat-containing protein

CHAPTER 1

LITERATURE REVIEW

I. OVARIAN CANCER

Ovarian cancer comprises three major categories namely: epithelial, germ cell and stromal cancers. Epithelial ovarian cancer (EOC) is the deadliest and the most common ovarian type which accounts for almost 90% of all reported cases [1]. Therefore, the focus of this study will be on EOC and its subtypes. The low survival rate for women with EOC results from the inability to detect the disease at an early curable stage, the vagueness of accompanying symptoms, the lack of effective treatment for the advanced stages and from our incomplete understanding of the mechanism by which EOC develops. All these factors contribute to make EOC the most lethal cancer among all gynaecological malignancies, and the 5th leading cause of cancer death in women [2].

I. 1. Etiology and Epidemiology

In 2018, an estimated 22,240 new ovarian cancer cases and 14,070 deaths were reported in the United States [3]. In Canada, each year, 2800 Canadian women will develop EOC, of which 1800 will die as a direct consequence of disease [4]. This rate ranks ovarian cancer as the fifth leading cause of cancer-related death among women [5]. Despite the ongoing efforts to develop treatment regimens and effective surgery, the overall rate of survival for ovarian cancer is still relatively low, mainly due to late stage diagnosis [6, 7]. The success rate of conventional ovarian cancer therapies, such as chemotherapy and cytoreductive surgery, can be as high as 90% if the disease is diagnosed at an early stage. The late-stage diagnosis of ovarian cancer is often due to minimal symptoms of the disease that are often confused with gastrointestinal problems [7, 8]. As ovarian cancer affects a large number of women worldwide, it is highly important to understand the molecular mechanism by which ovarian cancer develops and progresses in order to improve therapeutic efficacy and patient outcomes.

I. 2. Stages and Grades of Epithelial Ovarian Cancer

EOC stage is determined by the level of cancer dissemination within the patient's body. Identifying the correct cancer stage is vital for choosing proper treatment methods and prognosis [9]. Generally, four different stages of ovarian cancer are described. In stage I, the tumor is confined to the ovaries and is characterized by the lack of ascites formation, which is the accumulation of fluid in the abdominal cavity as a secondary result of cancer progression. During stage II, malignant cells from the primary tumor begin to metastasize to other pelvic tissues, like the uterus and fallopian tubes, via the ascites fluid, which also contains cytokines and growth factors that sustain tumor progression [10-12]. Stage III is marked by the extension of the tumor to the omentum or the visceral peritoneum, yet they are still limited to the true pelvis. Stage IV begins when tumors progress further, infiltrate one or both ovaries, and metastasize into distant organs [13]. Cancer stage is a key factor in prognosis and is directly correlated with survival rate as it declines rapidly from 93% with Stage I, to as low as 19% with Stage IV [14].

EOC is classified into grades according to the degree of cell differentiation of malignant cells [13]. Grade I tumor cells are well differentiated, grade II tumors are little differentiated, while grade III and IV tumors are poorly differentiated [13]. In general, tumors showing a high degree of cell differentiation resemble and behave similarly to the surrounding healthy tissues [13].

I. 3. Histopathological Subtypes of EOC

In the past, the majority of research identified EOC as one disease. However, it is well established now that ovarian cancer is a heterogeneous disease. Recent studies classify ovarian cancer as several distinct diseases rather than one disease with different subtypes [15]. The focus of this review will be on EOC and its different subtypes which include: serous,

endometrioid, clear cell and mucinous. Each subtype has a distinct molecular profile, prognosis and progression models.

I. 3.1 Serous Carcinoma

I. 3.1.a. High-Grade Serous Carcinoma

High-grade serous carcinoma (HGSC) is the most common subtype, accounting for about 75% of EOCs. A pathologic examination of HGSC reveals solid or papillary growth with grooves and tumor cells that are characterized by rapid cell proliferation, abnormal cell nuclei with variability in size and shape. Generally, HGSCs is accompanied with disseminated tumor masses in the omentum, ovaries, and other intra-abdominal locations with or without ascites. Only less than 5% of patient cases can be diagnosed in the first stage while the cancer is still contained within the ovaries [16, 17]. Due to the late detection of HGSC, it is challenging to study any earlier events of this subtype. However, recent studies suggested that HGSC originates from the fallopian tube epithelium rather than from the ovary [16, 17]. Also, the genetic instability of HGSC could be due to frequent mutations in *BRCA2*, *BRCA1*, and *TP53* tumor suppressor genes.

I. 3.1.b. Low-Grade Serous Carcinoma

Low-Grade serous carcinoma (LGSC) is characterized by the appearance of papillary structures, uniform small nuclei, and low mitotic activity. LGSCs are less common than HGSC [17]. Patients with LGSC are often diagnosed at an early stage (usually stage I), and tend to have a higher survival rate. However, patients with advanced stage LGSC have a lower survival rate [18-20], likely due to the relatively high chemoresistance of the recurrent LGSC compared to HGSC [21]. Molecularly, LGSC is often marked with distinct mutations in *KRAS*, *BRAF* and/or *ERBB2* [22, 23].

Despite the similar naming, LGSC rarely develops into HGSC, and the two serous carcinomas mostly do not have any overlap in mutational patterns [23]. Furthermore, LGSC is

likely to be present in premenopausal women around the age of 45-50, compared to HGSC, which usually affects women around the age of 60 and older [4].

I. 3.2. Endometrioid Carcinoma

Endometrioid Carcinoma (EC) is one of the two major subtypes of ovarian carcinoma that has a well-defined endometriosis (ectopic endometrial tissue) association [24-26]. 50% of patients with EC are diagnosed in stage I of which, 15% percent of the cases affect both ovaries [27]. The early intervention of EC is usually effective as patients diagnosed with stage I cancer are likely to have promising outcomes [28]. However, when detected at later stages, the overall 5-year survival is poor [28]. There is a number of genes that are typically mutated within the endometrioid carcinomas including: the characteristic mutation in *CTNNB1,* as well as in *KRAS, PPP2R1A, ARID1A, PIK3CA* and *PTEN* [29].

I. 3.3. Clear Cell Carcinoma

Clear cell carcinoma (CCC) was given this name due to the abundance of the clear intracytoplasmic glycogen. Like the endometrioid carcinoma, the majority of CCC is detected in stage I. However, studies showed a fairly unfavourable outcome prediction for women diagnosed with this type of tumor [30-32]. CCC is the second type of ovarian cancer that is related to endometriosis and is often associated with either benign tumors known as clear cell adenofibroma or with cysts. Nevertheless, CCC developing from adenofibroma is less likely correlated with endometriosis compared to the cystic CCC [33]. About 50% of CCC have mutations in *ARID1A* and approximately 36% contain *PIK3CA* mutations [34, 35]. In addition, most CCC cases also have mutations, but at a lower frequency, in *PPP2R1A*, *PTEN*, *KRAS*, and *TP53* [36-38].

I. 3.4. Mucinous Carcinoma

Benign mucinous carcinoma (MC) is the least common type of ovarian carcinomas, and represents approximately 12% of the total ovarian tumors and if diagnosed early, have a high survival rate [39, 40]. Most ovarian MC cases are the result of metastases initiated in distal locations like biliary and gastrointestinal tracts or the pancreas [41-45]. MC is usually glandular in shape and composed of stratified columnar cells that are characterized by having basally located pale-staining mucin, and nuclei at the apical cytoplasm [45, 46]. However, it can sometimes be difficult to differentiate metastatic from primary MCs as many mucinous carcinomas show intestinal-type differentiation evidence [46]. In approximately 50% of invasive MC, both *TP53* and *KRAS* genes are mutated within the same tumors [47]. On the other hand, in 19% of them, *ERBB2* is amplified [48]. Expectedly, *KRAS* mutation and *ERBB2* amplification can be linked to survival rate alteration [48]. The lack of information on other molecular alteration frequency in mucinous carcinomas makes this type of cancer difficult to diagnose.

I. 4. Origin of EOC Subtypes

Although they are all called ovarian cancers, the origin of different EOC subtypes has been debated. For nearly half a century, it was widely believed that EOC develops from the ovarian surface epithelium (OSE), or from the coelomic epithelium, which is a single layer of mesoepithelial cells with multipotent properties that covers the ovarian surface [49]. More recently however, accumulating evidence suggests that not all these subtypes originate from the ovaries, and that they may originate from other tissues such as fallopian tubes or endometrial-type epithelium [49, 50] (Figure 1.1). It has been reported that the most common form of EOC, serous ovarian cancer, originates from the fallopian tube epithelial cells, particularly from the secretory cells at the fimbriated end of the fallopian tube [51]. Moreover,

recent experiments performed on mice, proposed that serous carcinomas may occur in cell populations that have stem-cell-like properties found in areas covered with peritoneal mesothelium, OSE and fallopian tube epithelium [52, 53].

On the other hand, other studies have shown that up to 50% of the EC and CCC cases are associated with endometriosis and that patients with endometrioses are significantly more susceptible to ovarian cancer [54]. The mechanism by which endometriosis develops is still unclear. It was believed that implantation of endometrial tissues may take place outside the endometrium walls through retrograde menstruation [55]. However, it is now believed that endometriosis arises from endometrial stem cells or progenitor cells that differentiate after menarche [56]. In other cases, genetic and morphological studies showed a transition from endometriotic cysts to EC or CCC [33, 57, 58]. The common mutational range of ovarian cancers associated with endometriosis and uterine EC are likely to have a common origin that is attributed to the endometriosis.

There is a lot of uncertainty about the origin of the MC subtype. This is probably because the intestinal cell-like differentiation is not typical of epithelia in the female genital tract and that only a small subset of MC show endocervical differentiation suggesting a Müllerian origin [6]. However, studies carried out recently concluded that MC may be derived from multiple layers of ovarian germ cell tumors, known as teratomas [59, 60]. This least common subtype of EOC may be the only ovarian cancer type that has been proven to be developed from ovarian cells [61].

In summary, only a small portion of ovarian carcinomas has been proven to originate in the ovaries. This paradigm shift has moved the focus from the ovaries as the sole cause of all ovarian carcinomas into also considering other neighbouring organs [62]. In addition, understanding the origin of these EOC subtypes is important to the development of better diagnosis and detection techniques and treatment options to help improve patients' prognosis.

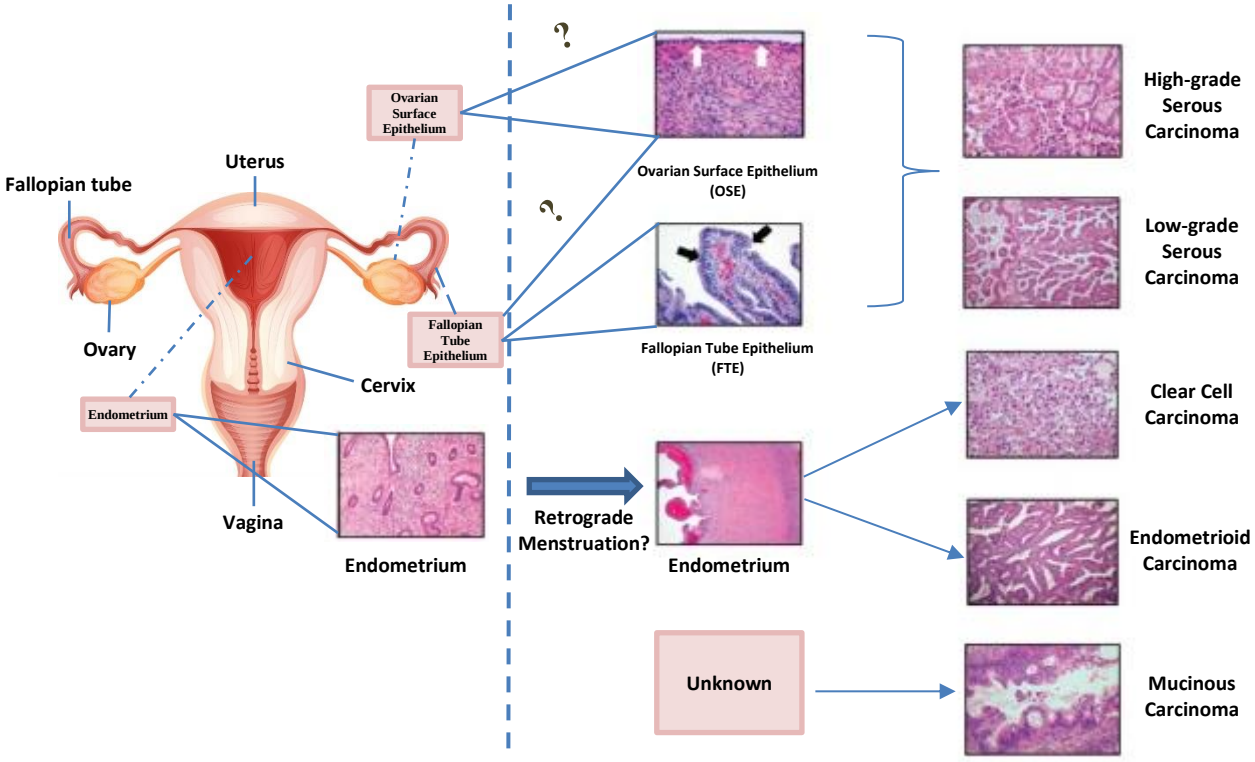

Figure 1.1: Suggested cellular origins of ovarian carcinomas. Studies suggest that several ovarian cancer subtypes have an origin outside the ovaries. The progression and origins of these carcinomas remain to be confirmed. In pictures, white arrows indicate ovarian surface epithelium (OSE), and black arrows indicate fallopian tube epithelium (FTE). Reprinted with modifications from [6] and photographs of pathology slides reprinted from Kathleen Cho (2016) with permission.

I. 5. Molecular and Genetic Abnormalities of EOC Subtypes

Modern analytical procedures have allowed researchers to perform in-depth studies on ovarian cancer using genomic and wide transcriptome screens. In addition, it is now possible to perform metabolic and proteomic screens [63]. The introduction of these new methods allowed better analysis of EOC molecular markers, protein interactions, and metabolism [64].

In general, cancer develops either due to the accumulation of genetic modifications or other molecular defects, but most genetic modifications result in anomalous cellular functions such as immune evasion and uncontrolled cell division [65]. Although some inherited mutations through the germline may lead to cancer development, the disease sequentially develops through an acquired somatic mutation in the site of origin. These mutations in genes encoding proteins that can cause either activation of oncogenes or inactivation of tumor suppressors. (Table 1).

I. 5.1. Inherited Mutations

Patients with a family history of ovarian cancer are more likely to be at higher risk for developing it. Mutations in *BRCA1* and *BRCA2* genes are typical ovarian cancer indicators, and they account for almost 15% of all cases of ovarian carcinomas [66]. In a study on Jewish Ashkenazi women, *BRCA1* and *BRCA2* were responsible for 40-50% and 20-30%, respectively, of ovarian cancer total lifetime risk [67]. These mutations also contribute to about 5-10% of acquired breast cancers and 20-25% of the inherited ones [68, 69]. However, *BRCA1* and *BRCA2* are not the only genes associated with ovarian cancer, and others include: *MLH1*, *EPCAM*, *PMS2*, *MSH1*, *MSH6* and *TP53* [70]. Most of these vital genes are involved in the DNA repair process. Therefore, women with a mutation in one or more of these genes are at a higher risk of developing ovarian carcinomas [71].

I. 5.2. Acquired Mutations

More than 95% of HGSC patients are diagnosed with a mutation in *TP53* [72-74]. Despite the fact that most ovarian serous tumors grow as *de novo* high-grade lesions with *TP53* modification, it is now believed that the tumors may also arise from an already established low-grade tumor. [75]. A control experiment shows that the majority of these cases were not identified as HGSC [76]. In addition, previous genetic studies conducted on serous carcinomas were not accurate. This is due to the inclusion of other subtypes of non-serous ovarian carcinomas.

Almost one-third of the HGSC cases are characterized by having somatic mutations in *BRCA1* and *BRCA2* [77]. A statistical study conducted recently on putative homologous recombination in gene mutation, showed rare somatic disorders in *BRIP1*, *RAD51C* and *CHEK2* in the advanced stages of HGSC [78]. The Cancer Genome Atlas (TCGA), carefully sequenced exomes of more than 300 cases. It was found that almost all these cases have mutations in *BRCA1*, *BRCA2* and *TP53*. In addition, *FAT3* and *NF1* were also identified as rare mutated genes in approximately 3% of the cases studied. Similarly, *PIK3CA*, *MYC*, *CCNE1* and *KRAS* were abundantly expressed suggesting that these particular genes can be used as markers to help in early prognosis [78]. Additionally, deletions in other genes such as *PTEN*, ZBTB7A, *CDKN2A* and *NFI* can also affect diagnosis and treatment results [79].

Table 1: Characteristic mutations in epithelial ovarian carcinoma subtypes.

Carcinoma Subtype	Potential cellular origin	Gene Activation	Gene Inactivation
HGSC	Mostly fallopian tube epithelium. Also ovarian surface epithelium	No frequent mutations	*BRCA1*, *BRCA2*: tumor suppressor genes that help repair DNA damage or destroy cells if DNA cannot be repaired *TP53*: a tumor suppressor commonly mutated in cancers and crucial for genomic stability and DNA repair
LGSC	Serous border line tumors	*BRAF*: an oncogene involved with intracellular signaling involved with directing cell growth *KRAS*: an oncogene that recruits and activates proteins necessary for tumor growth	Unknown
EC	Endometriosis	*KRAS* *CTNNB1*: operates as a signal transducer to regulate gene transcription and cell–cell adhesion *PIK3CA*: promotes cell survival, growth, and migration *PPP2R1A*: regulates signaling pathways that inhibit cell growth and division	*BRCA1*, *BRCA2* *ARID1A*: regulates gene by altering the accessibility of transcription factors to DNA *PTEN*: a tumor suppressor that inhibits cellular growth. This gene is often mutated in cancer
CCC	Endometriosis/ Uncertain	*KRAS* *PIK3CA* *PPP2R1A*	*TP53* *PTEN* *ARID1A*
MC	Unknown	*BRAF, KRAS* *ERBB2*: a receptor tyrosine kinase that can interact with signaling molecules to promote tumor growth and block cell death. It is commonly amplified or overexpressed in cancers	*TP53, CDKN2A*: a tumor suppressor that induces cell cycle arrest *RNF43*: a tumor suppressor that inhibits WNT signaling pathway

Adapted from [6].

II. MICRORNAs

MicroRNAs (miRNAs) are small noncoding RNAs expressed endogenously in eukaryotes and are important elements in post-transcriptional regulation of gene expression [80-83]. In 1993, the first microRNA, *lin-4*, was identified in *C. elegans* in pioneer papers by the Ambros and Ruvkun groups [84, 85]. Despite the importance of *lin-4* for the control of larvae development timing, it did not encode for a protein. However, it suppressed the expression of lin-14 by the interaction between the *lin-4* and the 3'UTR of *lin-14*. It was believed for several years that this RNA-RNA interaction is an exclusive phenomenon to nematodes development and to *lin-4*. In 2000, another newly discovered microRNA, *let-7*, in *C. elegans* was reported to be able to target the 3′UTR of several mRNAs. In addition, the 3′UTR of one mRNA can harbour many target sites for several microRNAs [86]. The presence of miRNA in several cell types among the eukaryotes was then revealed through intense cloning effort. These findings suggest a more spread role of miRNAs in regulating gene expressions than what was thought previously [80]. In March, 2018, the miRNA database (miRBase) has listed ~ 1900 annotated and predicted miRNAs in the human genome. The function of many of these miRNAs is still unknown; however, it is now well accepted that miRNAs are involved in regulating many biological processes, such as cell proliferation, apoptosis, differentiation, and development [87]. In addition, the use of miRNAs as potential diagnostic and therapeutic molecules has been suggested [88, 89].

II. 1. Biogenesis and miRISC Assembly

miRNAs can generally be classified as "intragenic" or "intergenic" depending on their genomic location. Almost half of all annotated miRNAs in humans are located within host genes, mainly within the introns of protein-coding genes or other non-coding RNA genes [90]. The biogenesis process of miRNAs is relatively consistent. Expression of intronic

miRNAs are usually coupled with their host gene, while the transcription of intergenic miRNAs is directed by their own promoters. However, it was shown recently that the expression of some miRNAs are decoupled from their host genes through independent transcription mechanisms and alternative splicing [91].

The 18–22 nucleotide (nt) mature miRNA molecules are initially transcribed by RNA polymerase II into primary miRNA (pri-miRNA) transcript, containing a 5′ m^7G cap and a 3′ poly-A tail [92, 93]. Subsequently, pri-miRNAs go through extensive processing within the nucleus. The primary maturation step changes pri-miRNA into ~70 nt hairpin miRNA precursors (pre-miRNAs). Pri-miRNA cleavage is facilitated by the microprocessor complex, which consists of an RNase III endonuclease, DROSHA, and the double-stranded-RNA-binding protein, DGCR8 (DiGeorge syndrome Critical Region 8) [81, 94-96]. The pre-miRNA is then exported to the cytoplasm via a member of the nuclear transport receptor family Exportin 5 (XPO5) [94, 97, 98].

In the cytoplasm, the pre-miRNAs are further processed into mature miRNAs by a different RNase III endonuclease, Dicer, [81, 94, 99]. Specifically, Dicer slices pre-miRNA near the terminal loop freeing a short, ~ 22 nt, RNA duplex [99-101] (Figure 1.2). Lastly, the fully processed mature miRNA molecules are integrated into the miRNA-induced silencing complex (miRISC) [102, 103].

The core element of miRISC is a member of the Argonaute (AGO) protein family that binds miRNA. AGO family proteins comprise four members in humans (AGO1-4). The miRISC loading complex facilitates miRNA loading into AGO, where the 5′ or 3′ ends of the miRNAs are clamped to different domains of AGO [81, 104]. miRNA loading involves ATP-dependent loading of the miRNA duplex into AGO and its subsequent unwinding [105].

miRNA duplex consists of a “guide strand” and a “passenger strand”. The guide strand will serve in target transcript recognition, while the passenger strand will be ejected

from the AGO protein. However, the criteria of strand selection remain unclear [106]. Some studies, however, suggested that the more thermodynamically stable 5′ end of the miRNA will be ejected through miRISC maturation, while the strand with less stable 5′ end will be anchored to AGO. The AGO is then interacting with the strategically positioned phosphate backbone of the guide strand, while the 5′ and 3′ ends are anchored exposing the "seed-region" (nucleotides 2-8, from the 5′ end) where miRNA-loaded miRISC recognizes the 3′ UTR of target mRNAs [107-110].

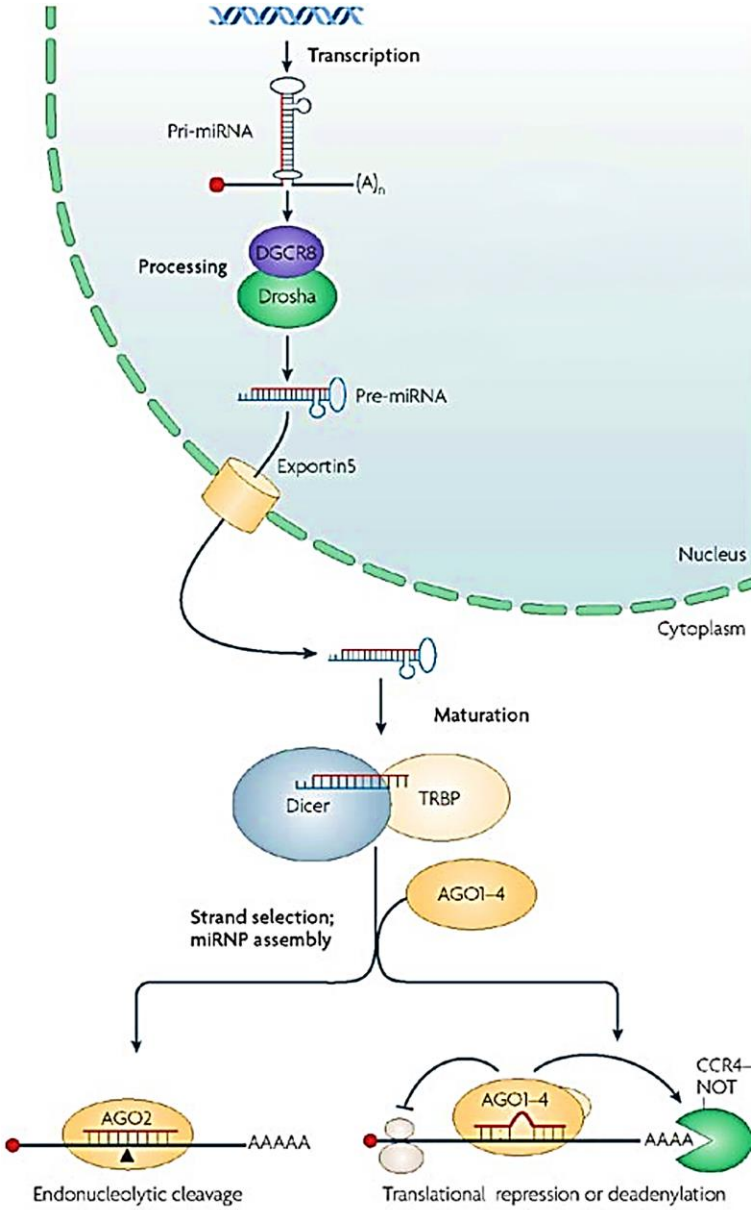
Transcription
Pri-miRNA
(A)n
Processing
DGCR8
Drosha
Pre-miRNA
Exportin5
Nucleus
Cytoplasm
Maturation
Dicer
TRBP
AGO1–4
Strand selection;
miRNP assembly
AGO2
AAAAA
Endonucleolytic cleavage
AGO1–4
CCR4–
NOT
AAAA
Translational repression or deadenylation

Figure 1.2. MicroRNA biogenesis and RNA-induced gene silencing. Transcription of primary micro RNA (Pri-miRNA), that contain a double-stranded stem, a loop, ssRNA tails, a 5′ cap and 3′ poly-A tail, from miRNA genes is followed by cleavage to precursor mRNA (Pre-miRNA) by the Drosha nuclear RNase III and DGCR8. The Pre-miRNA is then exported to the cytoplasm by Exportin 5 via nuclear pores. In the cytoplasm, Pre-miRNA is further processed by RNase activity of Dicer and TRBP to the mature microRNA duplex. The duplex loads onto Argonaut ribonucleases in the miRISC complex and separates. One of the mature miRNA strands (red strand) mediates small interfering RNA silencing by degrading the target mRNA or interfering with translation. The outcome of miRISC formation varies with the degree of complementarity of the seed sequence of miRNA and 3′ untranslated regions (UTR) of the target mRNA. AGO2 loaded miRNA can lead to endonucleolytic cleavage of the recognized target or translational repression and deadenylation. Reprinted with permission from [111].

II. 2. MiRNA Nomenclature

The newest report from miRBase, Release 22: March 2018, shows 38589 identified miRNAs across different species, albeit the function of many of these miRNAs remains to be explored and validated [112-114]. miRNA nomenclature has changed over time as well, as our understanding of miRNA biogenesis and mechanism. The genes discovered in early genetic studies were named following their phenotypes (for instance, *lin-4*, *let-7* and *lsy-6*), whereas the majority of miRNAs discovered from cloning or sequencing were given numerical names (for instance, the lin-4 homologues in other species are known as mir-125). Pre-miRNA hairpins are referred to as "mir", while the mature miRNAs are referred to as "miR". Genes encoding miRNA species are marked with lettered suffixes (for instance, mir-125a and mir-125b). To differentiate mature miRNA species transcribed from different genomic loci with 100% sequence identity, numeric suffixes are inserted after the names of the miRNA (for instance, mir-125b-1 and mir-125b-2). Each miRNA's name begins with a prefix indicating the species of origin.

Initially, one strand of miRNA duplex was believed to be the main strand, while the other one was believed to be non-functional and subject to degradation. The later-degraded strand was denoted with a "*". Further investigation showed that the majority of the "*" strands are fully functional and may have similar rates of maturation to that of the guide strands, as well as exert a unique biological function [115, 116]. While a locus may contain a cluster of multiple miRNAs, every pre-miRNA generates two mature miRNAs: one from the 3′ strand and one from the 5′ strand of the precursor. Currently, the old "*" naming system is seized and replaced with the modern system -3p and -5p, which processed from the 3′ and 5′ arm respectively. For instance, the precursor hairpin of miRNA 590 would be mir-590, and the two arms of the mature miRNA would be miR-590-3p and miR-590-5p [116].

II. 3. Mechanism of miRNA-Mediated Gene Regulation

Despite the lack of a unified model, several mechanisms have been proposed to describe the miRNA action. Generally, the repressive effect of miRNAs is exerted by either mRNA cleavage, mRNA decay, or repressing translation [117] (Figure 1.2). It is widely believed that miRNAs bind to a specific sequence at the 3′ UTR of their selected mRNA, which induces mRNA deadenylation and decapping as well as translational repression [118]. More recently, it has been shown that miRNAs can also have binding sites on other regions of the mRNA including, coding sequence and 5′ UTR, or to DNA promoter regions [119]. Interestingly, it was found that when miRNA interacts with the promoter region, it can induce transcription, while binding to the coding region or the 5′ UTR represses gene expression and exerts silencing effects [120-122].

miRNA guide strand and AGO are the minimally required components to form miRISC [123]. The loaded miRNA gives miRISC its target specificity via complementary miRNA:mRNA interactions. The region of target interaction is termed the miRNA response element (MRE). Depending on the degree of the complementarity between miRISC and MRE, one of two routes can be taken, 1- AGO2-dependent splicing can cleave fully complementary target mRNAs or 2- miRISC-mediated translational initiation inhibition and target mRNA deadenylation and decay [124]. A perfect complementary between miRNA and MRE will induce the endonuclease activity of AGO2 and leads to mRNA cleavage [124]. Nonetheless, this perfect matching disrupts the interaction between AGO and 3′ end of the miRNA promoting its degradation [125]. Although the target mRNA cleavage is the main mechanism found in plant miRNAs and siRNAs, it is infrequently observed in miRNA:mRNA interactions in human [111]. In mammalian cells, the majority of miRNA-MRE interactions possess a central or 3′ mismatch. This imperfect coupling prevents AGO2 endonuclease activity allowing a mediating role for AGO2 in RNA interference [126]. Albeit all four AGO proteins in humans

interact with miRNAs, only AGO2 has endonucleolytic activity [127].

The second gene silencing mechanism mediated by miRNA is via suppression of translation initiation and/or degradation of target mRNA. This process is mediated through the interaction between AGO and GW182, which is an essential member of a protein family regulating the downstream repression stages [107]. In addition to binding to AGO, GW182 can bind to the poly-A binding proteins on the mRNA poly-A tail. Also, it is capable of interacting with cellular deadenylases like the CCR4/NOT complex to promote deadenylation and indirectly mRNA decapping, which results in target mRNA instability and degradation [128]. The last mechanism is through repression of translation. However, it is still unclear how exactly miRNA mediates it. However, some evidence refers to the miRNA's ability to interfere with the translation initiation process [129]. This translation repression was initially observed in the lin-4 mediating lin-14 protein level without affecting the mRNA levels [85].

II. 4. Dysregulation of miRNA Expression in Cancer

Studies have shown that 30-60% of human protein-coding genes are regulated by miRNAs [130]. miRNAs are reported to modulate many biological processes including: differentiation, cell cycle, apoptosis, proliferation, and immune reaction [87]. In cancer, miRNA expression dysregulation was attributed to both genetic and epigenetic factors and mechanisms. Those factors may include one of the following: 1- alteration of miRNA genes by amplification or deletion. 2- histone acetylation and methylation at the miRNA promoter and epigenetic modifications, or 3- abnormalities in miRNA biogenesis and defects in transcriptional control machinery (Figure 1.3).

In chronic lymphocytic leukemia, chromosomal region (13q14) is frequently deleted. This region was shown to encode for miR-15 and miR-16 that target the anti-apoptotic factor B cell lymphoma 2 (BCL2). Both miRNAs showed expression alteration in cancer cases [131].

In addition, another study in ovarian cancer demonstrated the association between mutations at genomic loci containing miRNA genes and cancer. The study showed that many miRNA loci at chromosomal fragile sites, and almost half of these miRNA located in a frequently translocated region in cancer cases [132, 133].

During cancer, gene duplication and/or abnormal methylation of the miRNA promoter can induce transcription of pri-miRNA [134]. DNA hypo- or hyper-methylation and histone hypo- or hyper-acetylation at the promoter of miRNAs was reported to alter miRNA genes [134, 135]. On the other hand, acetylation of histone H3 lysine 9 or 14 (H3K9ac and H3K14ac) and tri-methylation of histone H3 lysine 4 (H3K4me3) are reported to affect miRNA gene promoters [136, 137].

Abnormalities in miRNA biogenesis and defects in transcriptional machinery were also associated with cancer progression [138-140]. In the mouse germ line, deletion of *Dicer1* leads to early embryonic fatality around embryonic day 7.5 [141], and *Dicer1*-knockout in embryonic stem cells significantly affected cell differentiation and proliferation [142, 143], while partial deletion of *Dicer1* or *Drosha* induced tumorigenesis phenotypes [144]. In addition, mutation in Exportin 5 (XPO5) prevented the exportation of miRNA from the nucleus and resulted in carcinoma progression [145].

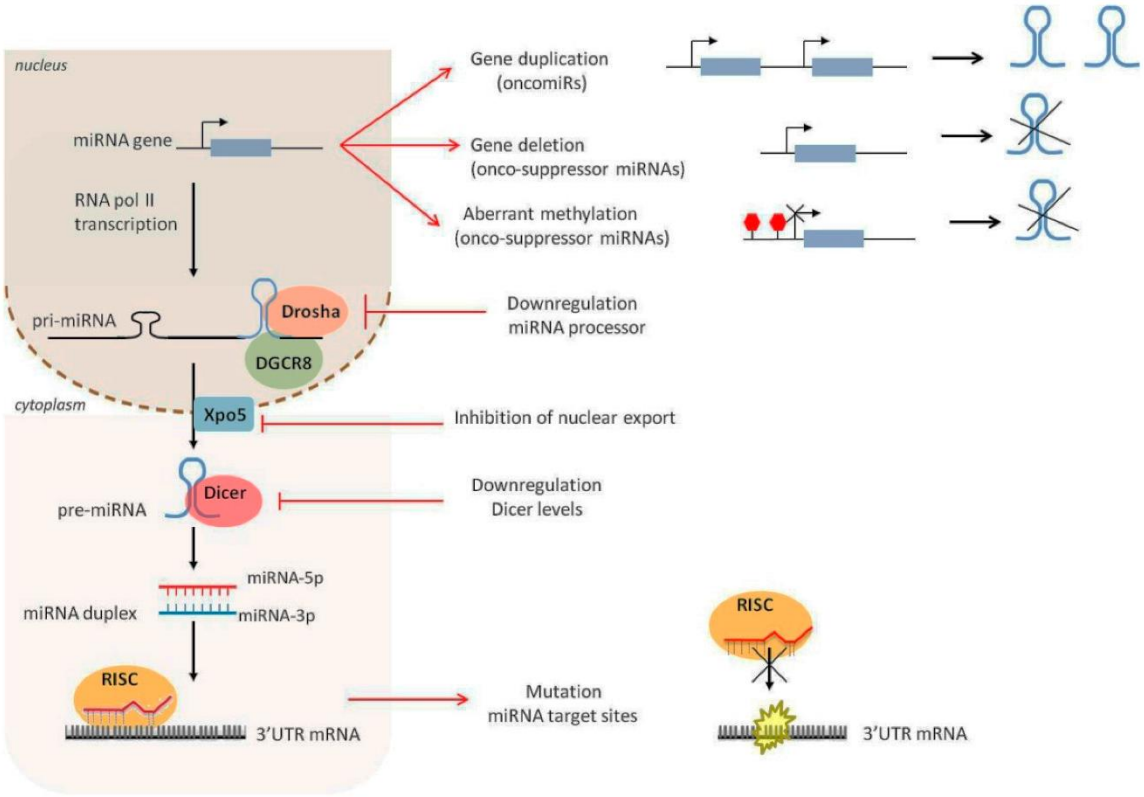

Figure 1.3. microRNA (miRNA) biogenesis dysregulation during cancer initiation and progression [146].

II. 5. MicroRNA-590 (miR-590)

MicroRNA-590-3p (miR-590-3p) is located on chromosome 7q11.23 (Figure 1.4) and is contained within an intron of the eukaryotic translation initiation factor 4H (eIF4H) gene. eIF4H has been shown to stimulate translation in rabbit reticulocytes [147]. It has also been reported that eIF4H was overexpressed in most human ovarian cancer tissues [148], suggesting a critical role for eIF4H in carcinogenesis. miR-590 is expressed in heart, breast, nerves, stomach, and ovaries. In addition, it plays a significant function in cell differentiation, proliferation, and tumor regulation, indicating that miR-590 is engaged in several physiological processes. In a recent study, miR-590-3p was shown to promote cardiomyocyte proliferation and induce cardiac regeneration after myocardial infarction [149]. These findings are in accordance with other previous studies where miR-590-3p promoted ovarian cancer [150], lymphoblastic leukaemia [151], colorectal [152], glioblastoma [153] and colon cancer [154]. Both the mature miR-590-3p and mir-590-5p (Figure 1.5) were reported to have an independent function from each other, and can be associated with both promoting and inhibiting cancers [151, 152, 154-156]. This dual function of miR-590 would likely be attributed to differential mRNA target sets between the 5p and 3p strands and will be further discussed in (chapter 2).

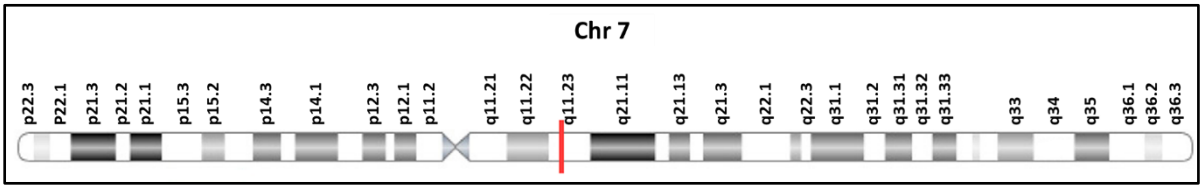

Figure 1.4. Gene location of miR-590.

has-miR-590-3p
56 – uaauuuuauguauaagcuagu- 76

has-miR-590-5p
16 – gagcuuauucauaaaagugcag - 37

Figure 1.5. Sequences of miR-590-3p and miR-590-5p

III. THE FORKHEAD BOX (FOX) SUPERFAMILY

The Forkhead box (FOX) proteins are transcription factors that play critical roles in several processes. The FOX gene family encodes for proteins which control the transcription of genes taking part in functions such as proliferation, organ development or regulating metabolic homeostasis [157]. The FOX superfamily comprises 50 *FOX* genes in the human genome and 44 in the mouse, and are divided into 19 subfamilies (Table 2) [158]. Depending on the family member and cell type, *FOX* genes are differentially expressed in various cancers. However, they can play either a tumor suppressing or a tumor promoting role and gene expression can be regulated during transcription or translation.

Forkhead (*fkh*) was the first *FOX* gene discovered in Drosophila [159], followed by *FOXA1* identification and characterized in rats [160]. In 1990, some protein groups were found to share a similar DNA-binding domain, later called the Forkhead domain (FHD), which was found to be highly conserved among the entire *FOX* family [161]. In 1993, the crystal structure of the DNA-bound Forkhead domain was solved for *FOXA1* [162]. Many other FOX structures followed, including the DNA-binding domains of *FOXM1, FOXO1, FOXO3, FOXO4, FOXP1, FOXP2, FOXK1,* and *FOXK2* [162].

Unified naming system

Prior to 2000, *FOX* genes lacked an integrated naming convention and were named by the investigators who found them. This old naming system was used until the Winged helix/Forkhead nomenclature committee implemented a unified nomenclature system for the FOX family members. This system described the FOX family as the set of genes that have sequence homology to the canonical Winged helix/Forkhead DNA-binding domain. In addition, subclasses *FOXA* and *FOXO* were defined according to a phylogenetic study of the Forkhead domain [163].

Table 1.2: List of the FOX genes in humans and mice, chromosomal locations and percentage sequence similarity between the human and mouse orthologous proteins.

Human		Mouse		% Similarity
Protein	**Chromosome**	**Orthologue**	**Chromosome**	
FOXA1	14q12-q13	FOXA1A	12	96.2
FOXA2	20p11	FOXA2	2	97.4
FOXA3	19q13.2-q13.4	FOXA3	7	90.4
FOXB1	15q22	FOXB1	9	99.7
FOXB2	9q21.2	FOXB2	19	92.6
FOXC1	6p25	FOXC1	13	95.1
FOXC2	16q24.1	FOXC2	8	92.6
FOXD1	5q12-q13	FOXD1	13	85.8
FOXD2	1p34-p32	FOXD2	4	94.3
FOXD3	1p31.3	FOXD3	4	90.8
FOXD4	9p24.3			
FOXD4L1	2q14.1	FOXD4	19	63.7
FOXD4L2	9p12			
FOXD4L3	9q13			
FOXD4L4	9q13			
FOXD4L5	9q13			
FOXD4L6	9q12			
FOXE1	9q22	FOXE1	4	91.2
FOXE3	1p32	FOXE3	4	79.3
FOXF1	16q24	FOXF1	8	97.4
FOXF2	6p25.3	FOXF2	13	94.6
FOXG1	14q11-q13	FOXG1	12	96.3
FOXH1	8q24	FOXH1	15	76.3
FOXI1	5q34	FOXI1	11	89.9
FOXI2	10q26.2	FOXI2	7	78.6
FOXI3	2p11.2	FOXI3	6	84.5
FOXJ1	17q25.1	FOXJ1	11	94.5
FOXJ2	12p13.31	FOXJ2	6	93.2
FOXJ3	1p34.2	FOXJ3	4	96.5
FOXK1	7p22	FOXK1	5	92
FOXK2	17q25	FOXK2	11	95
FOXL1	16q24	FOXL1	8	73
FOXL2	3q23	FOXL2	9	96.8
FOXM1	12p13	FOXM1	6	88.6
FOXN1	17q11-q12	FOXN1	11	90.9
FOXN2	2p22-p16	FOXN2	17	48
FOXN3	14q24.3-q31	FOXN3	12	90
FOXN4	12q24.12	FOXN4	5	86.2
FOXO1	13q14.1	FOXO1	3	95.4
FOXO3	6q21	FOXO3	10	96.1
FOXO4	Xq13.1	FOXO4	X	93.3
FOXO6	1p34.2	FOXO6	4	86
FOXP1	3p14.1	FOXP1	6	94.6
FOXP2	7q31	FOXP2	6	99.7
FOXP3	Xp11.23	FOXP3	X	91.4
FOXP4	6p21.1	FOXP4	17	80.5
FOXQ1	6p25	FOXQ1	13	93.6
FOXR1	11q23.3	FOXR1	9	77.7
FOXR2	Xp11	FOXR2	X	73
FOXS1	20q11.1-q11.2	FOXS1	2	83.3

Adapted from [158]

III. 1. FOXA Subfamily

Forkhead box A2 (*FOXA2*) is a transcription factor involved in embryonic development, metabolism and homeostasis [164]. It was formerly known as hepatocyte nuclear factor 3β (*HNF3β*) due to its function in regulating specific gene expression patterns in the liver [160]. The *FOXA2* gene is located on chromosome 20p11.21, and the translated protein can bind to the DNA consensus sequence 5-[AC]A[AT]T[AG]TT[GT][AG][CT]T[CT]-3 [162]. This gene participates in cell signal transduction, inhibition or activation of the transcriptional activity of target genes [165], and controls metabolism [166]. In addition, it plays an important role in the development [167] and maturity of organs and tissues [168].

It was believed that *FOXA1* and *FOXA2* have some functional redundancy. Although a recent study showed that *FOXA2* is involved in tumor development, *FOXA2* role as a tumor-suppressor has been also reported in lung cancer [169, 170], pancreatic cancer [171], as well as in gastric tumors [172]. Interestingly, FOXA2 has been reported as both a tumor promoter and tumor suppressor in breast cancer [200, 201]. On the other hand, in liver cancer, the function of *FOXA2* development is sexually dimorphic, as it has a tumor-promoting function in males and tumor-suppressing function in females [173].

III. 2. Structure of FOXA2

The *FOXA2* gene is ~ 2400 bp in length and is located in chromosome 20p11.21. As a FOXA family member, *FOXA2* has a Forkhead domain that can form a complex to target DNA motifs [162]. Recently, FOXA was identified as a pioneer factor, regulating chromatin accessibility to other factors, and also binds to enhancers and promoters [164, 174, 175]. In addition, *FOXA2* is the only FOX member that has an AKT2/PKB phosphorylation site at the N terminus of the FHD which suggests additional unique regulatory function [164]. Structurally, *FOXA2* also contains two nuclear localization sequences (NLS) that flank the FHD [176, 177] (Figure 1.6).

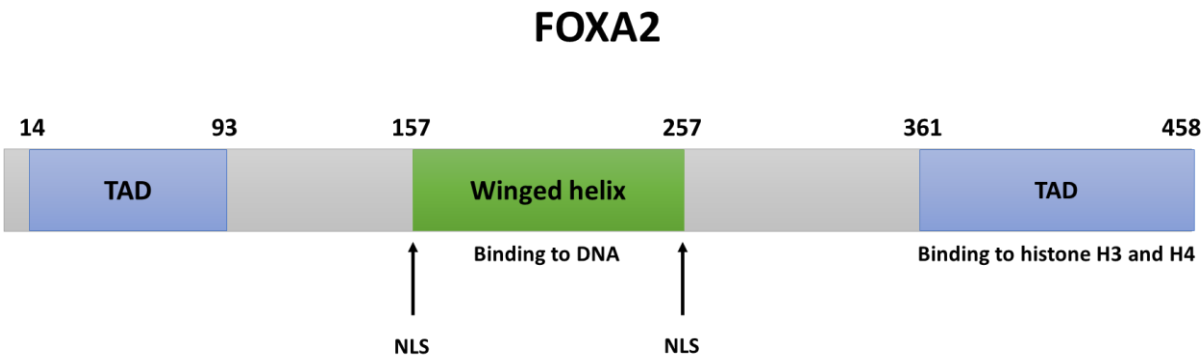

Figure 1.6: Structure of Forkhead box protein A2 protein. FOXA2 has two nuclear localization sequences and two transactivation domains. FOXA2 possesses a winged helix, which located in the center of FOXA2, two Transcription Activation Domain (TAD), one at each end. NLS refers to nuclear localization sequences. Reprinted (with modifications) from [178].

III. 3. FOXs in Diseases

Given their primary function in the expression of numerous genes that influence cell survival and proliferation, it was suggested that FOX family members may play a role as cancer therapeutic targets. *FOX* family members were reported to have either up- or down-regulating effects in several cancer types. *FOXP1* has been shown to act as an oncogene and/or as an anti-oncogene, based on the cell type, even though these observations are principally dependent on correlations between mRNA levels and clinical results [179]. Likewise, FOXM1 is considered an oncogene that is widely expressed in several carcinomas and expressed at lower levels in normal cells [180].

Breast and prostate cancers are the two major cancers that are influenced by hormones. It has been reported that FOXA1/2 play a crucial role in the regulation of estrogen-receptor-alpha positive (ERα) and androgen receptor (AR) [181-183], and the expression of FOXA in ERα-positive breast cancers and AR-positive prostate cancers were observed [183, 184].

Metastasis is responsible for ~ 90% of cancer deaths [6]. The epithelial–mesenchymal transition (EMT) is considered an important requirement for metastasis in most carcinomas, allowing cancer cells to disassociate from the primary tumor by enhancing cell motility, invasion, and cell adhesion molecule profiles, such as E-cadherin [185]. FOXA2 was reported to strongly inhibit metastasis while decreased expression levels promoted cancer progression in lung cancer [169, 170]. In addition, FOXA2 was reported to regulate epithelial marker, E-cadherin, expression [186]. This indicates its role in EMT regulation, and its importance in suppressing tumor metastasis via EMT down-regulation.

Moreover, FOXA1/2 were reported to be essential for sexual dimorphism in liver cancer. In FOXA1/2 mutant mice, it was shown that tumors' sizes were increased in females, while decreased in males. This dimorphism effect was essentially achieved through the recruitment of ERα and androgen receptor (AR) to their relevant targets in the liver [173].

IV. VERSICAN

Versican (VCAN) is a large chondroitin sulfate proteoglycan that provides a loose hydrated matrix during key events in development and disease [187]. VCAN is one of the main components of the extracellular matrix (ECM). Besides providing necessary support for the physical shape of the cell and its behaviour, ECM is a key element in cell adhesion, proliferation, migration and differentiation [188]. ECM remodelling takes place through 1- signal transduction, which in turn results in behavioural changes in cell motility and proliferation, and 2- through the expression of proteins that control the dynamic process of ECM composition and decomposition in tissues [189].

VCAN is comprised of 15 exons located within chromosome 5 (5q14.2-q14.3), and is encoded by the *VCAN* gene. It has a molecular mass of ~500 kDa, and it was first detected in human's healthy and cancerous brain tissue [190].

VCAN has a glycosaminoglycan-domain (GAG domain), a globular G1-domain at its N-terminal, and a globular G3-domain at the C-terminal. All isoforms have these G1 and G3 globular domains [191]. Alternate splicing of the GAG-domain leads to four different isoforms of VCAN; namely, V0, V1, V2, V3 many of which have been discovered in a variety of tissues [192-194] (Figure 1.7). V0 has a GAG-α exon and a GAG-β exon. V1 has a GAG-β exon. V2 has the GAG-α exon. V3 contains only the two globular domains, G1 and G3. As a result, this latter isoform exists as a glycoprotein and not as a proteoglycan [195]. The size difference of chondroitin sulphate attachment regions in between the isoforms may lead to functional and structural diversity.

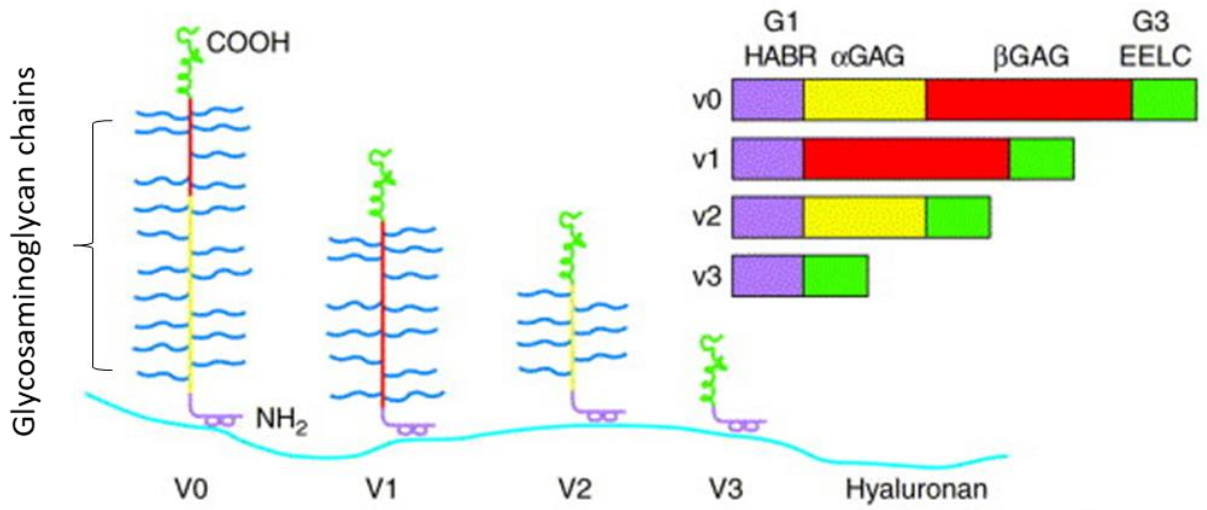

Figure 1.7: Structure of different versican isoforms. Alternative splicing of the mRNA transcript leads to the formation of four different versican isoforms, V0, V1, V2 and V3. All isoforms interact with hyaluronan. Reprinted with permission from [196]

IV. 1. The Role of Versican Isoforms in Normal and Cancer Tissues

The function of each VCAN isoform in normal and cancer tissues is still unclear [197]. During late embryonic developmental stages, V0 and V1 isoforms are expressed prominently; however, V0 isoform expression diminishes in adult tissues. To date, it has not been demonstrated that the most common isoforms, V0 and V1, can play different roles [198] but studies showed that V1 promotes cell proliferation and can protect fibroblasts from apoptosis [199]. In contrast, isoform V2 was shown to inhibit cell proliferation and does not appear to be involved in apoptosis resistance [199]. Interestingly, some studies have suggested that the smallest VCAN variant, V3, which contains only G1 and G3-domains may have a different role and properties from the other isoforms [200]. V3 was reported to be expressed in growth factors or cytokines activated endothelial cell cultures; however, the exact function of V3 in activated endothelium is yet to be identified. On the other hand, V3 overexpression in smooth muscle cells of the artery increased their adhesion to cell culture plates but inhibited cell proliferation and migration in wound-healing assays [200]. Also, although V3 overexpression significantly decreased melanoma cancer cells' growth *in vivo* and *in vitro*, it promoted cells metastasis into the lung, suggesting a dual role of V3 in cancer development and progression [201, 202].

Many other studies have confirmed elevated expression levels of VCAN in several cancers such as brain tumors, melanomas, osteosarcomas, lymphomas, as well as breast, prostate, colon, lung, pancreatic, and ovarian endometrial cancers [203-210]. In general, higher VCAN level was correlated with poor outcomes and cancer recurrence in prostate, breast and many other cancer types [198]. In ovarian cancer, serous epithelial cancers were correlated with high stromal VCAN level and this was linked to a reduction in survival rates. On the other hand, early stage clear cell carcinoma was associated with high VCAN levels which promoted recurrence-free survival. In normal ovaries, however, VCAN expression is precisely regulated

[211]. Researchers have shown that different mechanisms are accountable for differentially controlling localization, protein expression, and for the biological role of VCAN [212]. For example, VCAN level is induced in the ovary as a result of the natural wound-healing [213], follicle growth [211], and inflammation [214] events that follow the release of the ovum. Although it has been reported that the VCAN level is positively correlated with patient's poor outcome, VCAN level cannot be used as a prognostic marker for EOC progression [215].

V. CYCLIN G2

Cyclins are an important family of cell cycle regulators [216]. They achieve their function via activation of specific cyclin-dependent kinases in order to promote cell cycle progression [217-219]. One of these cell cycle controllers is Cyclin G2, a protein encoded by the *CCNG2* gene in humans [220, 221]. Although the function of *CCNG2* is not completely understood, a recent study suggested that it has an important role as a tumor suppressor [216]. It has also been reported that the level of *CCNG2* is inversely correlated with the progression of breast cancer [223], acute leukaemia [224], oral [225], thyroid [226], as well as gastric cancers [224, 227]. Our lab has previously shown that *CCNG2* modulated *Nodal*-regulated anti-proliferative effect in EOC cells, and that Cyclin G2 is highly unstable [228, 229]. In addition, we recently showed that overexpression of *CCNG2* significantly suppresses cell proliferation, migration and invasion both *in vitro* and *in vivo* [216].

The G-type cyclin members, including, cyclin G1, cyclin G2 and cyclin I, possess a relatively similar sequence homology and functional resemblance [220, 230]. While cyclin G2 has a high sequence identity with various G-types cyclins (41% homology to cyclin I and 71% homology to cyclin G1) [231], there are some differences in their promoter sequence, regulation, and expression, indicating a non-compensatory physiological function [220, 232].

V. 1. Structure and Expression Profile of Cyclin G2

The protein structure of cyclin G2 is classified into three main domains: the amino-terminal domain, the carboxyl-terminal domain, and a cyclin box of nearly a 110 amino acids [221]. Both cyclin A and cyclin G2 have a similar cyclin box, which interacts with CDK-2 to regulate cell transition from one phase to the next [233]. However, the means by which CDK-2 binds to any cyclin-dependent kinase partner is still unknown [231, 234]. As a result, cyclin

G2-association with other regulatory members of the cell cycle may be possible. However, this association probably does not occur through the cyclin box domain [234].

Cyclin G2 is conserved in primates and other species [235], and it has been reported to have an inverse correlation between cyclin G2 expression with age in some species [235]. Monitoring cyclin G2 levels in the mice liver over time showed that protein levels vary from 3-6 weeks of age. When the tissue ages and becomes mitotically silent, cyclin G2 levels decrease more than two-fold when compared with younger tissues [235].

V. 2. Functions of Cyclin G2

Cyclin G2 is an unconventional cyclin which does not follow the behaviour of the other cyclin family members [232]. High levels of cyclin G2 are correlated with cell cycle quiescence in several cell types [225, 231, 232, 234]. Its expression fluctuates greatly during the cell cycle. In response to DNA damage and growth inhibitory signals, it has been observed that cyclin G2 protein level is consistently up-regulated [225, 230, 231, 234]. In addition, cyclin G2 expression was greatly reduced during proliferation, while it is mainly expressed during cell cycle arrest and during the G_0 phase [230, 234].

In the tightly regulated process of the cell cycle, the progression of cell differentiation was also associated with cyclin G2 expression, as its level is often the highest in terminally differentiated tissue [236]. Moreover, cyclin G2 overexpression following implantation induces uterine stromal cells differentiation [237].

V. 3 Cyclin G2 Dysregulation in Cancer

Malignancy progression is highly influenced by many other cellular processes, including DNA damage, cell differentiation, and indeed cell cycle control. Thus, it is suggested that cyclin G2 association with its protein targets regulates its tumor suppressing effect. On the

other hand, when the oncogenic signaling pathways result in a reduction of cyclin G2 expression level, its ability to associate or bind to its partners is also affected, and this leads to the progression of diseases [238-240].

Studies have shown that several oncogenic signaling pathways can result in the reduction of cyclin G2 expression, while some growth-inhibitory signals are able to upregulate its expression. Furthermore, cyclin G2 expression is induced by several anticancer drugs [238-240]. Interestingly, many studies showed that cyclin G2 overexpression inhibits cell proliferation in human cell lines [225, 232, 241] and inhibits colony and spheroid formation as well as tumor formation *in vivo*. Cyclin G2 was also found to positively associate with survival, but to negatively correlate with cancer progression [216].

VI. WNT/β-CATENIN SIGNALING

The Wnt signaling pathway is a crucial pathway that regulates cell survival, proliferation, polarity, and the fate of stem cells in both embryonic and adult tissues [242]. The Wnt pathway is characterized into β-catenin dependent (canonical), which will be the focus of this review, and β-catenin independent (non-canonical) signaling pathways. While components of non-canonical Wnt signaling have not been well-characterized, multiple elements of canonical Wnt signaling (Wnt/β-catenin) have been identified.

One of the important dynamic proteins regulating the canonical Wnt pathway is β-catenin. β-catenin is located in several subcellular compartments within the cytoplasm, or within the junctions where it plays a role in the cell-cell contact stabilization. In addition, β-catenin may also be located within the nucleus where it stimulates the expression of target genes by binding to transcription factors (Figure 1.8) [243]. Disruption of the Wnt/β-catenin pathway or mutations in β-catenin is associated with many different diseases including cancer [243, 244].

Wnt signaling involves in the regulation of target genes associated with cell cycle progression [245, 246], reduction of cell-cell contact [247], and EMT genes [248]. Canonical Wnt signaling cascades are activated by the binding of extracellular Wnt ligands to its receptors. Wnt ligands family comprises 19 glycoprotein members [249]. Upon production, Wnts are readily secreted by signaling cells [250, 251]. Once they reach the membrane of a target cell, Wnt ligands bind to the membrane receptors Frizzled (Fz) [252]. Lipoprotein receptor-related protein (LRP) 5 or 6 are another important trans-membrane receptor [253, 254]), which interacts with Fz to form a Wnt receptor complex and initiate Wnt signaling [255]. The cytosolic β-catenin level is highly regulated by the β-catenin destruction complex. The destruction complex is composed of tumor suppressor proteins Axin, Adenomatous polyposis coli (APC), glycogen synthase kinase 3 (GSK3) and casein kinase I (CKI), Protein

phosphatase 2 (PP2A) and β-transduction repeat-containing protein (β-TrCP) [256].

Axin acts as a scaffold protein that binds to and brings CKI, GSK3, and β-catenin into close proximity. This binding promotes phosphorylation and subsequent inhibition of β-catenin activity [257, 258]. In the presence of Wnt signaling, LRP is phosphorylated by CKI and GSK3, inducing the translocation of the β-catenin destruction complex closer to the membrane [259] and increasing the binding between GSK3 and LRP. Dishevelled (Dvl) molecule is then interacts with LRP leading to the activation of DVL and inactivation of GSK3β, which leads to the dissociation of Axin and GSK3. The GSK3 plasma membrane-associated pool is essential to activate signaling by phosphorylation of CKI and LRP, while the GSK3 destruction complex associated pool phosphorylates CKI and β-catenin to inhibit signaling. Consequently, the disruption of the destruction complex prevents β-catenin phosphorylation and degradation subsequently. The stability of β-catenin by Wnt signaling results in the translocation of β-catenin to the nucleus and activation of Wnt target genes through interactions with TCF/Lef transcription factors; however, β-catenin cannot bind DNA directly and serves as a co-activator [260]

VI. 1. TCF/Lef Transcription Factor Family

In the absence of Wnt signaling, TCF/Lef possess limited transcriptional activity due to their interaction with Groucho transcriptional repressors [261, 262]. As β-catenin enters the nucleus, it displaces Groucho, forming a transcriptionally active complex with TCF and other co-activators [263]. TCF/ β-catenin transcriptional activity is modulated through a variety of signals: (i) TCF/Lef isoforms lacking the β-catenin binding domain can antagonize TCF/ β-catenin complex activity [264, 265], (ii) expression of nuclear antagonists, Chibby and ICAT, which can bind to β-catenin to limits its interaction with transcription factors and co-activators, promoting its nuclear exclusion [266, 267], and (iii) post-translational modifications such as

phosphorylation and acetylation that can lead to activation, repression, or degradation of TCF/Lef proteins [264, 265].

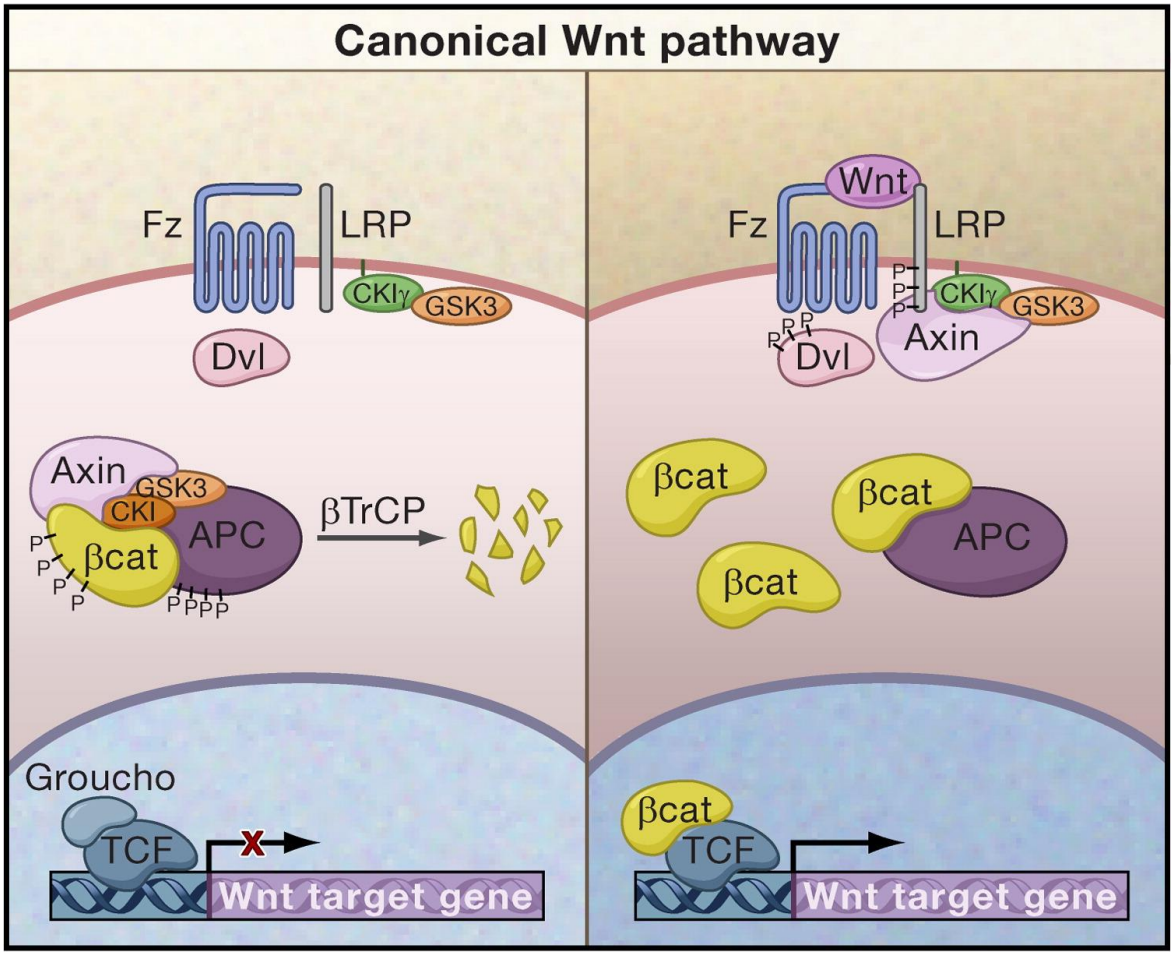

Figure 1.8: Wnt/ β-catenin signaling pathway. In the absence of Wnt signaling (left), the destruction complex phosphorylates β-catenin. β-TrCP then ubiquitinates β-catenin leading to its degradation. In the presence of Wnt signaling (right), Wnt binds to its Fz receptor and recruits Disheveled (Dvl). Dvl promotes the phosphorylation of LRP5/6 co-receptor through CK1 and GSK3β. This leads to a high-affinity binding of Axin and subsequent disruption of the destruction complex. When the destruction complex is inactivated, β-catenin is accumulated, stabilized and translocated to the nucleus. In the nucleus, β-catenin binds to DNA-binding proteins of the T-cell factor (TCF) and lymphoid enhancer-binding factor 1 (Lef-1) to regulate Wnt target gene transcription. Reprinted with permission from [243].

VI. 2. β-Catenin Protein Characteristics and Its Physiological Functional Roles

β-catenin is a highly conserved protein [268]. The β-catenin function is strongly correlated with the structural components that allow it to form complexes with several proteins. The flexible structures of the C- and N- terminals of β-catenin facilitate the interaction with transcription factors as well as allows for its phosphorylation. On the other hand, the central region acts as a platform that mediates protein-protein interactions [269] (Figure 1.9).

In addition, β-catenin levels are highly dependent on a delicate balance of phosphorylation events through the interaction with members of the destruction complex, Axin, APC, CK1 and GSK3β. These phosphorylation events allow β-catenin to be recognized, and subsequently ubiquitinated by the β-transduction repeat-containing protein E3 ubiquitin ligase β-TrCP and hence, result in its proteasomal degradation [268, 270].

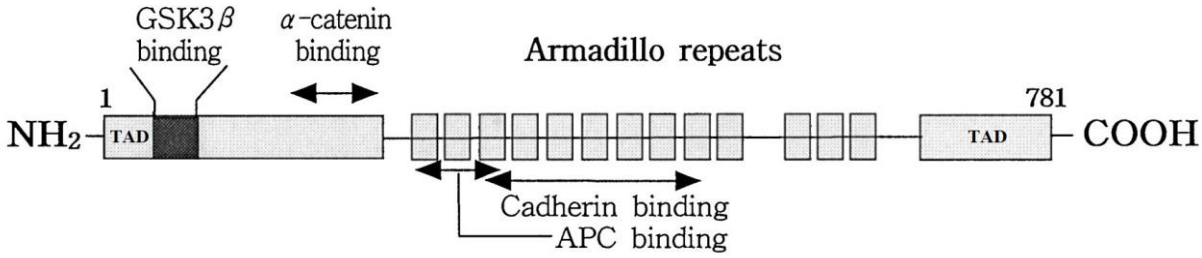

Figure 1.9: The structure of β-catenin. β-catenin consists of a highly conserved Armadillo repeat domain and relatively unstructured N- and C- terminal domains. β-catenin N-terminal GSK3β and CKI phosphorylation sites are required for proteasome-mediated destruction by β-TrCP. The transcriptional activation domains (TAD) are required for nuclear signaling. Within the Armadillo repeat domain, many of the β-catenin partners compete for the same binding site. Adapted and reprinted with permission from [80].

VI. 3. β-Catenin Dysregulation and Cancer

Dysregulation of β-catenin signaling can affect many cellular processes such as proliferation, survival, and stem-cell biology; all of which are frequently associated with malignancy development, progression and transformation [271-273]. Activating mutations in β-catenin gene were observed in several types of tumors [274]. In ovarian cancer, as well as many other types of cancer, alterations in the levels of protein components within Wnt/β-catenin pathway have been shown to play a vital role in the tumorigenesis [275]. In endometrioid carcinoma, β-catenin nuclear expression is widely observed suggesting that the activation of the β-catenin-TCF signaling pathway facilitates the development of this carcinoma subtype [276]. Also, the dysregulation of the Wnt signaling components in other ovarian cancer subtypes may promote cancer development [216, 277]. Furthermore, recent studies have indicated that Wnt/β-catenin pathway promotes ovarian cancer stem cell self-renewal [279, 280], chemoresistance [281], and metastasis [278].

In a previous study on EOC cells, we showed that cyclin G2 exerts anti-tumor effects by attenuating β-catenin signaling, and enhances the recruitment of the destruction complex [216]. CCNG2 was found to downregulate key Wnt components LRP6 and DVL2, leading to a decrease in total β-catenin and an increase in phosphorylated β-catenin [216]. This regulation leads to β-catenin degradation and suppression of β-catenin/TCF transcriptional complex activity as the consequence. With high level of CCNG2 and low level of β-catenin in the cytoplasm, the accumulation of β-catenin in the nucleus will be limited and signal transduction will be inhibited. In contrast, inhibition of CCNG2 expression results in accumulation of β-catenin in the nucleus, thus inducing TCF/Lef signaling to activate the transcription of its target genes and affecting cell-cell adhesion [282]. In fact, β-catenin accumulation in the nucleus can be considered a marker for metastasis progression [283-287]. This is likely attributed to the transcriptional activation of mesenchymal genes that results in

epithelial-to-mesenchymal transition (EMT), a hallmark of cancer initiation and development [288]. Given its important regulatory role in regulating pathways, β-catenin has become an important target of many potential therapeutic treatments [289].

VII. RATIONALE, HYPOTHESIS, AND OBJECTIVES

Ovarian cancer is the deadliest of the gynecologic malignancies, and is the fifth leading cause of cancer-related death among women [5]. In part, this is due to absence of effective early screening methods for EOC when the disease is at its early, and more manageable, stage. As such, the low survival rate for women with EOC is in part due to the lack of effective treatment for the advanced cancer, as well as from our incomplete understanding of how exactly EOC develops [290].

After their discovery in 1993, miRNA research quickly rose in popularity leading to ~1900 validated miRNAs being identified in the human genome in 2017 [291-293]. miRNAs have shown to regulate nearly all physiological and pathological processes. In cancer therapy miRNAs have shown great promise as both therapeutic targets and potential biomarkers. Therefore, we were interested in studying the effect of miRNAs in regulating ovarian cancer and their potential use as early diagnostic markers of EOC. Since we have found that CCNG2 exerts tumor-suppressing effects in EOC [228], we searched for miRNAs that may target CCNG2. Among the several miRNAs tested, miR-590-3p exhibited the strongest effect on promoting cell proliferation. At the beginning of our study, little was known about the function of miR-590-3p, with one report about its role in promoting cardiomyocyte proliferation and induce cardiac regeneration after myocardial infarction [149], and another report about its role in hepatocellular carcinoma [294]. Although the role of miR-590-3p in ovarian cancer was unknown, it was identified as one of the dysregulated miRNAs in EOC tumors [295], suggesting its potential role in EOC development.

Based on these findings, we hypothesize that miR-590-3p promotes ovarian cancer progression. Thus, the objectives of my Ph.D. study were to determine the function of miR-590-3p in EOC development and to investigate the mechanisms by which miR-590-3p exerts tumorigenic effects on EOC cells.

CHAPTER 2

MICRORNA-590-3P PROMOTES OVARIAN CANCER GROWTH AND METASTASIS VIA A NOVEL FOXA2-VERSICAN PATHWAY

miRNA-590-3p promotes ovarian cancer growth and metastasis via a novel FOXA2-versican pathway

Mohamed Salem[1], Jacob A. O'Brien[1], Stefanie Bernaudo[1], Heba Shawer[2], Gang Ye[1], Jelena Brkic[1], Asma Amleh[2], Barbara C. Vanderhyden[3], Basel Refky[4], Burton B. Yang[5], Sergey N. Krylov[6,7], Chun Peng[1,7*]

Published in: *Cancer Res; 78(15); 4175–90. ©2018 AACR.*

[1]Department of Biology, York University, Toronto, Canada
[2]American University in Cairo, New Cairo, Egypt
[3]Department of Cellular and Molecular Medicine, University of Ottawa, Ottawa, Canada
[4]Department of Surgical Oncology, Mansoura Oncology Center, Mansoura, Egypt
[5]Sunnybrook Research Institute, Sunnybrook Health Science Centre, Toronto, Canada
[6]Department of Chemistry, York University, Toronto, Canada
[7]Centre for Research on Molecular Interactions, York University, Toronto, Canada
[*] Corresponding author and to whom reprint requests should be addressed to:
Dr. Chun Peng, Department of Biology, York University, Toronto, Ontario, Canada M3J 1P3. cpeng@yorku.ca

Authors' Contributions

Conception and design: M. Salem, J.A. O'Brien, S. Bernaudo, A. Amleh, C. Peng

Development of methodology: M. Salem, J.A. O'Brien, H. Shawer, G. Ye, A. Amleh, S.N. Krylov, B.B. Yang

Acquisition of data: M. Salem generated data for most figures. J.A. O'Brien performed the TCGA database analysis and generated Figure 2.6 and supplementary figures S2.4-2.6. S. Bernaudo helped in designing experiments. H. Shawer performed the experiment in figure 2.1A and 2.1C. G. Ye assisted in the in vivo studies presented in figure 2.2 . J. Brkić generated the heatmap in figure 2.3A.

Analysis and interpretation of data: M. Salem, J.A. O'Brien, S, Bernaudo, H. Shawer, J. Brkić, A. Amleh, C. Peng

Patient samples: B. Vanderhyden, B. Refky

Manuscript drafting and revision: M. Salem, C. Peng, J.A. O'Brien, S. Bernaudo, H. Shawer, J. Brkić, A. Amleh, C, B. Vanderhyden, B.B. Yang

Study supervision: C. Peng

ABSTRACT

miRNAs play important roles in gene regulation, and their dysregulation is associated with many diseases, including epithelial ovarian cancer (EOC), which is the fifth leading cause of cancer-related death among women. In this study, we determined the expression and function of miR-590-3p in EOC. miR-590-3p levels were higher in high-grade carcinoma when compared with low-grade or tumors with low malignant potential. Interestingly, plasma levels of miR-590-3p were significantly higher in patients with EOC than in subjects with benign gynecologic disorders. Transient transfection of miR-590-3p mimics or stable transfection of mir-590 increased cell proliferation, migration, and invasion. *In vivo* studies revealed that mir-590 accelerated tumor growth and metastasis. Using a cDNA microarray, we identified forkhead box A2 (FOXA2) and versican (VCAN) as top downregulated and upregulated genes by mir-590, respectively. miR-590-3p targeted FOXA2 3′ UTR to suppress its expression. In addition, knockdown or knockout of FOXA2 enhanced cell proliferation, migration, and invasion. Overexpression of FOXA2 decreased, whereas knockout of FOXA2 increased VCAN mRNA and protein levels, which was due to direct binding and regulation of the VCAN gene by FOXA2. Interrogation of the TCGA ovarian cancer database revealed a negative relationship between FOXA2 and VCAN mRNA levels in EOC tumors, and high FOXA2/low VCAN mRNA levels in tumors positively correlated with patient survival. Finally, overexpression of FOXA2 or silencing of VCAN reversed the effects of mir-590. These findings demonstrate that miR-590-3p promotes EOC development via a novel FOXA2–VCAN pathway.

INTRODUCTION

Epithelial ovarian cancer (EOC) is the most common form of ovarian cancer and has the highest mortality rate among all gynecologic malignancies [1]. There are no effective early screening methods for EOC; thus, most cases are not detected until late stages when the cancer has spread to other organs. Ovarian cancer cells detached from primary tumors often settle on the peritoneum and omentum, as well as adjacent organs [2]. However, tumor cells have also been detected in the blood of patients with ovarian cancer, suggesting an additional hematogenous path by which cancer cells invade through blood and lymph vessels to establish secondary tumors [3].

miRNAs are small noncoding RNAs that regulate gene expression primarily at the posttranscriptional levels. miRNA genes are transcribed into primary miRNAs, processed into precursor (pre)-miRNAs, and exported from the nucleus. Within the cytoplasm, pre-miRNAs are further processed into mature miRNAs [4]. It is well accepted that miRNAs play critical roles in many developmental and physiologic events. Moreover, aberrant miRNA expression has been implicated in the pathogenesis of human diseases, including cancer [4].

miR-590-3p is contained within an intron of the eukaryotic translation initiation factor 4H gene. miR-590-3p was first reported to enhance cardiomyocyte proliferation and cardiac regeneration after myocardial infarction [5]. More recently, the effects of miR-590-3p on several types of cancer have been reported [6-8]. Although the role of miR-590-3p in ovarian cancer is unknown, an RNA sequencing (RNA-seq) study has identified miR-590-3p as one of the miRNAs dysregulated in EOC tumors [9], suggesting its potential role in EOC development.

Forkhead box A2 (FOXA2) is a transcription factor involved in the regulation of embryo development, as well as metabolism and homeostasis [10]. Recent studies suggest that FOXA2 also plays a role in cancer development. Tumor-suppressive effects of FOXA2 have

been reported in pancreatic cancer [11], lung cancer [12, 13], and gastric cancer [14]. In breast cancer, both tumor-suppressing [15] and tumor-promoting effects [16] have been found. Interestingly, the role of FOXA2 in liver cancer development is sexually dimorphic, with tumor-suppressive effects in females and tumor-promoting effects in males [17].

Versican (VCAN) is a large proteoglycan and a major component of the extracellular matrix. Numerous studies have shown that VCAN is frequently overexpressed in tumor tissues and promotes processes associated with tumor development, such as adhesion, proliferation, migration, invasion, and angiogenesis [18]. In advanced stage serous ovarian cancer, high VCAN expression in the tumor stroma is associated with shorter survival [19], and *in vitro* studies suggest that VCAN promotes ovarian cancer cell invasion [20].

The aim of this study was to investigate the role of miR-590-3p in ovarian cancer development. Herein, we report that miR-590-3p is upregulated in tumor tissues and plasma samples of patients with EOC and exerts tumor-promoting effects. We further demonstrate that FOXA2 is a direct target of miR-590-3p and identify FOXA2 as a negative regulator of VCAN. Finally, we show that lower FOXA2 and higher VCAN levels in the same tumors are significantly associated with decreased survival rates in patients with ovarian cancer.

METHODS AND MATERIALS

Patient specimen

Two sets of samples were used in this study. The first set, which contained tissues and plasma samples, was collected at Mansoura Oncology Center in Egypt (Supplementary Table S1A) with approval by the Institutional Review Board of the American University in Cairo. The other set of tumor samples was obtained from the Ottawa Ovarian Cancer Tissue Bank (Supplementary Table S1B) through a protocol approved by the Research Ethics Board of The Ottawa Hospital (Ottawa, Canada). For the first set of samples, control ovarian tissues were taken from women who underwent hysterectomy and/or oophorectomy for benign gynecologic conditions. Blood samples were collected prior to surgery. All patients provided written informed consent. The studies were conducted in accordance with the ethical guidelines of Canadian Tri-Council and U.S. Common Rule.

Cell culture and transient transfection

EOC cell lines, ES-2, SKOV3.ip1, and HEY, were obtained and cultured, as reported previously [21]. The SKOV3.ip1 was transfected with a luciferase plasmid (pMIR-REPORT, Ambion) to allow for bioluminescent imaging. OVCAR3 was purchased from ATCC and cultured in RPMI1640 media (HyClone) supplemented with 20% FBS and 0.01 mg/mL insulin. All cell lines have been authenticated using short tandem repeat profile (IDEXX BioResearch). Cells were routinely tested to ensure they were free of Mycoplasma contamination using Mycoplasma Detection Kit-QuickTest (BioMake) and DAPI staining. Transient transfection of plasmids (0.25–1.5 μg), miRNA mimics, inhibitors, or siRNAs (150–200 nmol/L) was carried out in 6-well plates using Lipofectamine 2000 or Lipofectamine RNAiMAX (Life Technologies) following the manufacturer's suggested protocols. siRNAs, nontargeting negative control (NC), and miR-590-3p/5p mimic were purchased from GenePharma Co. Anti–

miR-590-3p/5p and its corresponding NC were purchased from RiboBio. Their sequences are listed in Supplementary Table S2. The FOXA2 expression plasmid was purchased from GenScript.

Generation of mir-590 stable cell lines

A fragment containing hsa-mir-590 stem-loop sequence was generated using specific primers (Supplementary Table S2). PCR was carried out using Phusion DNA Polymerase, and the resulting product was cloned into the pRNAT-CMV3.2/Hygro Expression Vector (GenScript). Positive clones were selected using PCR and validated by sequencing. The clone with the correct sequence was subsequently transfected into ES-2, SKOV3.ip1, and HEY cells. To generate control cells, the same cell lines were transfected with pRNAT-CMV3.2/Hygro, without the mir-590 insert. Following transfection, cells were cultured with hygromycin (0.6 mg/mL for SKOV3.ip1 and HEY cells and 0.8 mg/mL for ES-2) to select mir-590–positive cells.

RNA extraction, reverse transcription, and real-time PCR

Total RNA was extracted from cells or tissues using TRIzol reagent (Invitrogen) and reverse transcribed into cDNA, as described previously [22]. qRT-PCR was carried out using EvaGreen qPCR Master Mix (ABM), following the manufacturer's suggested protocol. The levels of mRNAs were normalized to GAPDH. Primer sequences are listed in Supplementary Table S2. To measure miR-590-3p and miR-590-5p levels, small RNA–enriched total RNA was extracted using TRIzol reagent (Invitrogen) as reported previously [22, 23]. The miR-590 levels in cells and tissues were measured using TaqMan PCR Kit (Thermo Fisher Scientific) and normalized to U6 snRNA. RNA was extracted from plasma samples using Qiagen miRNeasy Serum/Plasma Kit. A synthetic *C. elegans* cel-miR-39 miRNA mimic spike-in was

used as an internal control. Relative quantification of mRNAs and miRNAs were calculated using the $2^{-\Delta\Delta}C_t$ method.

Migration, invasion, and proliferation assays

Transwell migration and invasion assays were performed as described previously [21] with the modification that migrated and invaded cell numbers were counted using an automated quantification plugin for ImageJ [24]. Cell proliferation assays were conducted using manual cell counting or a real-time live-cell imaging system IncuCyte S3 (Essen Bioscience). Briefly, transfected cells were detached using Accutase (Corning) and seeded into a 96-well plate at the density of 2.5×10^3 cells/well. Four hours after seeding, images were taken every 4 hours for 68 hours.

Clonogenic assay

A total of 500 cells, stably overexpressing either mir-590 or its empty vector (EV), were seeded in a 6-well plate. After 15 to 20 days, colonies were fixed with 3.7% paraformaldehyde for 5 minutes, and stained with 0.05% crystal violet for 30 minutes. Plates were then washed, and the number of visible colonies were counted.

Microarray analysis

Total RNA was extracted from the ES-2 cell line overexpressing mir-590 and its EV-transfected control cell line ($n = 3$ wells). The cDNA microarray and subsequent analyses were conducted by the Princess Margaret Genomics Centre, Toronto, Canada (https://www.pmgenomics.ca/pmgenomics/). Hybridization was carried out using the Human HT-12 V4 BeadChip and data were imported in GeneSpring (v13.0) for analysis. The data were first normalized using a standard (for Illumina arrays) quantile normalization followed by a

"per probe" median centered normalization. Data were then filtered to remove the confounding effect probes that show no signal may have on subsequent analysis. Only probes that were above the 20th percentile of the distribution of intensities in 100% of any of the 1 of 2 groups were allowed to pass through this filtering. The final set contained 38,146 probes. A one-way ANOVA with a Benjamini–Hochberg false discovery rate–corrected $P < 0.05$ showed 4,259 significantly varying probes. A *post hoc* Tukey HSD test was used after the ANOVA and resulted in 2,483 significant probes. The microarray dataset has been deposited to the Gene Expression Omnibus repository under the accession number GSE113440. Genes that showed a difference between the EV and mir-590 groups by 2.0-fold or more were organized into a heatmap using the Multi Experiment Viewer (MeV) Microarray Software Suite. The Cancer Genome Atlas (TCGA) ovarian cancer dataset in Oncomine (www.oncomine.org) was interrogated to determine whether these genes are dysregulated in EOC.

Protein extraction and immunoblotting

Cell lysates were prepared as described previously [21]. To detect FOXA2, proteins were separated by 10% SDS-PAGE gels, then transferred to PVDF membranes (Immobilon-P, Millipore Corp.) for 1 hour. To resolve VCAN samples and GAPDH on the same gel, samples were loaded into 4% to 15% gradient gels and transferred to PVDF membranes for 14 hours using 40 volts in a cold room at 4°C. Membranes were blocked in 5% blocking buffer (5% skim milk in Tris-buffered saline and Tween-20) for 1 hour at room temperature and then incubated overnight with primary antibody at 4°C. Membranes were subsequently probed using horseradish peroxidase–conjugated secondary antibody (1:5,000) at room temperature for 2 hours. Protein signals were visualized using Luminata Classico Western HRP Substrate (EMD Millipore Corp.). FOXA2 antibody was obtained from Cell Signaling Technology (dilution

1:1,000), VCAN antibody was obtained from Boster (1:1,000), and GAPDH antibody was purchased from Santa Cruz Biotechnology (1:10,000).

Chromatin immunoprecipitation assay

Chromatin immunoprecipitation (ChIP) assays were conducted as reported previously [25]. Briefly, cells were crosslinked and cell lysates were sonicated and precleared with Pierce Protein A/G Magnetic Beads (Thermo Fisher Scientific) for 1 hour at 4°C. The samples were incubated with fresh magnetic beads conjugated with either FOXA2 antibody or control IgG (Cell Signaling Technology) overnight at 4°C. DNA was extracted from the precipitated samples using the phenol–chloroform method. To design primers for VCAN, the VCAN gene was analyzed for consensus FOXA2-binding sites, 5′-[AC]A[AT]T[AG]TT[GT][AG][CT]T[CT]-3′, obtained from UniProt [26] using a program developed by us (source code available from http://peng.lab.yorku.ca/bioinformatics-tools). The VCAN promoter region was predicted using transcription start site–proximal TF-binding sites, promoter-associated histone markers (H3K4Me3 and H3K27Ac), and DNase hypersensitivity sites from the UCSC Genome Browser [27]. Three sets of primers were designed to target: (i) a predicted FOXA2 binding site on the promoter; (ii) an intragenic site with two proximal predicted FOXA2-binding sites overlapping an open chromatin region with regulatory potential; and (iii) an intragenic site that overlaps an open chromatin region with no predicted FOXA2-binding sites, which serves as a negative control.

Luciferase assay

A fragment of FOXA2 3′ UTR, containing the predicted miR-590-3p–binding site, was generated by PCR using specific primers (Supplementary Table S2). The resulting PCR amplicon was cloned into pMIR-REPORT, downstream of the luciferase coding sequence.

Cells were seeded in 12-well plates at a density of 7.5×10^4 cells/well, transfected with the FOXA2 3′ UTR construct, together with miR-590-3p mimics or its NC. At 24 hours after transfection, luciferase activity was measured using the Dual Luciferase Reporter Assay System (Promega) according to the manufacturer's instructions, as reported previously [23].

Tumor xenograft assays

The use of animals for this study was approved by York University Animal Care Committee. Five to 6-week-old female CD-1 nude mice were purchased from Charles River Laboratories and were housed under sterile conditions in Microisolator cages, fed standard chow diet with water, and maintained in a 12-hour light/dark cycle. To study tumor formation, mice were injected subcutaneously with 1.5×10^6 control or mir-590 stable ES-2 cells suspended in 150 μL PBS. Tumor size was measured every 2 days throughout the course of the experiment. The endpoint of the study was determined when tumor size reached 17 mm or if the animal showed any sign of sicknesses such as hunched posture, inactivity, hypothermia, or ulceration at the tumor site. To study tumor metastasis, two experiments were performed. In the first experiment, mice were injected intraperitoneally with 1×10^6 SKOV3.ip1-luc cells expressing EV or mir-590, suspended in 200 μL of PBS. Animals were monitored daily and the experiment was terminated at day 70 when some of the mice showed excessive abdominal distension or moribund. Mice were anaesthetized using Ketamine (100 mg/kg) and Xylazine (10 mg/kg; CDMV) and then sacrificed. The number of nodules, as well as tumor weight and volume, were determined. In the second experiment, mice were injected with 5×10^6 SKOV3.ip1-luc control or mir-590 stable cells, and at 8, 16, and 23 days after cell inoculation, mice were anaesthetized and injected intraperitoneally with D-luciferin (150 mg/kg, Thermo Fisher Scientific), and bioluminescence signals were detected using an animal imager (ART Optix MX3).

Generation of FOXA2 knockout cells

To knockout *FOXA2*, two single guide (sg)RNAs targeting human *FOXA2* (Supplementary Table S2), designed by the Zhang laboratory [28] and cloned into pLentiCRISPR v2, were purchased from GenScript. Lentiviral packaging plasmids (pMDLg/pRRE and pRSV-Rev) and the envelope plasmid (pMD2.G) was obtained from Addgene. To produce virus, 293T cells, seeded at a density of 2.5×10^6 cells/10-cm plate, were infected with 20 μg of each of the pLentiCRISPR v2 with or without FOXA2 sgRNA, 10 μg of pMDLg/pRRE, 5 μg of pRSV-Rev, and 6 μg of pMD2.G. Supernatants were collected and used to infect ES-2 and SKOV3.ip1 cells to generate the control with EV as well as the two *FOXA2* knockout lines: FOXAΔ1 and FOXAΔ2. After infection, cells were cultured with puromycin at a concentration of 1 μg/mL to select infected cells.

TCGA data analysis and bioinformatics

To investigate the correlation of FOXA2 and VCAN expression with multiple clinical attributes, portions of the TCGA Provisional dataset published on June 31, 2016, for ovarian serous cystadenocarcinoma (https://cancergenome.nih.gov) were downloaded from cBioPortal.org [29]. This dataset contains 603 samples with associated clinical characteristics and 307 of those samples have undergone RNA-seq and Illumina HM27 methylation analysis, which were used in this study. Investigation of the preceding 2011 dataset was limited as it contained fewer samples, no RNA-seq/DNA methylation data, and far fewer clinical attributes. For these reasons, we report bioinformatical findings from the more comprehensive provisional dataset only. Sample data were aggregated from multiple files into a single comma delimited file using a custom C++ program (available from http://peng.lab.yorku.ca/bioinformatics-

tools) compiled using Microsoft Visual Studio 2015 and analyzed in Microsoft Excel 2016. The analysis was independently completed at least twice to ensure a high degree of fidelity.

To determine the association between FOXA2 or VCAN and the clinical outcomes, samples were grouped into FOXA2 or VCAN "low" and "high" expression groups based on whether the expression levels were below or above, respectively, the mean value. These groups were then divided into subgroups based on the sample SDs from the mean (SD 1.0, SD 1.25, SD 1.5) where SD 0.0 represents all samples in the low or high group. In this way, subgroups represent increasing extremes of mRNA expression values. The following criteria were used to define the groups (Eq. A):

$$If\ x_i < \bar{x} - (s * m) \rightarrow Low\ group$$
$$If\ x_i > \bar{x} + (s * m) \rightarrow High\ group \qquad \textbf{(A)}$$

Where x_i represents each sample's FOXA2 or VCAN mRNA expression value, $\bar{x}$ the mean, s the sample standard deviation, and m the number of SDs from the mean; SD 1.0 is represented by $m = 1.0$. FOXA2 or VCAN mRNA expression groups and subgroups were calculated independently from each other.

To examine the effects of anticorrelated FOXA2 and VCAN mRNA expression samples, they were first assigned a Δ coefficient to represent the relative difference between FOXA2 and VCAN mRNA expression. mRNA expression values were converted to SDs from the mean (SDM) and then VCAN SDM was subtracted from FOXA2 SDM for each sample to calculate Δ (Eq. B):

$$\Delta = \frac{x_i^{FOXA2} - \bar{x}^{FOXA2}}{s^{FOXA2}} - \frac{x_i^{VCAN} - \bar{x}^{VCAN}}{s^{VCAN}} \qquad \textbf{(B)}$$
$$\Delta < 0 \Rightarrow \downarrow FOXA2, \uparrow VCAN$$
$$\Delta > 0 \Rightarrow \uparrow FOXA2, \downarrow VCAN$$

The definition of variables is the same as those described for Eq.A.

Samples were shown or hidden based on the criteria above using conditional 'IF' statements in Excel. This allowed quick manipulation of groups and subgroups by changing m (Eq. 1) or ranges of Δ. Data retrieval was then based on samples passing the desired criteria and containing queried data (e.g. methylation) and then formatted to be copied to GraphPad. Binary data such as 'Recurred/Progressed' and 'Disease-free' were converted to 1 and 0, respectively. Likewise, clinical attributes for Survival and Invasion indicators were also converted to binary; 'DECEASED' and 'Yes' = 1, 'LIVING' and 'NO' = 0, respectively.

Statistical analysis

All *in vitro* experiments were done at least three times with at least triplicates in each group. The results are expressed as mean ± SEM in bar graphs and line graphs. Statistical analyses were performed using SigmaStat and GraphPad prism 6. Multiple groups were analyzed by one-way or two-way ANOVA, followed by Tukey *post hoc* test. Student *t*-test was used for comparison between two groups. Clinical samples were presented as box–whisker plots and analyzed by Kruskal–Wallis test, followed by Wilcoxon rank test for multiple group comparison or Wilcoxon rank test when only two groups were compared. For TCGA clinical samples, binary data were analyzed using one-tailed Student *t-test*. Kaplan–Meier survival and disease-free graphs were analyzed using the Mantel–Cox test; $P < 0.05$ was considered statistically significant.

RESULTS

miR-590-3p is upregulated in ovarian cancer and promotes cell growth, migration, and invasion

Using EOC tissue samples collected at Mansoura Oncology Center (Supplementary Table S2.1A) and Ottawa Ovarian Cancer Tissue Bank (Supplementary Table S2.1B), we found that miR-590-3p levels in grade II/III ovarian tumors were significantly higher than in grade I tumors or normal ovarian tissues (Fig. 2.1A). Similarly, miR-590-3p levels were also upregulated in high-grade serous tumors when compared with tumors of low malignancy potential (Fig. 2.1B). In another histologic subtype of EOC, endometrioid ovarian cancer, high-grade tumors also had higher miR-590-3p levels than the low-grade ones (Supplementary Fig. S2.1A). Circulating miR-590-3p levels were also significantly higher in patients with EOC than in subjects with benign gynecologic disorders (Fig. 2.1C). To determine the effect of miR-590-3p on cell proliferation, migration, and invasion, EOC cell lines ES-2, SKOV3.ip1, and OVCAR3 were transiently transfected with miR-590-3p mimic, anti–miR-590-3p, or NCs. miR-590-3p significantly increased cell numbers (Fig. 2.1D; Supplementary Fig. S2.1B), migration, and invasion (Fig. 2.1E; Supplementary Fig. S2.1C–S2.1E). On the other hand, inhibition of miR-590-3p by anti–miR-590-3p resulted in a significant decrease in cell proliferation (Fig. 2.1D) and migration (Supplementary Fig. S2.1D).

Stable overexpression of mir-590 enhances tumor development and metastasis

To further investigate the function of miR-590-3p in EOC development, SKOV3.ip1 cells expressing luciferase, ES-2, and HEY cells stably transfected with mir-590 or its corresponding EV were generated (Supplementary Fig. S2.2A). Real-time PCR revealed that both miR-590-3p and miR-590-5p were significantly higher in cells transfected with mir-590, when compared with the EV (Supplementary Fig. S2.2B). Overexpression of mir-590

significantly enhanced cell proliferation (Fig. 2.1F), invasion (Fig. 2.1G), and colony formation (Fig. 2.1H; Supplementary Fig. S2.2C). To confirm that the observed effects of mir-590 were due to miR-590-3p and/or miR-590-5p overexpression, we transfected EV and mir-590 cells with anti–miR-590-3p, anti–mir-590-5p, or their nontargeting control. Both anti–miR-590-3p and anti–miR-590-5p reduced invasion in EV and mir-590 cells in ES-2 cells. However, in SKOV3.ip1 cells, only anti–miR-590-3p had a significant effect of cell invasion in the EV control group (Fig. 2.1I).

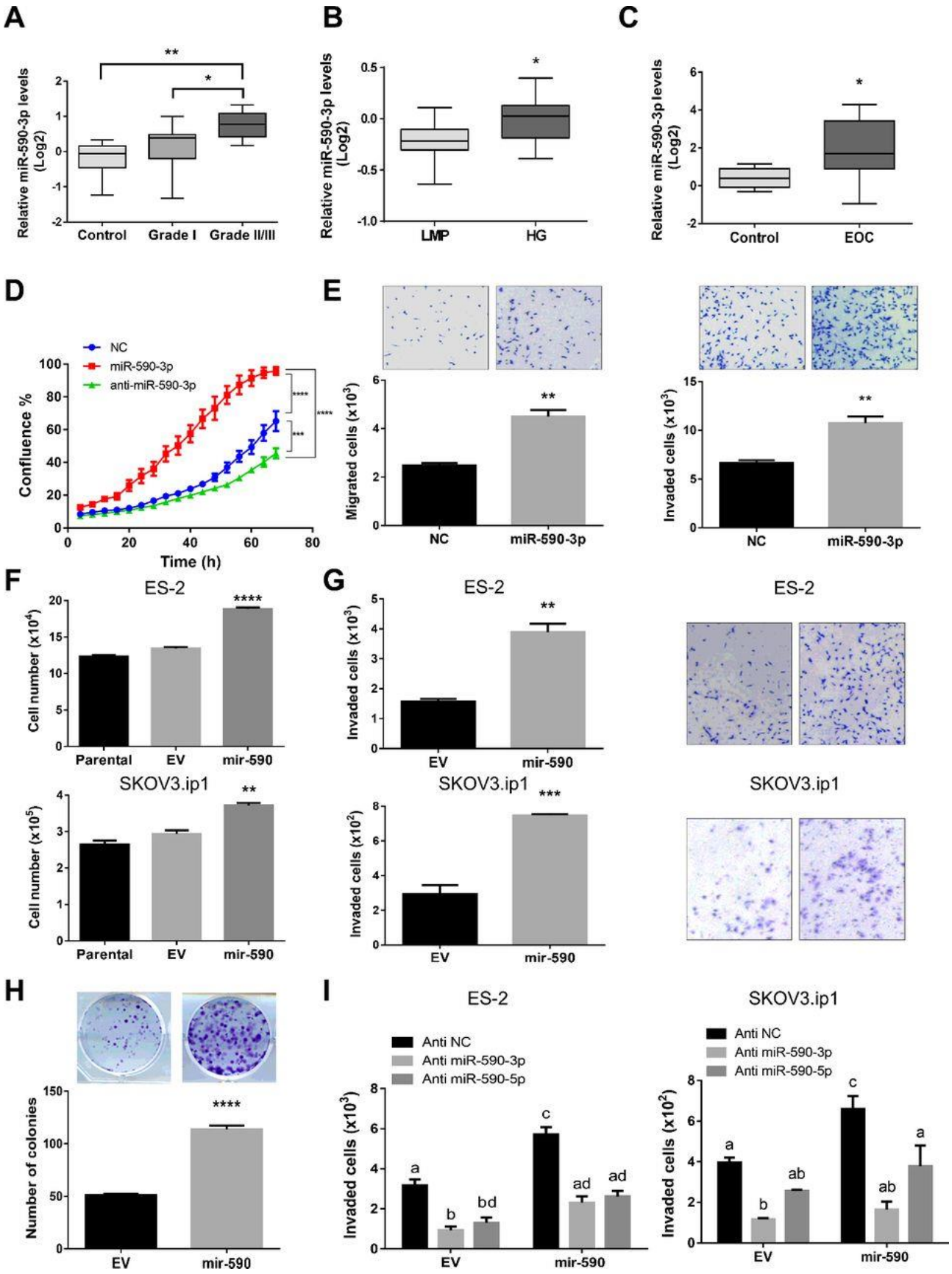
A
Relative miR-590-3p levels (Log2)
Control
Grade I
Grade II/III
B
Relative miR-590-3p levels (Log2)
LMP
HG
C
Relative miR-590-3p levels (Log2)
Control
EOC
D
NC
miR-590-3p
anti-miR-590-3p
Confluence %
Time (h)
E
Migrated cells (x10^3)
NC
miR-590-3p
Invaded cells (x10^3)
NC
miR-590-3p
F
ES-2
Cell number (x10^4)
Parental
EV
mir-590
SKOV3.ip1
Cell number (x10^5)
Parental
EV
mir-590
G
ES-2
Invaded cells (x10^3)
EV
mir-590
SKOV3.ip1
Invaded cells (x10^2)
EV
mir-590
H
Number of colonies
EV
mir-590
I
ES-2
Anti NC
Anti miR-590-3p
Anti miR-590-5p
Invaded cells (x10^3)
EV
mir-590
SKOV3.ip1
Anti NC
Anti miR-590-3p
Anti miR-590-5p
Invaded cells (x10^2)
EV
mir-590

Figure 2.1. miR-590-3p is upregulated in EOC and exerts tumor-promoting effects *in vitro*. A, miR-590-3p levels were elevated in higher grade EOC tumors compared with normal ovarian tissue or low-grade tumors. RNA was extracted from normal ovary (n = 6), grade 1 (n = 11), or grade 2/3 EOC samples (n = 9), and miR-590-3p level was determined by real-time PCR. **B,** miR-590-3p levels were higher in high-grade serous ovarian tumors (HG; n = 14) than in tumors with low malignancy potential (LMP; n = 16). **C,** Plasma miR-590-3p levels were significantly higher in patients with EOC (n = 13) than in subjects with benign gynecologic disorders (n = 6). Data in **A–C** are converted to $\log_2$ and plotted in box–whisker plots. **D,** miR-590-3p enhanced cell proliferation. SKOV3.ip1 cells were transiently transfected with NCs, miR-590-3p mimic, or anti–miR-590-3p. Cell confluency was monitored by IncuCyte for 68 hours (n = 7). **E,** miR-590-3p enhanced cell migration and invasion. ES-2 cells were transiently transfected with miR-590-3p or its NC, and transwell migration and invasion were determined at 24 hours after transfection (n = 3). **F,** Stable overexpression of mir-590 increased cell proliferation in both ES-2 and SKOV3.ip1 cells when compared with parental or control cells transfected with EV (n = 3). **G,** Cells overexpressing mir-590 invaded faster than cells expressing the EV (n = 3). **H,** In a clonogenic assay, cells overexpressing mir-590 formed more and larger colonies than the ones expressing the EV (n = 3). **I,** Effects of anti–miR-590-3p and anti–miR-590-5p on mir-590–induced cell invasion. ES-2 and SKOV3.ip1 cells stably transfected with EV or mir-590 were transiently transfected with anti–miR590-3p, anti–miR-590-5p, or their negative control (anti-NC). Transwell assays were performed (n = 3). Data represent median flanked by 25th and 75th percentiles (**A–C**) and mean ± SEM (**D–I**). *, P < 0.05; **, P < 0.01; ***, P < 0.001; ****, P < 0.0001. Different letters above bars denote statistical significance.

To determine whether mir-590 affects tumor formation *in vivo*, ES-2 cells stably overexpressing mir-590 or its control vector were injected subcutaneously into female CD-1 nude mice and tumor size was measured over 21 days. The mir-590 cells formed significantly larger tumors at multiple time points measured (Fig. 2.2A). To examine the effect of mir-590 on metastasis, control and mir-590–expressing SKOV3.ip1 cells were injected intraperitoneally into the nude mice. It was observed that mice injected with mir-590 cells had a higher number of nodules throughout the peritoneal cavity (Fig. 2.2B) and formed larger tumors when compared with the control (Fig. 2.2C). Live animal imaging revealed that mice inoculated with mir-590 cells had stronger bioluminescent signals than mice injected with control cells (Fig. 2.2D).

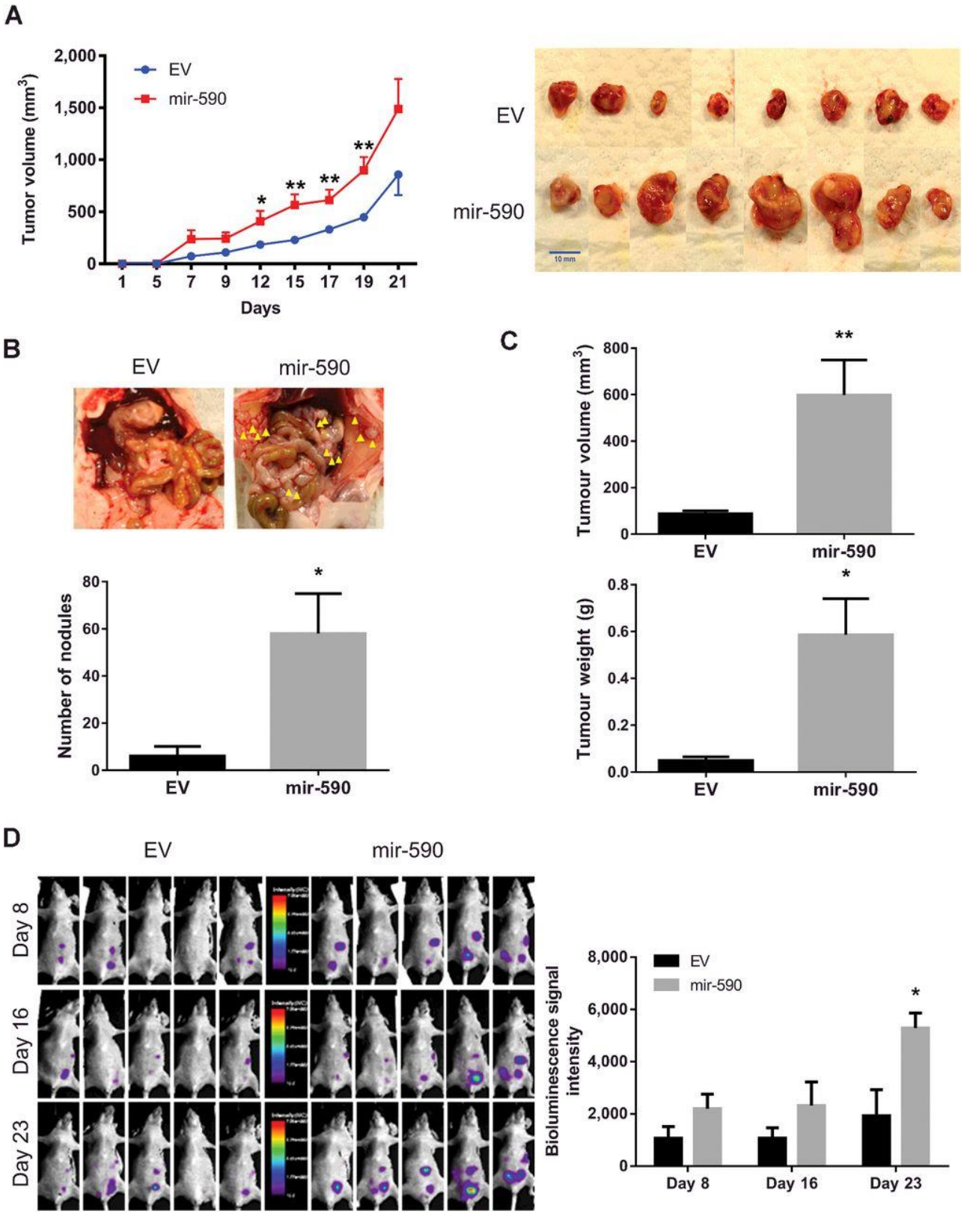
A
Tumor volume (mm3)
2,000
1,500
1,000
500
0
EV
mir-590
1 5 7 9 12 15 17 19 21
Days
*
**
**
**
EV
mir-590
10 mm
B
EV
mir-590
Number of nodules
80
60
40
20
0
*
EV
mir-590
C
Tumour volume (mm3)
800
600
400
200
0
**
EV
mir-590
Tumour weight (g)
0.8
0.6
0.4
0.2
0.0
*
EV
mir-590
D
EV
mir-590
Day 8
Day 16
Day 23
Bioluminescence signal intensity
8,000
6,000
4,000
2,000
0
EV
mir-590
*
Day 8
Day 16
Day 23

Figure 2.2. mir-590 promotes tumor formation and metastasis *in vivo*. A, mir-590 accelerates tumor growth. ES-2 cells stably transfected with EV or mir-590 were injected subcutaneously into female CD-1 nude mice, and tumor volumes were measured (n = 8). **B** and **C**, mir-590 promotes tumor metastasis. SKOV3.ip1 cells stably transfected with luciferase and EV or miR-590 were injected intraperitoneally into CD-1 nude mice and the mice were examined at 70 days after tumor cell inoculation. The number of nodules (B) and total tumor volumes and weight (C) were significantly higher in mice injected with mir-590 cells when compared with the control. **D,** Bioluminescent imaging of mice inoculated with control or mir-590 cells. Mice were injected intraperitoneally with SKOV3.ip1 cells expressing the vector or mir-590 (n = 5). Bioluminescence images were taken at day 8 to day 23 after injection. Data, mean ± SEM. *, $P < 0.05$; **, $P < 0.01$.

miR-590-3p regulates FOXA2 and VCAN

To determine the molecular mechanisms by which mir-590 exerts tumor-promoting effects on EOC, cDNA microarray was performed. Genes that were either up- or downregulated by mir-590 by 2-fold or more were organized into a heatmap (Fig. 2.3A). Genes that were downregulated were analyzed for miR-590-3p/5p–binding sites using tools at microRNA.org. It was found that most of these genes have predicted miR-590-3p–binding sites and a few have predicted miR-590-5p sites (Supplementary Table S2.3A). Interrogation of the TCGA dataset revealed that most of the top mir-590–downregulated genes were underexpressed in ovarian cancer samples when compared with normal ovary (Supplementary Table S2.3A). Among them, FOXA2 is the most strongly downregulated gene that has a miR-590-3p–binding site and is also downregulated in the TCGA dataset (Supplementary Table S2.3A). On the other hand, among all upregulated genes by mir-590, VCAN is the most strongly upregulated in the TCGA database (Supplementary Table S2.3B) and known to play a role in EOC development [29]. Therefore, we further investigated the expression, regulation, and function of FOXA2 and VCAN.

Using the tumor samples collected from the Ovarian Cancer Tissue Bank at Ottawa Research Institute, we found that FOXA2 mRNA levels were significantly lower, whereas VCAN mRNA levels showed the opposite trend, in the high-grade tumors than in tumors of low malignancy potential (Fig. 2.3B). Real-time PCR and Western blotting confirmed that FOXA2 was downregulated in ES-2 and SKOV3.ip1 cells overexpressing mir-590 (Fig. 2.3C). FOXA2 mRNA levels were also significantly downregulated in HEY mir-590 stable cells (Supplementary Fig. S2.3A). In tumors collected from mice grafted with ES-2 cells, FOXA2 mRNA and protein levels were also downregulated (Supplementary Fig. S2.3B). Conversely, VCAN protein and mRNA levels were higher in mir-590 cells than in the vector controls (Fig. 2.3D).

miR-590-3p targets FOXA2

To confirm that miR-590-3p directly targets FOXA2, luciferase reporter assays were performed. Transient transfection of miR-590-3p mimic or stable transfection of mir-590 significantly reduced the luciferase activity (Fig. 2.3E). Transient transfection of miR-590-3p also reduced FOXA2 mRNA and protein levels, whereas anti–miR-590-3p enhanced FOXA2 protein levels in ES-2 cells (Fig. 2.3F). Similarly, transfection of the miR-590-3p mimic in HEY, SKOV3.ip1, and OVCAR3 cells decreased FOXA2 protein levels (Supplementary Fig. S2.3C).

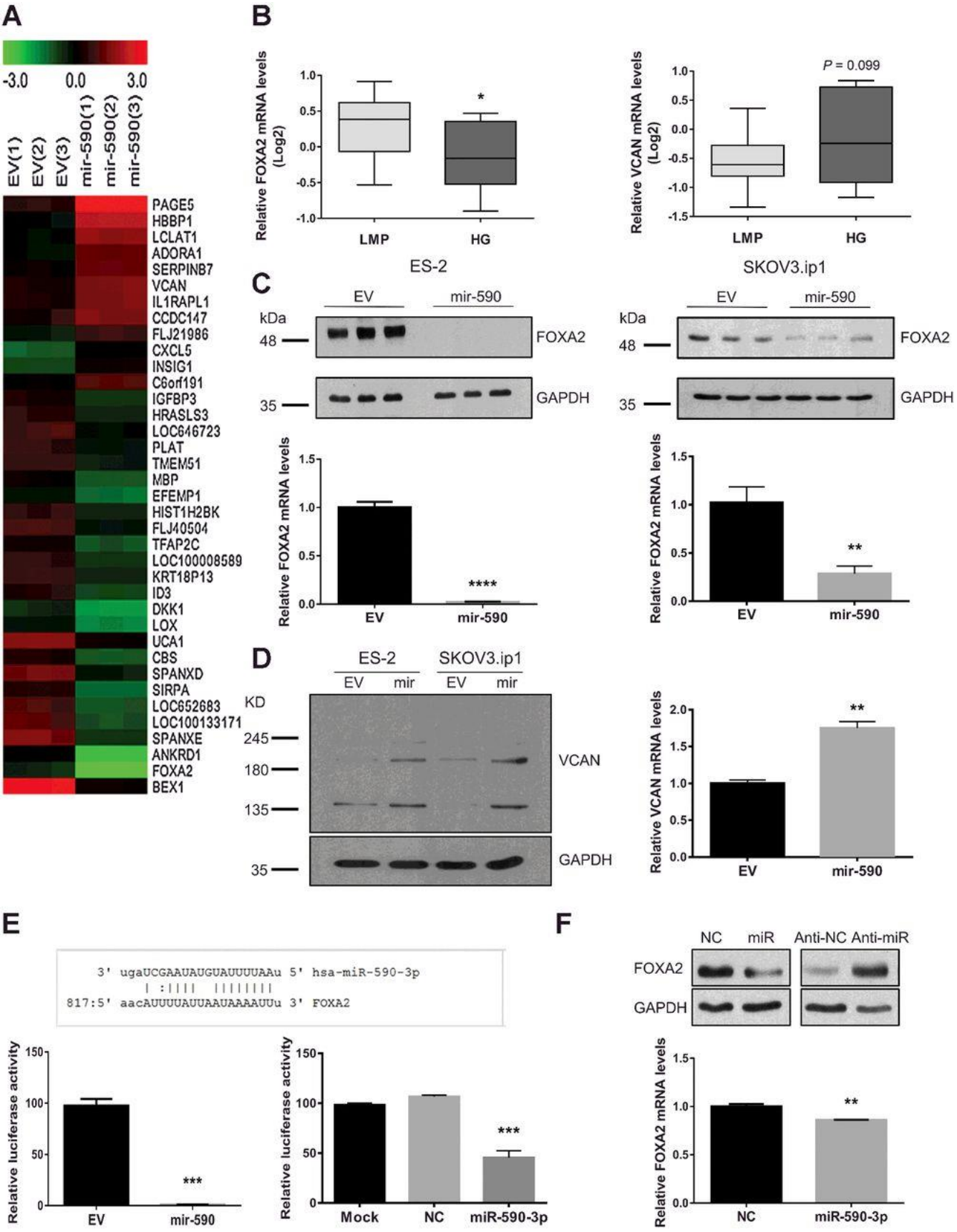
A
-3.0
0.0
3.0
EV(1)
EV(2)
EV(3)
mir-590(1)
mir-590(2)
mir-590(3)
PAGE5
HBBP1
LCLAT1
ADORA1
SERPINB7
VCAN
IL1RAPL1
CCDC147
FLJ21986
CXCL5
INSIG1
C6orf191
IGFBP3
HRASLS3
LOC646723
PLAT
TMEM51
MBP
EFEMP1
HIST1H2BK
FLJ40504
TFAP2C
LOC100008589
KRT18P13
ID3
DKK1
LOX
UCA1
CBS
SPANXD
SIRPA
LOC652683
LOC100133171
SPANXE
ANKRD1
FOXA2
BEX1
B
Relative FOXA2 mRNA levels (Log2)
LMP
HG
Relative VCAN mRNA levels (Log2)
P = 0.099
ES-2
SKOV3.ip1
C
EV
mir-590
kDa
48
35
FOXA2
GAPDH
Relative FOXA2 mRNA levels
D
ES-2
SKOV3.ip1
KD
245
180
135
VCAN
Relative VCAN mRNA levels
E
3' ugaUCGAAUAUGUAUUUUAAu 5' hsa-miR-590-3p
817:5' aacAUUUUAUUAAUAAAAUUu 3' FOXA2
Relative luciferase activity
Mock
NC
miR-590-3p
F
NC
miR
Anti-NC
Anti-miR
FOXA2
GAPDH
Relative FOXA2 mRNA levels

Figure 2.3. Regulation of FOXA2 and VCAN by mir-590. A, Heatmap of genes regulated by mir-590 revealed by cDNA microarray. Total RNA extracted from ES-2 cells stably transfected with mir-590 or EV control were subjected to a cDNA microarray analysis. Genes that were ≥2-fold down- or upregulated by mir-590 were included in the heatmap. **B,** FOXA2 mRNA levels (left) were significantly lower, whereas VCAN mRNA levels (right) showed an opposite trend in high-grade serous ovarian tumors (HG; $n = 13$) than in tumors with low malignancy potential (LMP; $n = 15$). **C,** Confirmation of FOXA2 downregulation by mir-590 using real-time PCR and Western blotting in both ES-2 and SKOV3.ip1 stable cells. **D,** Upregulation of VCAN by mir-590. Overexpression of mir-590 resulted in an increase in VCAN protein levels in both ES-2 and SKOV3.ip1 cells (left). Real-time PCR (right) revealed higher VCAN mRNA levels in mir-590–expressing in ES-2 cells ($n = 3$). **E,** FOXA2 is a target of miR-590-3p. A predicted miR-590-3p–binding site was found on FOXA2 3′ UTR. A luciferase reporter construct containing FOXA2 3′ UTR was generated. In ES-2 cells stably transfected with mir-590 (left), or transiently transfected with miR-590-3p (right), the luciferase activity was significantly decreased ($n = 3$). **F,** Transient transfection of miR-590-3p decreased FOXA2 mRNA levels ($n = 3$) and the protein levels, whereas transfection of anti–miR-590-3p increased FOXA2 protein levels. Statistical analyses were performed using Wilcoxon rank test (**B**), ANOVA/Tukey test (**E**, right), or *t-test* (all others). *, $P < 0.05$; **, $P < 0.01$; ***, $P < 0.001$; ****, $P < 0.0001$ versus their respective controls

FOXA2 exerts antitumor effects

To determine the role of FOXA2 in EOC development, we validated two siRNAs that decreased FOXA2 mRNA and protein levels (Fig. 2.4A). Transfection of these FOXA2 siRNAs in EOC cells accelerated proliferation (Fig. 2.4B) and invasion (Fig. 2.4C). To further confirm the role of FOXA2 in EOC cells, we used CRISPR/Cas9 gene editing tools to knockout *FOXA2* in both ES-2 and SKOV3.ip1 cells. Two sgRNAs were used to generate two populations of heterogeneous *FOXA2* knockout cells, designated as FOXAΔ1 and FOXAΔ2, respectively. *FOXA2* knockout diminished the expression of FOXA2 (Fig. 2.4D) and resulted in increased cell proliferation (Fig. 2.4E), migration (Fig. 2.4F), and invasion (Fig. 2.4G). Conversely, transient transfection of FOXA2 into several cell lines resulted in an inhibition of cell invasion (Fig. 2.4H; Supplementary Fig. S2.3D).

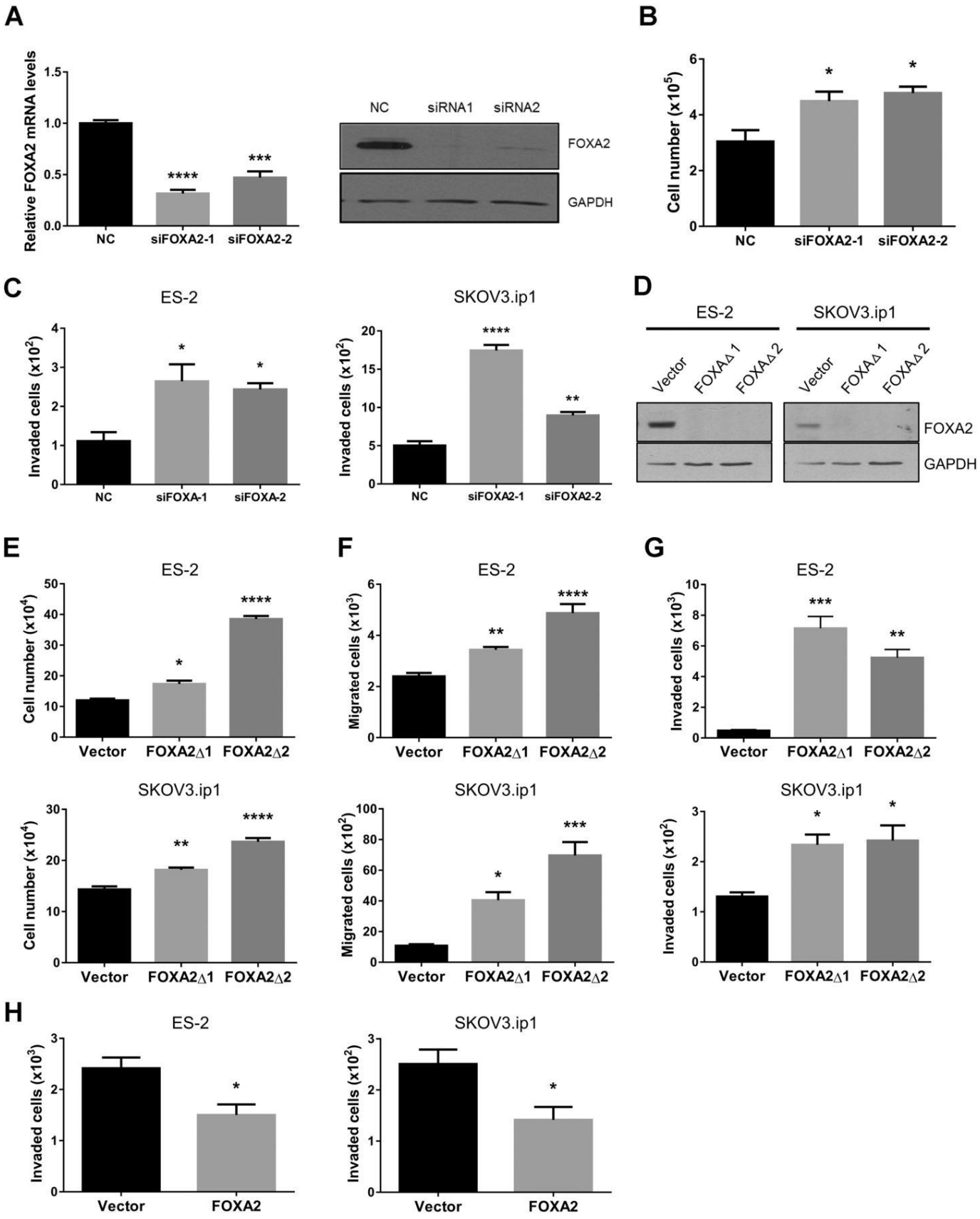
A
Relative FOXA2 mRNA levels
1.5
1.0
0.5
0.0
****
***
NC
siFOXA2-1
siFOXA2-2
NC
siRNA1
siRNA2
FOXA2
GAPDH
B
Cell number (x10^5)
6
4
2
0
*
*
NC
siFOXA2-1
siFOXA2-2
C
ES-2
Invaded cells (x10^2)
4
3
2
1
0
*
*
NC
siFOXA-1
siFOXA-2
SKOV3.ip1
Invaded cells (x10^2)
20
15
10
5
0
****
**
NC
siFOXA2-1
siFOXA2-2
D
ES-2
SKOV3.ip1
Vector
FOXAΔ1
FOXAΔ2
Vector
FOXAΔ1
FOXAΔ2
FOXA2
GAPDH
E
ES-2
Cell number (x10^4)
50
40
30
20
10
0
*
****
Vector
FOXA2Δ1
FOXA2Δ2
SKOV3.ip1
Cell number (x10^4)
30
20
10
0
**
****
Vector
FOXA2Δ1
FOXA2Δ2
F
ES-2
Migrated cells (x10^3)
6
4
2
0
**
****
Vector
FOXA2Δ1
FOXA2Δ2
SKOV3.ip1
Migrated cells (x10^2)
100
80
60
40
20
0
*
***
Vector
FOXA2Δ1
FOXA2Δ2
G
ES-2
Invaded cells (x10^3)
10
8
6
4
2
0
***
**
Vector
FOXA2Δ1
FOXA2Δ2
SKOV3.ip1
Invaded cells (x10^2)
3
2
1
0
*
*
Vector
FOXA2Δ1
FOXA2Δ2
H
ES-2
Invaded cells (x10^3)
3
2
1
0
*
Vector
FOXA2
SKOV3.ip1
Invaded cells (x10^2)
3
2
1
0
*
Vector
FOXA2

Figure 2.4. FOXA2 exerts antitumor effects in EOC cells. A, Validation of two different siRNAs targeting FOXA2. In ES-2 cells transfected with FOXA2 siRNAs, FOXA2 mRNA and protein levels were reduced, when compared with cells transfected with a nontargeting siRNA (NC). Total RNA and proteins were extracted at 48 hours after transfection. **B,** Knockdown of FOXA2 increased ES-2 cell proliferation. Cell numbers were measured 48 hours post transfection. **C,** Knockdown of FOXA2 increased cell invasion in ES-2 and SKOV3.ip1 cells. Cells were transfected with NC or one of the FOXA2 siRNAs, and 24 hours post transfection, cells were resuspended and an equal number of cells were then placed on the top chamber of the transwell inserts. Invaded cells were counted at 18 hours after plating. **D,** Generation of *FOXA2* knockout cells using CRISPR/Cas9. Two gRNAs were used and both eliminated FOXA2 protein in ES-2 and SKOV3.ip1 cells, as confirmed by Western blotting. **E–G,** Knockout of *FOXA2* increased cell proliferation (**E**), migration (**F**), and invasion (**G**). **H,** Transient transfection of FOXA2 plasmid into ES-2 and SKOV3.ip1 cells resulted in a decrease in cell invasion. Data, mean ± SEM ($n = 3$). *, $P < 0.05$; **, $P < 0.01$; ***, $P < 0.001$; ****, $P < 0.0001$ versus controls.

FOXA2 inhibits VCAN expression

Examination of a FOXA2 ChIP-seq dataset produced from mice revealed that *VCAN* was one of the genes enriched in FOXA2 antibody precipitated samples [30]. Analysis of the human *VCAN* gene identified multiple potential FOXA2-binding sites on the promoter and gene body; therefore, we tested the possibility that FOXA2 regulates VCAN expression. In cells transiently transfected with siRNAs targeting FOXA2, there was an increase in VCAN mRNA levels (Fig. 2.5A). In contrast, overexpression of FOXA2 reduced VCAN mRNA (Fig. 2.5B) and protein (Supplementary Fig. S2.3D) levels. Furthermore, VCAN protein levels were increased in *FOXA2* knockout cells and the reintroduction of FOXA2 strongly downregulated VCAN levels, as revealed by Western blotting (Fig. 2.5C). Finally, ChIP-qPCR assays were performed in ES-2 and SKOV3.ip1 cells using three sets of primers designed to target the *VCAN* promoter site, a potential regulatory site, and a distal negative control region with no predicted FOXA2 binding site (NC; Fig. 2.5D, top). In FOXA2 antibody precipitated samples, enrichment of VCAN DNA was observed in the regions where FOXA2-binding sites were predicted when compared with the IgG group, while there was no difference between the IgG and FOXA2 antibody groups in the region that had no FOXA2-binding sites (Fig. 2.5D, bottom).

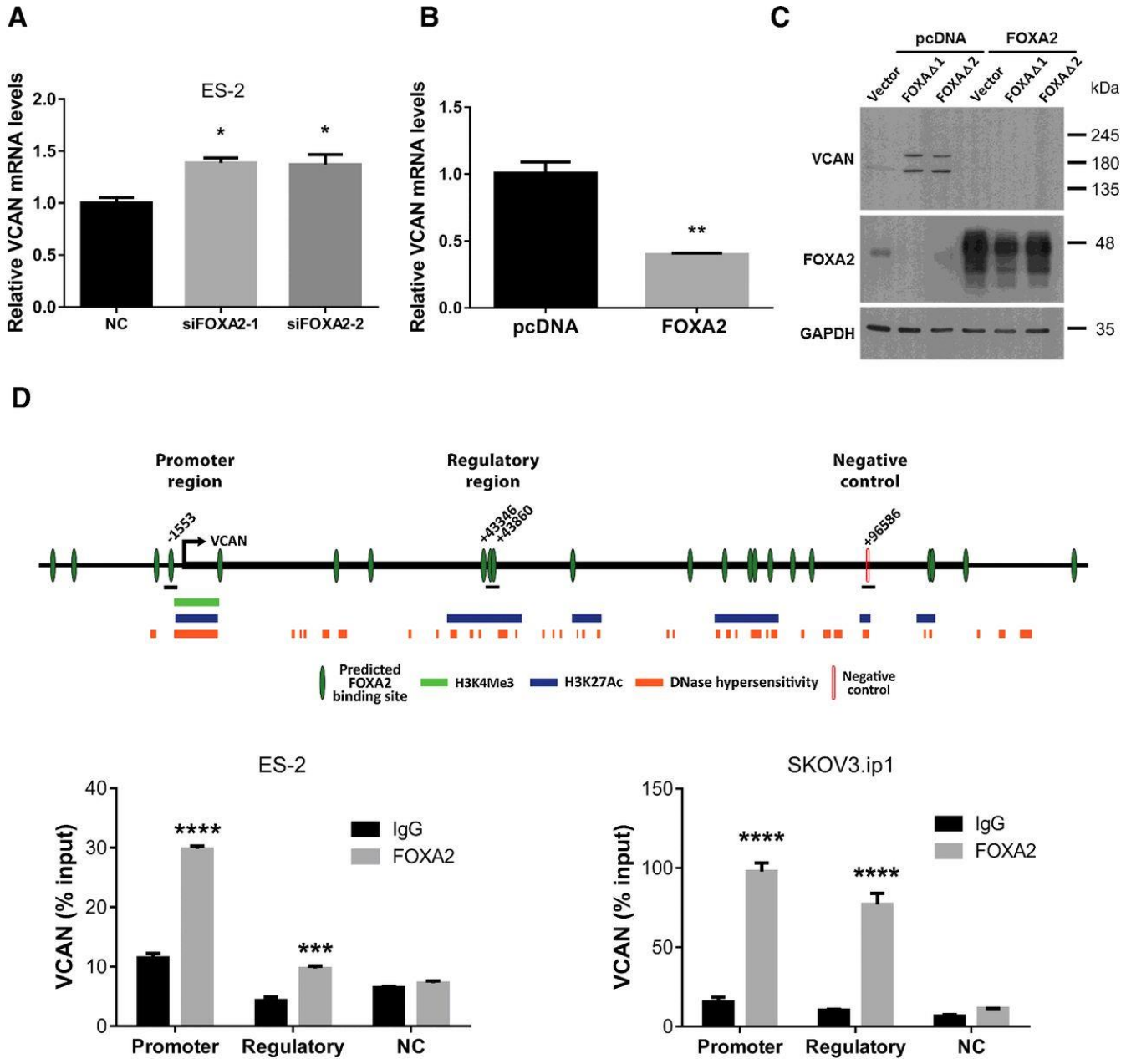
A
ES-2
Relative VCAN mRNA levels
2.0
1.5
1.0
0.5
0.0
*
*
NC
siFOXA2-1
siFOXA2-2
B
Relative VCAN mRNA levels
1.5
1.0
0.5
0.0
**
pcDNA
FOXA2
C
pcDNA
FOXA2
Vector
FOXAΔ1
FOXAΔ2
Vector
FOXAΔ1
FOXAΔ2
kDa
VCAN
245
180
135
FOXA2
48
GAPDH
35
D
Promoter region
Regulatory region
Negative control
-1553
VCAN
+43346
+43860
+96586
Predicted FOXA2 binding site
H3K4Me3
H3K27Ac
DNase hypersensitivity
Negative control
ES-2
VCAN (% input)
40
30
20
10
0
****
***
IgG
FOXA2
Promoter
Regulatory
NC
SKOV3.ip1
VCAN (% input)
150
100
50
0
****
****
IgG
FOXA2
Promoter
Regulatory
NC

Figure 2.5. FOXA2 regulates VCAN expression. A, ES-2 cells transfected with FOXA2 siRNAs increased the mRNA level of VCAN. **B,** In SKOV3.ip1 cells, transient transfection of FOXA2 decreased the mRNA level of VCAN. **C,** Knockout of *FOXA2* in ES-2 cells increased VCAN protein levels, but this effect was reversed by overexpression of FOXA2. **D,** FOXA2 binds to *VCAN* gene. Top, consensus FOXA2-binding sites were predicted in the *VCAN* promoter and within the gene body. Most of these predicted sites overlap DNA regions with histone modifications associated with regulatory potential and DNase hypersensitivity regions. Three pairs of primers were designed. The first pair targets the FOXA2-binding site in the promoter region (promoter; −1553 bp), the second pair spans two intragenic binding sites in a region with regulatory features (regulatory; +43346, +43860), and a distal region with no predicted FOXA2-binding site, which serves as a negative control (NC; +96586). Bottom, ChIP-qPCR was performed using FOXA2 antibody or IgG in both ES-2 and SKOV3.1p1 cells. VCAN DNA was enriched in the promoter, and to a lesser extent, the regulatory region (in ES-2), but not in the negative control. Data, mean ± SEM (**A**, **B**, and **D**; $n = 3$). *, $P < 0.05$; **, $P < 0.01$; ***, $P < 0.001$; ****, $P < 0.0001$ versus controls as analyzed by ANOVA/Tukey test (**A**) or *t-test* (**B** and **D**).

FOXA2 and VCAN are dysregulated in EOC

To further investigate the relationship between FOXA2 and VCAN and their significance in EOC development, we interrogated an ovarian cancer TCGA database. Initial sample-paired analysis of FOXA2 and VCAN mRNA levels displayed a slight negative correlation (Pearson: −0.1789, Spearman: −0.2249; Fig. 2.6A, left). To more closely evaluate the correlation between FOXA2 and VCAN mRNA levels and their possible effects on various clinical attributes, samples were divided into groups based on the deviation of their mRNA levels from the mean (Supplementary Fig. S2.4A and S2.4B). Groups were initially created in increments of 0.25 SDs. Because of the small sample sizes for groups with greater than 1.5 SD from the mean, they were excluded from the analysis. FOXA2 and VCAN mRNA levels were negatively correlated in most groups (Supplementary Fig. S2.4C). We adapted the minimal signal method from Adorno and colleagues [31] to produce a delta (Δ) coefficient for each sample such that a $\Delta<0$ represents samples with relatively low FOXA2 and high VCAN mRNA levels and oppositely for $\Delta>0$ (Fig. 2.6A, right; Supplementary Fig. S2.4D). Methylation of both FOXA2 and VCAN promoters was also examined. FOXA2 mRNA levels were negatively correlated with promoter methylation levels (Pearson: −0.3672, Spearman: −0.4232, $P < 0.0001$). Importantly, FOXA2 promoter methylation was positively correlated with VCAN mRNA levels (Pearson: 0.1750, Spearman: 0.3934, $P < 0.0001$; Fig. 2.6B). These samples were then divided into low or high groups based on their SD from their mean values (Supplementary Fig. S2.5A and S2.5B), and using delta groups with combined FOXA2 and VCAN expression profiles (Supplementary Fig. S2.5C). *FOXA2* promoter methylation was found to be increasingly polarized as both FOXA2 and VCAN mRNA levels moved further from the mean (Supplementary Fig. S2.5A and S2.5C, left). In contrast, VCAN promoter methylation was not correlated with either FOXA2 or VCAN mRNA levels (Supplementary Fig. S2.5B and S2.5C), except for the SD 1.5 high FOXA2 group (Supplementary Fig. S2.5B).

Next, we investigated the survival rates and disease-free statuses using the SD groups. We observed a trend that high FOXA2 (Supplementary Fig. S2.6A) or low VCAN (Supplementary Fig. S2.6B) is associated with longer survival. To determine whether the degree of negative correlation between FOXA2 and VCAN is associated with patient survival, we examined the delta coefficient groups. In the $\Delta > 0$ group that has high FOXA2 and low VCAN mRNA levels, both survival rates and disease-free statuses were increased with a median survival increase from 1,170 to 1,539 days ($P = 0.0036$) and disease-free period from 455 to 624 days ($P = 0.0029$; Fig. 2.6C). Interestingly, when examining the degree of vascular (VI) and lymphovascular (LVI) invasion, there was a significant positive correlation with VCAN and a trend of negative correlation with FOXA2 mRNA levels (Fig. 2.6D and 2.6E).

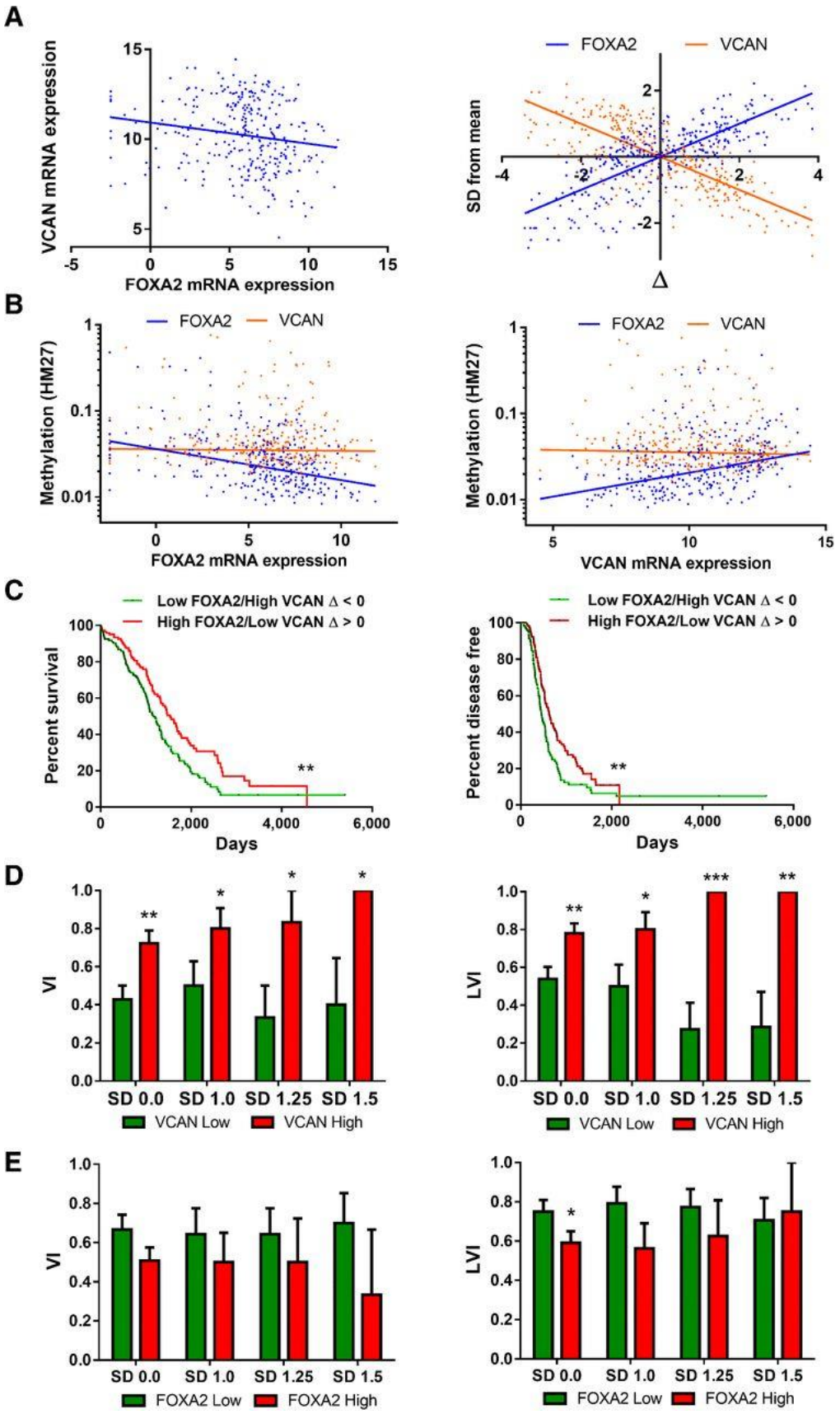
A
VCAN mRNA expression
FOXA2 mRNA expression
FOXA2
VCAN
SD from mean
Δ
B
Methylation (HM27)
FOXA2 mRNA expression
VCAN mRNA expression
C
Low FOXA2/High VCAN Δ < 0
High FOXA2/Low VCAN Δ > 0
Percent survival
Percent disease free
Days
D
VI
LVI
SD 0.0
SD 1.0
SD 1.25
SD 1.5
VCAN Low
VCAN High
E
FOXA2 Low
FOXA2 High

Figure 2.6. Analysis of FOXA2 and VCAN expression patterns in EOC tumors. A, FOXA2 and VCAN mRNA levels are negatively correlated in ovarian cancer samples. Left, sample-paired FOXA2 and VCAN mRNA levels (log_2; RNA-Seq V2 RSEM) in TCGA ovarian serous cystadenocarcinoma dataset were negatively correlated (n = 307). Pearson, −0.1789; P = 0.017. Spearman, −0.2249; P < 0.0001. Right, FOXA2 and VCAN mRNA levels were converted to their distance from the mean in SDs (Z-score). Delta (Δ) values were calculated for each tumor sample using SD from the mean of FOXA2 and VCAN mRNA expressions to group each sample based on the degree of relative anticorrelation in their expression. Delta values less than zero correlate with relatively low FOXA2 and high VCAN mRNA expression, whereas values greater than zero correlate with relatively high FOXA2 and low VCAN mRNA expression. **B**, Left, FOXA2 mRNA expression was negatively correlated with *FOXA2* promoter methylation (Pearson, −0.3672; P < 0.0001; Spearman, −0.4232; P < 0.0001). Right, VCAN mRNA expression was positively correlated with *FOXA2* promoter methylation (Pearson, 0.1750; P = 0.0024; Spearman, 0.3934; P < 0.0001). **C**, Kaplan–Meier graphs of either percent survival (left) or percent disease-free (right) were plotted using delta groups less than or greater than zero. Delta values less than zero correlate with relatively low FOXA2 and high VCAN mRNA expression, whereas values greater than zero correlate with relatively high FOXA2 and low VCAN mRNA expression. Median survival was significantly greater in the $\Delta > 0$ group based on the log-rank (Mantel–Cox) test; P = 0.0036. $\Delta < 0$: 1,169.7 d (n = 159); $\Delta > 0$: 1,539.3 d (n = 147). The median time of disease-free status was significantly longer in the $\Delta > 0$ group based on the log-rank (Mantel–Cox) test; P = 0.0029. $\Delta < 0$: 455.4 d (n = 159); $\Delta > 0$: 624.9 d (n = 147). **D** and **E**, Association between the proportion of subjects that were positive for vascular (VI; left) and lymphovascular (LVI; right) invasion indicators and VCAN or FOXA2 mRNA levels. Data, mean ± SEM. *, P < 0.05; **, P < 0.01; ***, P < 0.001.

The FOXA2–VCAN pathway mediates mir-590 effect

To confirm that the downregulation of FOXA2 and upregulation of VCAN contribute to the tumor-promoting effects of mir-590, rescue experiments were performed. We observed that overexpression of FOXA2 significantly reduced the ability of mir-590 to enhance cell migration and invasion (Fig. 2.7A). In addition, we determined whether silencing of VCAN would abolish the tumor-promoting effects of *FOXA2* knockout. *FOXA2* knockout cells expressed higher VCAN levels and significantly increased cell migration and invasion. However, these effects were significantly reduced when VCAN was knocked down in SKOV3.ip1 (Fig. 2.7B) and ES-2 (Fig. 2.7C) cells. Knockdown of VCAN also reduced the stimulatory effects of mir-590 on cell proliferation and invasion (Fig. 2.7D).

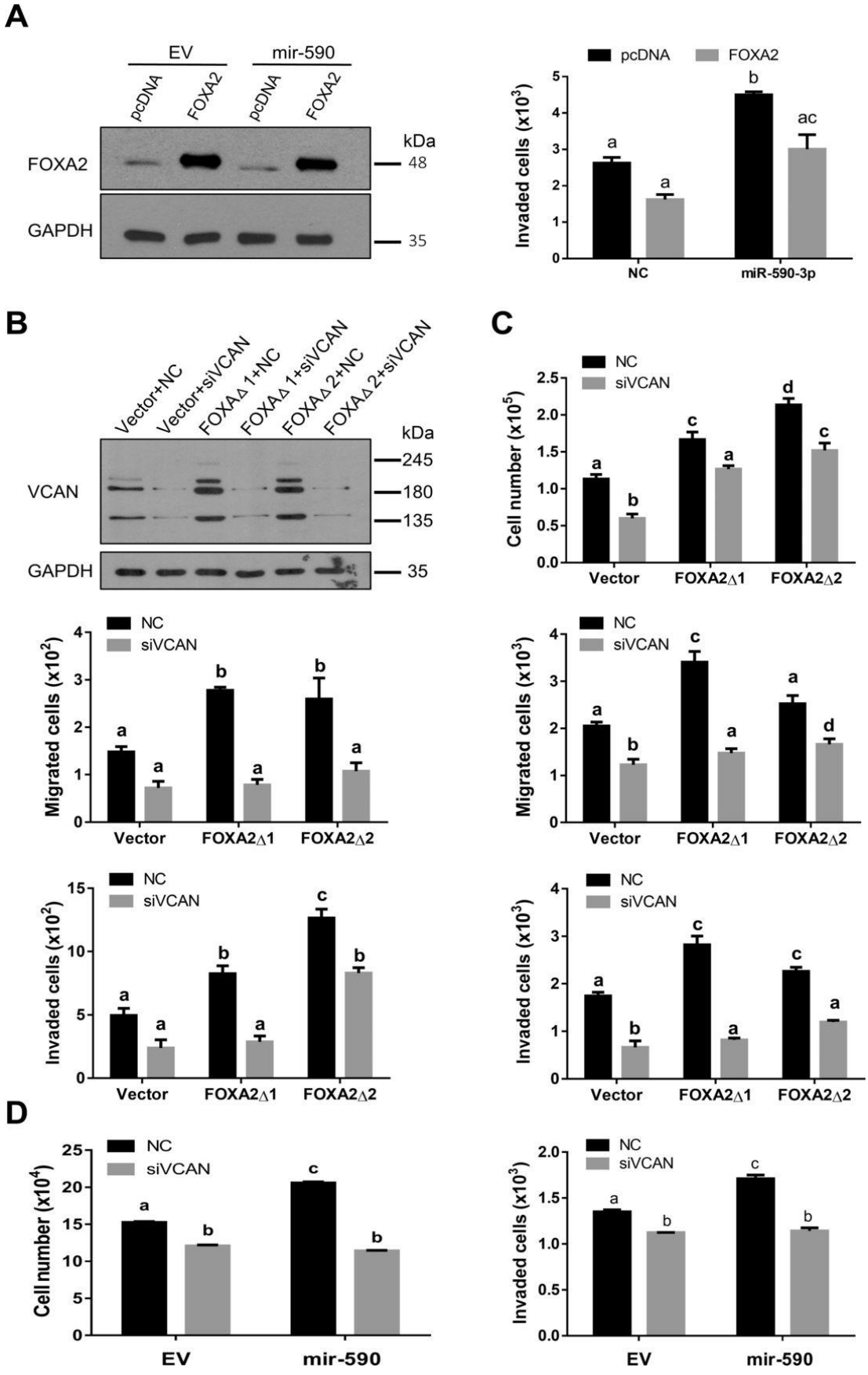
A
EV
mir-590
pcDNA
FOXA2
pcDNA
FOXA2
FOXA2
GAPDH
kDa
48
35
pcDNA
FOXA2
Invaded cells (x10³)
a
a
b
ac
NC
miR-590-3p
B
Vector+NC
Vector+siVCAN
FOXAΔ1+NC
FOXAΔ1+siVCAN
FOXAΔ2+NC
FOXAΔ2+siVCAN
kDa
VCAN
245
180
135
GAPDH
35
C
NC
siVCAN
Cell number (x10⁵)
Vector
FOXA2Δ1
FOXA2Δ2
Migrated cells (x10²)
Migrated cells (x10³)
Invaded cells (x10²)
Invaded cells (x10³)
D
Cell number (x10⁴)
EV
mir-590

Figure 2.7. FOXA2 and VCAN mediate the effects of mir-590 in EOC cells. **A**, Overexpression of FOXA2 in SKOV3.ip1 cells reversed the effect of mir-590. Control (EV) or mir-590 stable cells were transfected with either the control plasmid vector (pcDNA) or FOXA2-expressing plasmid. Overexpression of FOXA2 reduced the effects of mir-590 on invasion. **B**, Silencing of VCAN by siRNA reversed the effects of *FOXA2* knockout. Top, confirmation of VCAN knockdown by siRNA using Western blot analysis. Knockdown of VCAN significantly reduced cell migration (middle) and invasion (bottom) in *FOXA2* knockout SKOV3.ip1 cells. **C**, In ES-2 cells, knockdown of VCAN attenuated the effect of *FOXA2* knockout on cell proliferation (top), migration (middle), and invasion (bottom). **D**, Knockdown of VCAN reduced the effects of mir-590 on cell proliferation (left) and invasion (right). Statistical analyses were performed using ANOVA/Tukey test and groups significantly different from each other are denoted by a different letter.

DISCUSSION

In this study, we provided strong evidence to support a tumor-promoting role of miR-590-3p in ovarian cancer cells. We demonstrated that overexpression of miR-590-3p or its precursor, mir-590, significantly increased cell proliferation, migration, invasion, and colony formation *in vitro*. In addition, mir-590 promoted tumor growth and metastasis *in vivo*. Moreover, miR-590-3p levels were significantly elevated in high-grade EOC tumors when compared with normal ovaries or lower grade tumors. Finally, miR-590-3p plasma levels were higher in patients with EOC than in subjects with benign gynecologic disorders. These findings suggest that higher miR-590-3p is associated with a more aggressive disease.

Although the role of miR-590-3p in EOC has not previously been established, several studies have reported both tumor-promoting and tumor-suppressive effects of miR-590-3p in other types of cancer. For example, miR-590-3p promotes cell proliferation and invasion in T-cell acute lymphoblastic leukemia by inhibiting RB1 [6] and in colorectal cancer by targeting the Hippo pathway [7] and by promoting β-catenin signaling [32]. Similarly, tumor-promoting effects of miR-590-3p were observed in glioblastoma [33]. In contrast, miR-590-3p suppresses hepatocellular carcinoma growth [34] and inhibits proliferation and migration in bladder cancer cells [35]. In this study, we demonstrated that miR-590-3p enhanced colony formation, cell proliferation, migration, and invasion *in vitro*, and stimulated tumor growth and metastasis *in vivo*. These findings strongly support a tumor-promoting role of miR-590-3p in EOC. The differential role of miR-590-3p reported in different types of cancer is likely due to the differential targeting of genes by miR-590-3p and/or differential effects of its target genes. Indeed, we examined several reported target genes responsible for the antitumor effects of miR-590-3p, such as ZEB1 and ZEB2, and did not observe an inhibition by miR-590-3p or mir-590 in EOC cells. On the other hand, we found that DKK1, which was reported to be targeted by miR-590-3p in colon cancer [32], was strongly downregulated in our mir-590 cells. In addition,

the tumor-promoting effects of mir-590 observed in our study could also be attributed to miR-590-5p overexpression. We observed that both anti–miR-590-3p and anti–miR-590-5p attenuated the effect of mir-590, suggesting that miR-590-5p is also involved in EOC development.

In this study, we identified FOXA2 as a direct target of miR-590-3p and provided several lines of evidence to support a tumor-suppressive role of FOXA2 in EOC. First, FOXA2 mRNA levels were significantly downregulated in high-grade tumors when compared with tumors of low malignancy potential, suggesting that FOXA2 expression is associated with a less aggressive phenotype. Second, silencing of FOXA2 expression promoted cell proliferation, migration, and invasion, whereas overexpression of FOXA2 had the opposite effects. Finally, higher FOXA2 appeared to be associated with better patient survival. These findings are consistent with a previous study that identified FOXA2 as one of the 26 genes enriched in differentiated ovarian tumors with better prognosis [36]. The results are also in agreement with studies in lung cancer, which demonstrate that FOXA2 is a strong inhibitor of metastasis with decreased expression levels during cancer progression [12, 13]. Similarly, FOXA2 has been reported to suppress EMT and metastasis in breast cancer [15]. However, FOXA2 expression in triple-negative/basal-like breast carcinoma is positively associated with relapse and promotes cancer development [16]. Interestingly, in a mouse model of liver cancer, Foxa2 and Foxa1 suppress or promote liver cancer development, depending on whether they interact with estrogen receptor α (ERα) or androgen receptor, respectively [17]. This study also revealed that SNPs at FOXA2-binding sites, which impair the binding of both FOXA2 and ERα to their targets, correlate with liver cancer development in women. Thus, it is possible that the dual function of FOXA2 in cancer development is dependent, at least in part, on its interacting partners. It remains to be determined which factor(s) FOXA2 interacts with to exert the tumor-suppressive effects in EOC.

Findings from the current study identified a novel relationship between FOXA2 and VCAN. We demonstrated that knockdown or knockout of *FOXA2* enhanced, whereas overexpression of FOXA2 reduced, VCAN expression. In addition, ChIP-qPCR results showed that FOXA2 bound to the *VCAN* gene. These findings strongly suggest that FOXA2 is a transcriptional repressor of VCAN. This notion is further supported by the expression patterns of FOXA2 and VCAN in EOC tumor samples, which reveal a negative correlation between FOXA2 and VCAN mRNA levels. Importantly, we found that high FOXA2 and low VCAN mRNA levels in the same tumor sample were significantly associated with longer patient survival. Knockdown of VCAN reduced cell proliferation, migration, and invasion, supporting a tumor-promoting role of VCAN. It has been reported that VCAN can be produced from both ovarian cancer cells [37] and cancer-associated fibroblasts [20]. Because the tumor samples in the TCGA database most likely contain both cancer and fibroblastic stromal cells, it remains to be determined whether a negative relationship between FOXA2 and VCAN exists in both cancer and stromal cells.

Several isoforms of VCAN, namely V0, V1, V2, and V3, with molecular weights of approximately 370, 263, 180, and 74 kDa, respectively, are generated by alternative splicing [38]. Although V0 and V1 isoforms promote cancer development in many types of cancers, V2 and V3 isoforms have been reported to have antitumor effects [39]. Studies in EOC tumor samples revealed that V1 is the most abundant isoform [19]. The VCAN antibody that we used in this study detected several bands with molecular weights between 245 and 135 kDa. The intensity of all bands was reduced by the VCAN siRNA, indicating that they are all related to VCAN. Based on the molecule weight, the V3 isoform is not detected in our Western blots. It has been reported that in several EOC cell lines, including SKOV3 and OVCAR3, V2 isoform is not expressed [37]. In addition, V1 isoform can be processed into smaller fragments [40].

Thus, it is possible that miR-590-3p and FOXA2 regulate the expression of V1, and possibly V0.

Although it is widely believed that EOC metastasis occurs mainly within the peritoneal cavity [2], recent studies suggest that ovarian cancer cells can also spread via hematogenous metastasis [3]. In our analysis of VCAN levels in patients with ovarian cancer, we found that high VCAN levels were positively correlated with an increase in vascular and lymphovascular invasion indicator in the same samples. These observations, together with the finding that VCAN promotes invasion [20] and metastasis [37] in ovarian cancer, raise the interesting possibility that VCAN may play an important role in promoting hematogenous and lymphatic dissemination of EOC tumors.

One of the limitations of this study is the comparison of gene expression between tumor tissues and normal ovary or between tumors of different grades. EOC is a highly heterogeneous disease consisting of at least five histologic subtypes, high-grade serous carcinoma (HGSC), endometrioid carcinoma, clear cell carcinoma (CCC), low-grade serous carcinoma, and mucinous carcinoma, with HGSC accounting for 70% to 74% of EOC [41]. The different subtypes of EOC have distinct molecular features and tissue origins. It is believed that most HGSC originate from the fallopian tube epithelium, but some HGSCs may still arise from the ovarian surface epithelium [41]. The TCGA database contains data from ovarian serous cystadenocarcinoma and normal ovary, and therefore, we compared the expression of genes regulated by mir-590 between these two groups. This comparison is not ideal as most ovarian carcinomas originate outside the ovary. We therefore also compared miR-590-3p, FOXA2, and VCAN levels between the high-grade and low-grade tumors. However, such comparisons also have drawbacks because high- and low-grade tumors may have different tissue origins. Thus, we cannot exclude the possibility that the difference in gene expression patterns observed between carcinoma and normal ovary or between different grades of tumors may reflect the

different tissue origins. Nevertheless, the higher level of miR-590-3p in the more aggressive higher grade tumors, together with the finding that miR-590-3p promotes EOC cell invasion *in vitro* and metastasis *in vivo*, strongly suggests that miR-590-3p expression is associated with a more aggressive behavior of EOC. Our finding that plasma miR-590-3p levels were higher in patients with ovarian cancer than in control subjects further supports the notion that miR-590-3p is dysregulated during ovarian cancer development. However, it is not clear which factor(s) triggers the dysregulation of miR-590-3p during EOC development. A recent study reported that hypoxia increased miR-590-5p expression to promote colon cancer metastasis [42]. It remains to be investigated whether miR-590-3p is also induced by hypoxia.

ES-2 and SKOV3 cells are commonly used in ovarian cancer research. Most of the experiments in this study were conducted using ES-2 and SKOV3.ip1. SKOV3.ip1 was established from the ascites of a nude mouse injected intraperitoneally with SKOV3 cells [43] that is known to be a model for endometrioid carcinoma [41]. ES-2 originated from a CCC [44]; however, a recent study has placed ES-2 into the category of probably HGSC [45]. ES-2 is now listed as a cell line with mixed feature [41]. Because most of the samples used for bioinformatics analysis to determine the correlation between FOXA2/VCAN and patient survival were done using the TCGA dataset, which likely contains mostly HGSC tumors, we repeated some of the experiments in a HGSC cell line, OVCAR3 [41] and observed that, similar to ES-2 and SKOV3.ip1 cells, miR-590-3p enhanced cell invasion and decreased FOXA2 expression. On the other hand, FOXA2 suppressed cell invasion and inhibited VCAN expression. We have also obtained limited, but similar, results from the HEY cell line, which has also been used as a model for HGSC [46]. Based on these findings, it is possible that the miR-590-3p–FOXA2–VCAN pathway is preserved in multiple subtypes of EOC.

In summary, our study characterizes a previously unreported role of miR-590-3p in promoting EOC development in part by targeting FOXA2. We also provide evidence to support

a novel tumor-suppressive role of FOXA2 in EOC via inhibition of VCAN expression. Finally, our findings that low FOXA2/high VCAN mRNA levels in EOC tumors correlate with poor survival suggest that these genes may be prognostic markers for this deadly disease.

ACKNOWLEDGMENTS

This study was supported by grants from Canadian Institutes of Health Research (MOP-89931 and PJT-153146) and Canada Foundation for Innovation/Ontario Research Fund (project #35611) to C. Peng. J.A. O'Brien was a recipient of graduate scholarships from Ontario Graduate Scholarship (OGS) and York University. S. Bernaudo was a recipient of graduate scholarships from NSERC, OGS, and York University. J. Brkić was a recipient of graduate scholarships from QEII-GSST, OGS, and York University. The research performed in Egypt was supported by the American University in Cairo Internal Faculty Research Grant to A. Amleh and Graduate Student Research Grant to H. Shawer. We thank Dr. J. Liu for her help in statistical analyses of the clinical data, Dr. M.C. Hung for SKOV3.ip1 cells, E. Macdonald and the tumor bank at Ottawa Hospital Research Institute for providing the ovarian cancer samples, and Dr. Z. Wu for critical comments. The Ottawa Ovarian Cancer Tissue Bank is supported in part by Ovarian Cancer Canada. We are grateful to all patients who donated the samples.

CHAPTER 2

SUPPLEMENTARY DATA

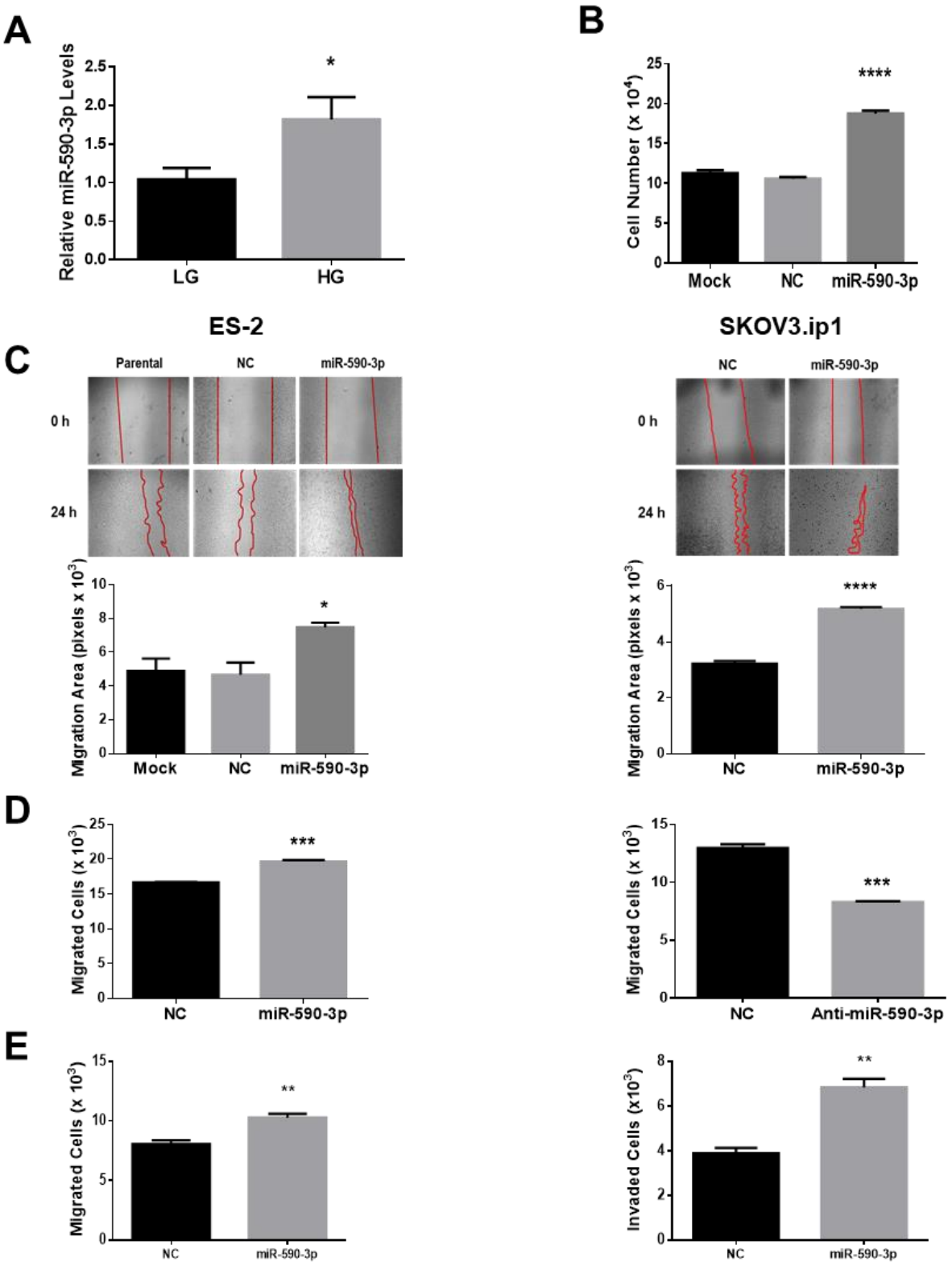
A
Relative miR-590-3p Levels
2.5
2.0
1.5
1.0
0.5
0.0
*
LG
HG
B
Cell Number (x 10^4)
25
20
15
10
5
0
****
Mock
NC
miR-590-3p
ES-2
SKOV3.ip1
C
Parental
NC
miR-590-3p
0 h
24 h
Migration Area (pixels x 10^3)
10
8
6
4
2
0
*
Mock
NC
miR-590-3p
NC
miR-590-3p
0 h
24 h
Migration Area (pixels x 10^3)
6
4
2
0
****
NC
miR-590-3p
D
Migrated Cells (x 10^3)
25
20
15
10
5
0
***
NC
miR-590-3p
Migrated Cells (x 10^3)
15
10
5
0
***
NC
Anti-miR-590-3p
E
Migrated Cells (x 10^3)
15
10
5
0
**
NC
miR-590-3p
Invaded Cells (x10^3)
8
6
4
2
0
**
NC
miR-590-3p

Fig. S2.1. miR-590-3p exerts tumor-promoting effects. **A,** miR-590-3p is upregulated in high grade (HG) compared with low grade (LG) endometrioid ovarian tumors (n=5). **B,** miR-590-3p enhances cell growth. SKOV3.ip1 cells were transiently transfected with non-targeting control (NC) or miR-590-3p mimic and cell numbers were counted at 48h after transfection. A mock transfection (with transfection reagents only) was also performed. **C,** miR-590-3p promotes migration in a wound-healing assay. ES-2 (left) or SKOV3.ip1 (right) cells were transfected with miR-590 or NC, or with transfection reagents only (mock). Cells transfected with miR-590-3p migrated faster than control cells. **D,** miR-590-3p promotes cell migration in a transwell migration assay. SKOV3.ip1 cells were transiently transfected with control or miR-590-3p mimic (left) or anti-miR-590-3p (right), and transwell migration assays were carried out. miR-590-3p increased, while anti-miR-590-3p decreased the number of cells migrated through the pores on the transwell inserts. **E,** miR-590-3p increases OVCAR3 cell migration and invasion. Cells were transfected with NC or miR-590-3p and transwell migration (left) and invasion (right) assays were performed. Data represent mean ± SEM (n=3). * $p < 0.05$, **, $p < 0.01$, *** $p < 0.001$, **** $p < 0.0001$ vs. controls.

A

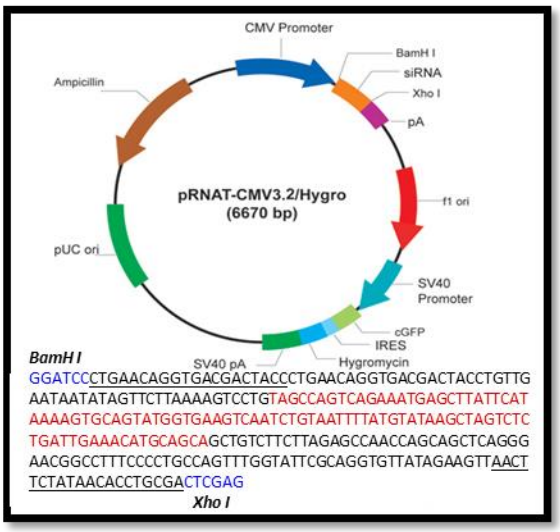
CMV Promoter
BamH I
siRNA
Xho I
pA
f1 ori
SV40 Promoter
cGFP
IRES
Hygromycin
SV40 pA
pUC ori
Ampicillin
pRNAT-CMV3.2/Hygro
(6670 bp)
BamH I
GGATCCCTGAACAGGTGACGACTACCCTGAACAGGTGACGACTACCTGTTG
AATAATATAGTTCTTAAAAGTCCTGTAGCCAGTCAGAAATGAGCTTATTCAT
AAAAGTGCAGTATGGTGAAGTCAATCTGTAATTTTATGTATAAGCTAGTCTC
TGATTGAAACATGCAGCAGCTGTCTTCTTAGAGCCAACCAGCAGCTCAGGG
AACGGCCTTTCCCCTGCCAGTTTGGTATTCGCAGGTGTTATAGAAGTTAACT
TCTATAACACCTGCGACTCGAG
Xho I

B

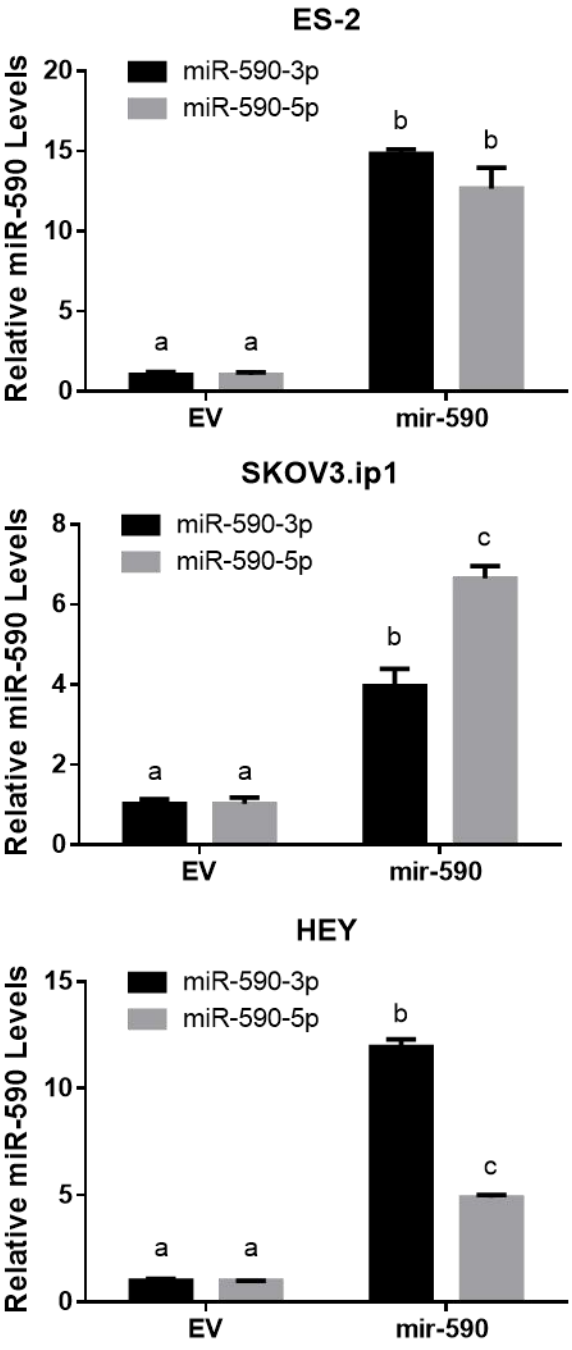
ES-2
miR-590-3p
miR-590-5p
Relative miR-590 Levels
20
15
10
5
0
a
a
b
b
EV
mir-590
SKOV3.ip1
miR-590-3p
miR-590-5p
Relative miR-590 Levels
8
6
4
2
0
a
a
b
c
EV
mir-590
HEY
miR-590-3p
miR-590-5p
Relative miR-590 Levels
15
10
5
0
a
a
b
c
EV
mir-590

C

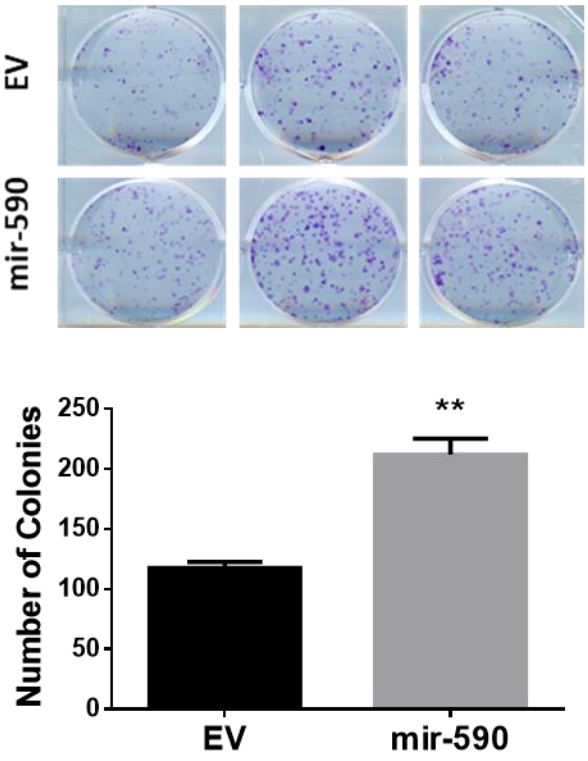
EV
mir-590
Number of Colonies
250
200
150
100
50
0
**
EV
mir-590

Fig. S2.2. Generation of cells stably expressing mir-590. A, mir-590 expression plasmid was generated by subcloning the mir-590 stem-loop sequence into the pRNAT-CMV3.2/Hygro expression vector. **B,** Levels of miR-590-3p and -5p in ES-2, SKOV3.ip1 and HEY cells stably transfected with mir-590 or the empty vector (EV) were measured by qRT-PCR. Different letters denote statistical significant. **C,** mir-590 overexpression increased colony formation in SKOV3.ip1 cells (n=3). ** $p < 0.01$ vs. empty vector control (EV).

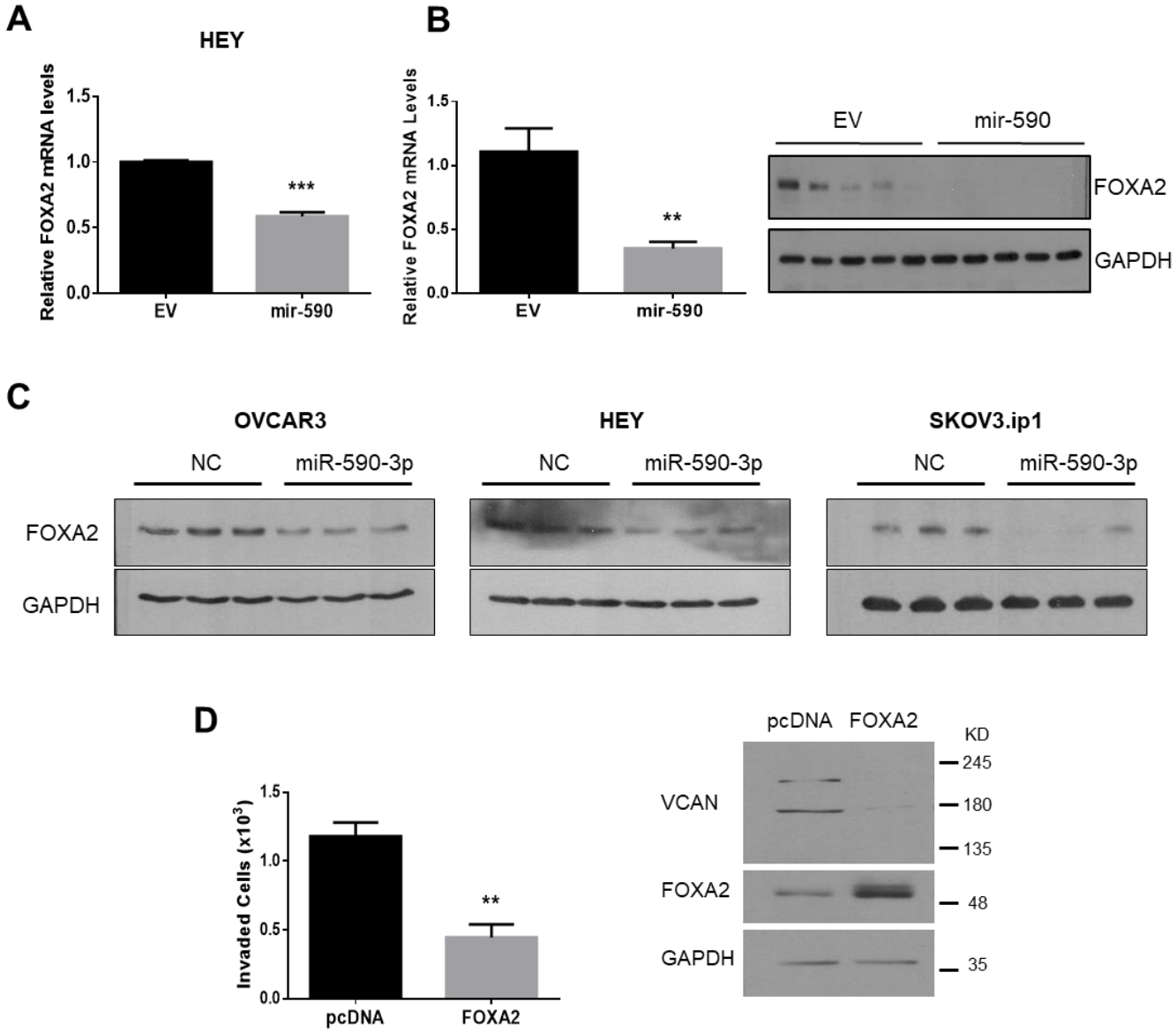

Fig. S2.3. Regulation of FOXA2 by miR-590-3p and effects of FOXA2 on cell invasion and VCAN expression. A, FOXA2 mRNA levels were reduced in HEY cells stably transfected with mir-590. **B,** FOXA2 mRNA and protein levels were down-regulated in tumors collected from mice grafted with control (EV) or mir-590-overexpressing ES-2 cells. **C,** Transient transfection of miR-590-3p decreased FOXA2 protein levels. **D,** Transient transfection of miR-590-3p into OVCAR3 cells resulted in a decrease in cell invasion (left) and VCAN protein levels (right). ** $p < 0.01$ and *** $p < 0.001$.

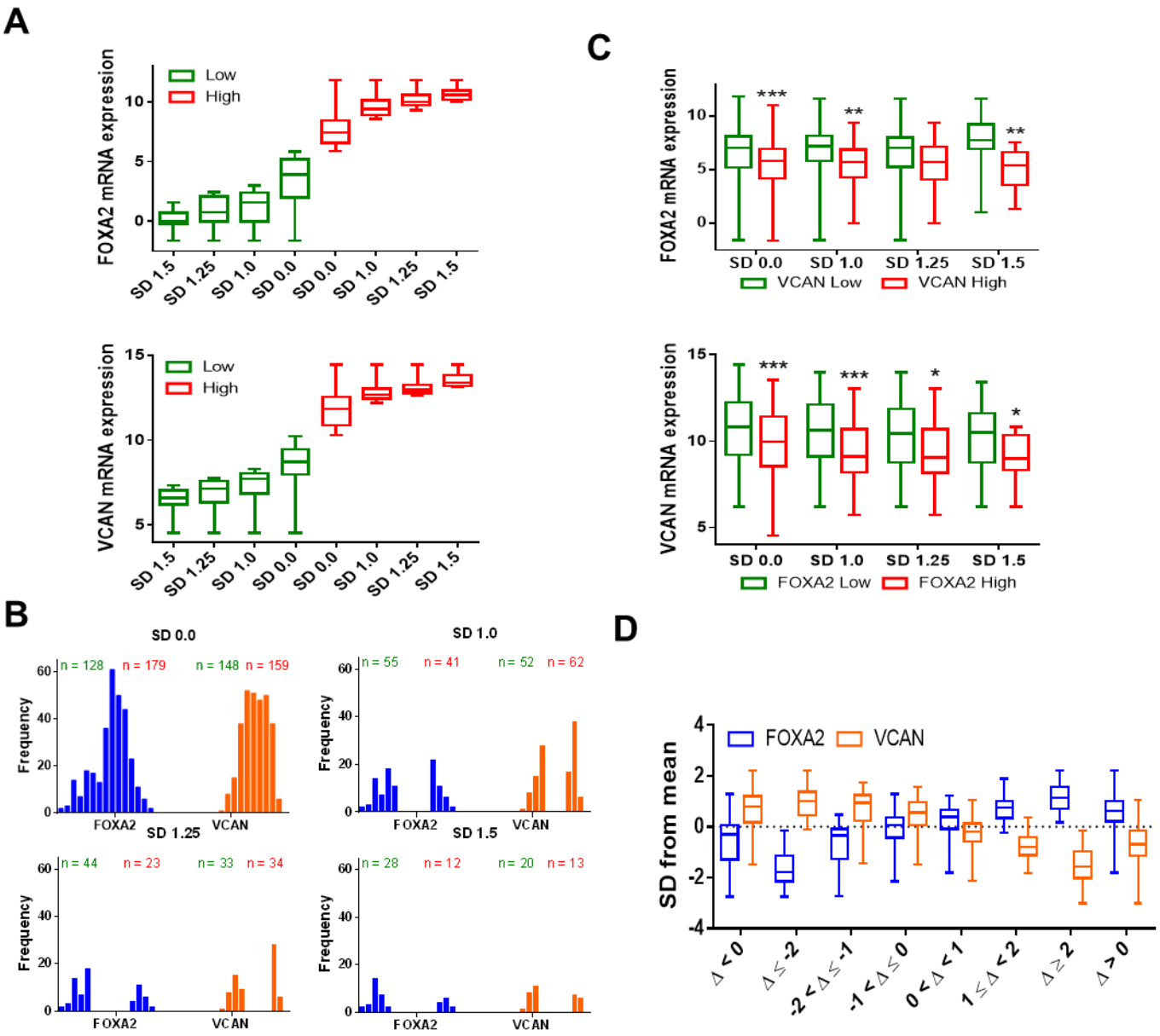
A
FOXA2 mRNA expression
Low
High
SD 1.5
SD 1.25
SD 1.0
SD 0.0
SD 0.0
SD 1.0
SD 1.25
SD 1.5
VCAN mRNA expression
B
SD 0.0
SD 1.0
SD 1.25
SD 1.5
Frequency
n = 128
n = 179
n = 148
n = 159
n = 55
n = 41
n = 52
n = 62
n = 44
n = 23
n = 33
n = 34
n = 28
n = 12
n = 20
n = 13
FOXA2
VCAN
C
***
**
VCAN Low
VCAN High
FOXA2 Low
FOXA2 High
D
SD from mean
Δ < 0
Δ ≤ -2
-2 < Δ ≤ -1
-1 < Δ ≤ 0
0 < Δ < 1
1 ≤ Δ < 2
Δ ≥ 2
Δ > 0

Fig. S2.4. Analysis of FOXA2 and VCAN expression in TCGA ovarian cancer database. **A,** Grouping of tumor samples based on their standard deviation (SD). Tumors were divided into groups based on either FOXA2 (top) or VCAN (bottom) mRNA expression (n = 307). The Low group (green) represents samples whose mRNA levels are less than the mean and the High group (red) greater than the mean. The SD 0.0 subgroups represent all samples less than (Low group) or greater than (High group) the mean. SD 1.0, 1.25, and 1.5 subgroups exclude samples whose mRNA levels are closer to the mean than 0.0, 1.0, or 1.25 SDs. Boxes represent 25^{th} and 75^{th} percentiles demarcated by the median. **B,** Frequency histograms of SD groups for FOXA2 (blue) and VCAN (orange) using a bin width of 1.0. **C,** FOXA2 and VCAN mRNA expression (log2) plotted against VCAN and FOXA2 groups, respectively. FOXA2 and VCAN mRNA expression were significantly negatively correlated throughout most SD subgroups. **D,** Grouped box and whiskers plot of FOXA2 and VCAN mRNA expression levels converted to SDs from the mean. Data is organised into Delta (Δ) groups ranging from -4 to +4, representing lower and upper limits respectively. A $\Delta < 0$ indicates samples with relatively low FOXA2 and high VCAN mRNA levels and $\Delta > 0$ represents samples with relatively high FOXA2 and low VCAN. * $p < 0.05$, ** $p < 0.01$, *** $p < 0.001$.

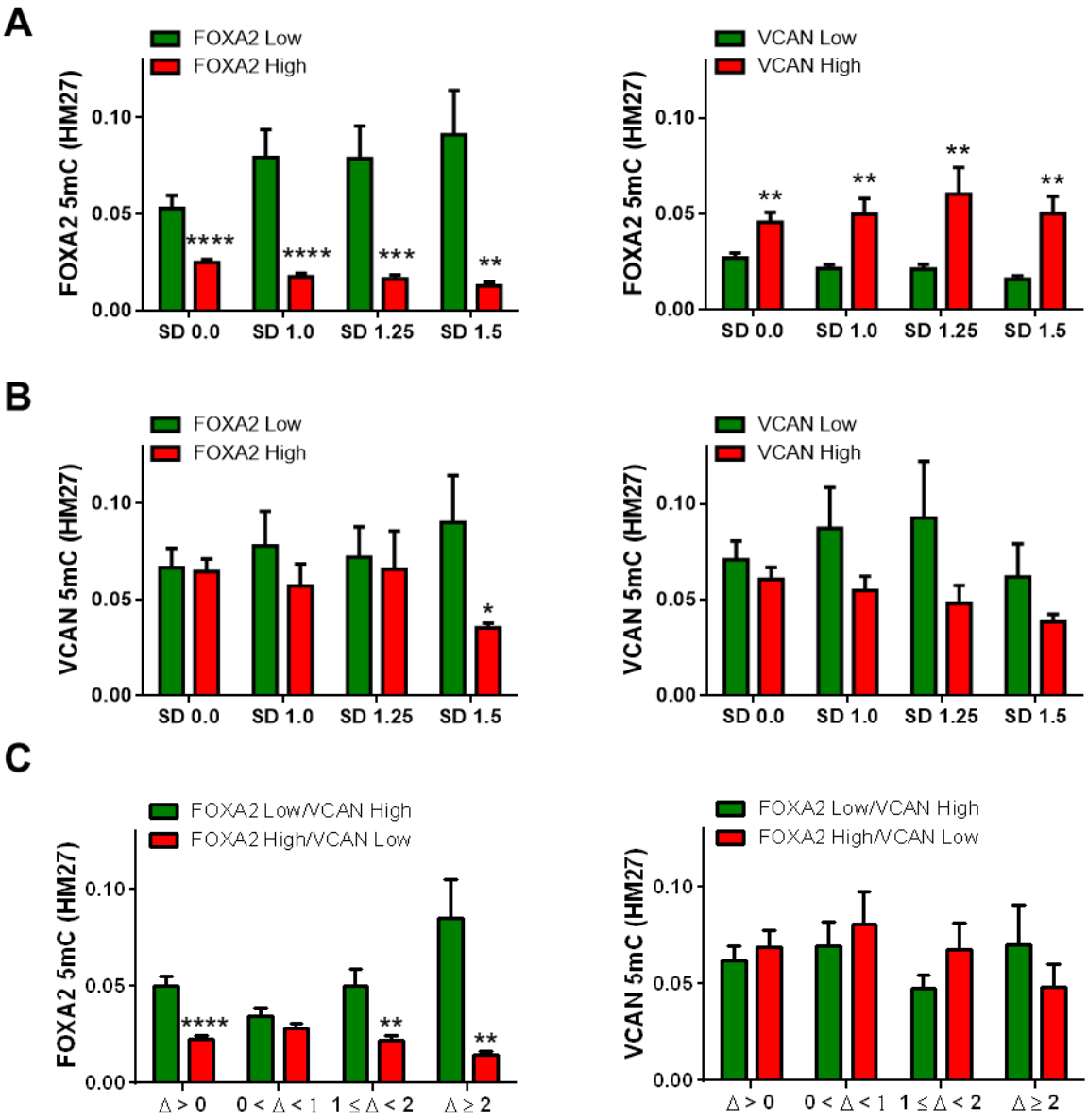
A
FOXA2 Low
FOXA2 High
FOXA2 5mC (HM27)
0.00
0.05
0.10
****
****
***
**
SD 0.0
SD 1.0
SD 1.25
SD 1.5
VCAN Low
VCAN High
FOXA2 5mC (HM27)
0.00
0.05
0.10
**
**
**
**
SD 0.0
SD 1.0
SD 1.25
SD 1.5
B
FOXA2 Low
FOXA2 High
VCAN 5mC (HM27)
0.00
0.05
0.10
*
SD 0.0
SD 1.0
SD 1.25
SD 1.5
VCAN Low
VCAN High
VCAN 5mC (HM27)
0.00
0.05
0.10
SD 0.0
SD 1.0
SD 1.25
SD 1.5
C
FOXA2 Low/VCAN High
FOXA2 High/VCAN Low
FOXA2 5mC (HM27)
0.00
0.05
0.10
****
**
**
Δ > 0
0 < Δ < 1
1 ≤ Δ < 2
Δ ≥ 2
FOXA2 Low/VCAN High
FOXA2 High/VCAN Low
VCAN 5mC (HM27)
0.00
0.05
0.10
Δ > 0
0 < Δ < 1
1 ≤ Δ < 2
Δ ≥ 2

Fig. S2.5. Relationship between FOXA2 and VCAN methylation status and their mRNA levels. A, FOXA2 promoter methylation is negatively correlated with FOXA2, but positively correlated with VCAN, mRNA levels. The proportion of FOXA2 promoter CpG methylation was significantly lower in the high FOXA2 expression group and across all high FOXA2 subgroups (left panel). FOXA2 promoter methylation plotted against low and high VCAN mRNA expression groups showed a significant positive correlation with VCAN mRNA expression. Methylation data was produced through the Illumina Infinium Human Methylation 27 (HM27) array. **B,** VCAN promoter methylation is not correlated with either FOXA2 or VCAN mRNA expression levels with the exception of FOXA2 High SD 1.5 subgroup. **C,** Delta groups show a significant negative correlation of FOXA2 promoter methylation and mRNA expression levels. Green bars represent relatively low FOXA2 and high VCAN mRNA expression levels and red bars relatively high FOXA2 and low VCAN mRNA expression levels. There is no correlation between VCAN promoter methylation and the FOXA2/VCAN mRNA levels. Data represent mean ± SEM. * $p < 0.05$, ** $p < 0.01$, *** $p < 0.001$, **** $p < 0.0001$.

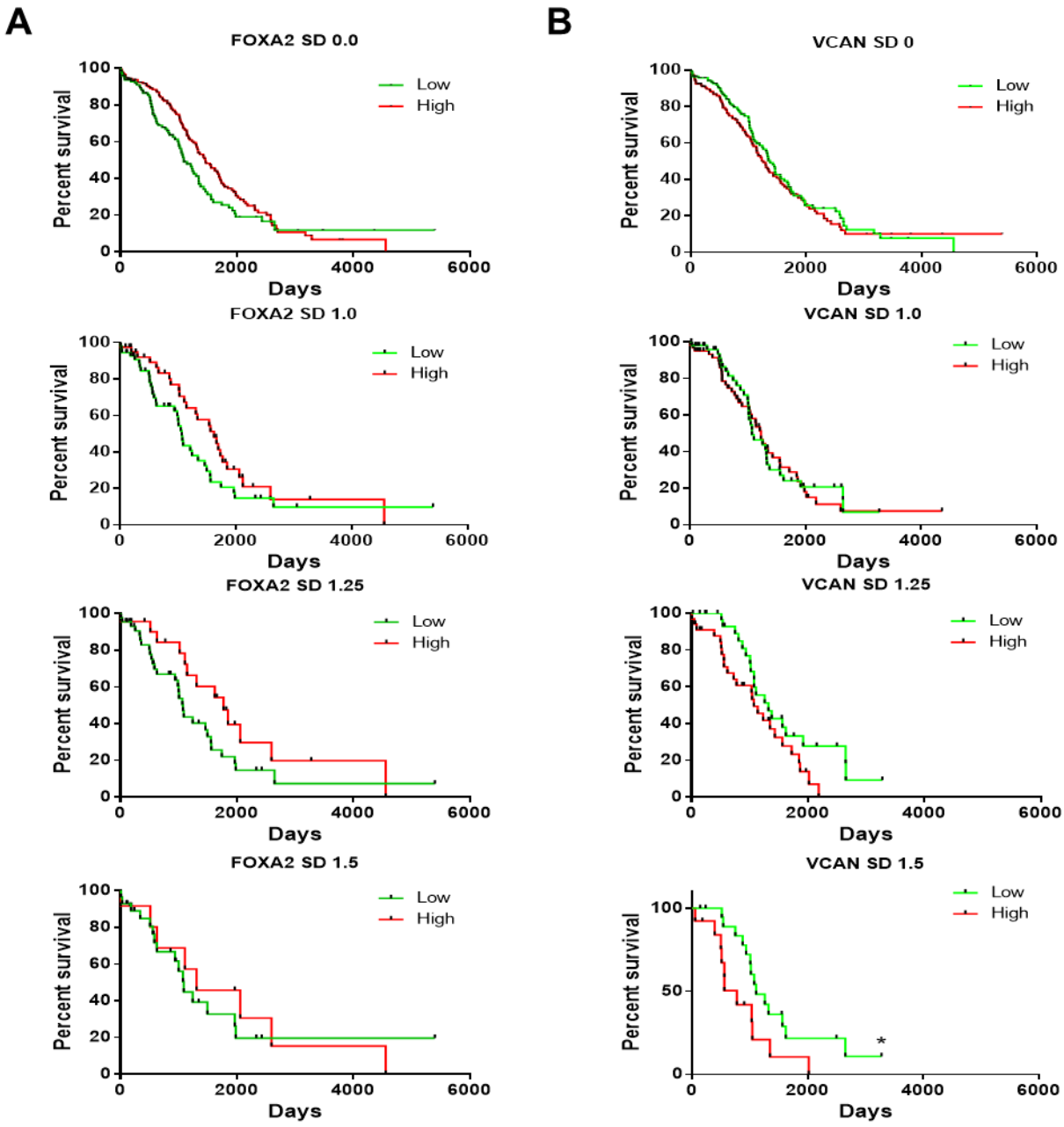

Fig. S2.6. Kaplan-Meier survival plots of all standard deviation groups. **A,** High FOXA2 groups show a trend of increased survival excluding SD 1.5. *Low FOXA2*: 1066.5 – 1089.9 days, *High FOXA2*: 1309.8 – 1773 days. **B,** No difference in survival was observed until the VCAN SD 1.5 group where low VCAN mRNA expression was correlated with increased survival. *Low VCAN*: 1075.2 – 1378.8 days, *High VCAN*: 775.5 – 1260.6 days. P-values were calculated using the Log-rank (Mantel-Cox) test. *$P < 0.05$.

Table S2.1: Clinical samples used in this study.

A. Tumor samples from Mansoura Oncology Center		
Grades/stage/subtype	**Tissue Samples**	**Plasma Samples**
Histological Subtypes		
Serous	18	13
Endometrioid	1	0
Mucinous	1	0
FIGO Stages		
IB	4	2
IIB	3	1
IIIC	10	8
IV	3	2
Histological Grade		
Grade I	11	6
Grade II	5	5
Grade III	4	2
B. Tumor samples from Ottawa Ovarian Cancer Tissue Bank		
Sample ID	**Stage**	**Histological Subtypes**
H1	IIIC	Serous high grade
H2	IIC	Serous high grade
H3	IIC	Serous high grade
H4	IIC	Serous high grade
H5	III	Serous high grade
H6	IIC	Serous high grade
H7	IIIC	Serous high grade
H8	IIIC	Serous high grade
H9	IIIC	Serous high grade
H10	IIC	Serous high grade
H11	IIIC	Serous high grade
H12	IIIC	Serous high grade
H13	IIIB	Serous high grade
L1	IC	LMP
L2	I	LMP
L3	IA	LMP
L4	Not identified	LMP
L5	III	LMP
L6	Not identified	LMP
L7	Not identified	LMP
L8	Not identified	LMP
L9	IIIA	LMP
L10	IIIA	LMP
L11	Not identified	LMP
L12	I	LMP
L13	IIIA	LMP
L14	Not identified	LMP
L15	III	LMP

Table S2.2: Oligonucleotides used in this study.

Name	Sequences	Source*
hsa-miR-590-3p mimic	5′- UAAUUUUAUGUAUAAGCUAGU -3′ 3′- AUUAAAAUACAUAUUCGAUCA -5′	GenePharma
hsa-miR-590-5p mimic	5′- GAGCUUAUUCAUAAAAGUGCAG -3′ 3′- CUCGAAUAAGUAUUUUCACGUC -5′	GenePharma
hsa-anti-miR-590-3p mimic	5′- ACUAGCUUAUACAUAAAAUUA -3	RiboBio
hsa-anti-miR-590-5p mimic	5′- CUGCACUUUUAUGAAUAAGCUC -3′	RiboBio
FOXA2 PCR primers	F 5′-TCTTAAGAAGACGACGGCTTCAG-3′ R 5′-TTGCTCTCTCACTTGTCCTCGAT-3′	[1]
VCAN PCR primers	F 5′- GTGACTATGGCTGGCACAAATTCC-3′ R5′- GGTTGGGTCTCCAATTCTCGTATTGC-3′	[2]
GAPDH PCR primers	F 5′-AAGGTCATCCCTGAGCTGAAC-3′ R 5′-ACGCCTGCTTCACCACCTTCT-3′	
FOXA2 siRNA1	5′- AAAUGGACCUCAAGGCCUAtt-3′ 3′-ttUUUACCUGGAGUUCCGGAU -5′	[3]
FOXA2 siRNA2	5′- GAACACCACUACGCCUUCAtt-3′ 3′ -ttCUUGUGGUGAUGCGGAAGU -5′	[3]
VCAN siRNA	5′- GCUGAACCCAUCUGCAUAtt-3′ 3′-ttCGACUUGGGUAGACGUAU -5′	
Non-targeting siRNA	5′ - UUCUCCGAACGUGUCACGUtt-3′ 3′ -ttAAGAGGCUUGCACAGUGCA -5′	GenePharma
VCAN ChIP (Promoter)	F 5′- AAGGTTGAAGTCTGATTCTGC-3′ R 5′- CTTTTGTTATTTATCAGCCCTCTGC-3′	
VCAN ChIP (Regulatory)	F 5′- GTTGCTTGACTTCACCCTTACC-3′ R 5′- CCATGAATCATAAGACCTCCCC-3′	
VCAN ChIP (NC)	F 5′- AGCAAAATCAAAGCATCCTAGC-3′ R 5′- GAATGTCTGATACCCACAGGC-3′	
mir-590 (clone)	F 5′ -CTGAACAGGTGACGACTACC-3′ R 5′ -AACTTCTATAACACCTGCGA-3′	
FOXA2 (3'UTR clone)	F 5′ -TACTGTGTAGACTCCTGCTTCTT-3′ R 5′ -TATGTCTGAAAATTTTATTAATA-3′	
FOXA sgRNA 1 (CRISPR/Cas9)	5′ -CATGAACATGTCGTCGTACG-3′	Genscript
FOXA sgRNA2 (CRISPR/Cas9)	5′ -AAGGGCACGAGCCGTCCGAC-3′	Genscript

*** All siRNAs taken from cited references or designed by us were synthesized by GenePharma. All primers, designed by others or us were ordered from Sigma.**

Table S2.3: Protein coding genes regulated by mir-590 and their expression profile in TCGA ovarian cancer dataset on Oncomine.

A: Down- regulated genes					
Gene symbol	**FC (mir/EV)**	**# of -3p binding**	**# of -5p binding**	**Dysregulation in EOC**	**p-value**
TMEM51	-2.011	1	0	-1.159	0.118
MBP	-2.107	0	0	-2.776	3.03×10^{-6}
EFEMP1	-2.116	6	0	-7.146	3.5×10^{-7}
HIST1H2BK	-2.158	0	1	1.498	3.58×10^{-5}
FLJ40504	-2.222	0	0	N/A	N/A
TFAP2C	-2.299	0	1	2.390	2.96×10^{-4}
ID3	-2.354	1	0	-2.263	0.001
DKK1	-2.411	1	0	1.176	0.007
LOX	-2.476	4	1	1.694	9.59×10^{-4}
UCA1	-2.555	1	1	N/A	N/A
CBS	-2.620	0	0	2.658	0.001
SIRPA	-3.256	1	0	-1.619	0.014
ANKRD1	-5.436	0	0	1.093	0.046
FOXA2	-6.113	1	0	-2.269	6.26×10^{-4}
BEX1	-6.209	0	0	-3.449	0.002

B: Up- regulated genes			
Gene symbol	**FC (mir/EV)**	**Dysregulation in EOC**	**p-value**
PAGE5	18.106	N/A	N/A
HBBP1	4.598	-1.037	0.184
LCLAT1	3.223	N/A	N/A
ADORA1	2.495	1.159	0.005
SERPINB7	2.231	1.247	1.51×10^{-4}
VCAN	2.230	3.744	1.03×10^{-6}
IL1RAPL1	2.103	-1.016	0.401
CCDC147	2.075	N/A	N/A
FLJ21986	2.048	-1.440	0.007
CXCL5	2.041	1.176	3.77×10^{-4}

N/A: No data available from TCGA database

REFERENCES

1. Zhen, G., et al., *IL-13 and Epidermal Growth Factor Receptor Have Critical but Distinct Roles in Epithelial Cell Mucin Production.* American Journal of Respiratory Cell and Molecular Biology, 2007. **36**(2): p. 244-253.
2. Arslan, F., et al., *The role of versican isoforms V0/V1 in glioma migration mediated by transforming growth factor-β2.* British Journal of Cancer, 2007. **96**(10): p. 1560-1568.
3. Song, Y., M.K. Washington, and H.C. Crawford, *Loss of FOXA1/2 is Essential for the Epithelial-to-Mesenchymal Transition in Pancreatic Cancer.* Cancer Research, 2010. **70**(5): p. 2115-2125.

CHAPTER 3

MIR-590-3P TARGETS CYCLIN G2 TO PROMOTE OVARIAN CANCER DEVELOPMENT

miR-590-3p Targets Cyclin G2 to Promote Ovarian Cancer Development

Mohamed Salem [1], Stefanie Bernaudo [1], Chun Peng [1, 2*]

[1]Department of Biology, York University, Toronto, Canada
[2]Centre for Research on Molecular Interactions, York University, Toronto, Canada

Abbreviated title: miR-590-3p targets cyclin G2 in ovarian cancer

Keywords: miR-590-3p, ovarian cancer, Cyclin G2, β-catenin

* **Corresponding author and to whom reprint requests should be addressed to:**

Dr. Chun Peng, Department of Biology, York University, Toronto, Ontario, Canada M3J 1P3.

cpeng@yorku.ca

This manuscript will be submitted to a peer reviewed journal

Authors' contributions:

M. Salem performed all experiments, S. Bernaudo generated the cell lines stably expressing CCNG2 and its control vector and, C. Peng supervised the study. All authors contributed to the writing of the manuscript.

ABSTRACT

Ovarian cancer is one of the leading causes of cancer death among women around the world. MicroRNAs (miRNAs) are small non-coding RNAs that interact with the 3' untranslated region (3′ UTR) of target genes to repress their expression. We have previously reported that miR-590-3p promotes ovarian cancer development in part by targeting FOXA2. In this study, we investigated other target genes of miR-590-3p and identified cyclin G2 (CCNG2) as a direct target of miR-590-3p. Transient transfection of miR-590-3p decreased the luciferase activity of a reporter containing CCNG2 3'UTR and CCNG2 mRNA levels. Stable overexpression of mir-590 also reduced CCNG2 mRNA and protein levels. miR-590-3p promoted cell proliferation, migration and invasion. In hanging drop cultures, overexpression of mir-590 induced formation of compact spheroids. Silencing of CCNG2 expression mimicked, while overexpression of CCNG2 reversed, these effects of miR-590-3p. Since we have shown that CCNG2 suppresses β-catenin signaling, we investigated if miR-590-3p regulates β-catenin activity. In TOPflash luciferase reporter assays, mir-590 increased β-catenin/TCF transcriptional activity and overexpression of CCNG2 attenuated the effect of mir-590. In addition, mir-590 increased the total β-catenin but decreased phospho-β-catenin levels. Taken together, these results suggest that miR-590-3p promotes ovarian cancer development, in part by directly targeting CCNG2 to enhance β-catenin activity.

INTRODUCTION

Ovarian cancer is the most lethal cancer of the female reproductive system and is one of the leading causes of cancer death in women [1]. There are many types of ovarian cancers, which are grouped into three categories; epithelial, stromal, and germ cell cancer. Epithelial ovarian cancer (EOC) is the most common form, representing approximately 90% of ovarian cancer cases [1] and the current treatment for advanced ovarian cancer is not very effective and many patients relapse [2]. One of the reasons for the patient's high mortality rate is the lack of effective early screening methods. In the majority of EOC cases, the disease is usually discovered when cancer has already disseminated outside the pelvis and spread throughout the abdominal cavity [3]. Another reason is due to the asymptomatic characteristics of EOC, which include the bloated feeling, a symptom that is frequently confused with unrelated diseases [4, 5]. This bloating is due to the accumulation of fluid in the peritoneal cavity corresponding to the formation of the malignant ascites [6]. Within the ascites fluid, malignant cells may present as single cells or aggregated spheroids. These spheroids were found to be highly resistant to many chemotherapeutic agents [7]. Although the precise mechanism involved in the production of excessive peritoneal fluid is still unclear [8-10], it is believed that the change in the cell behaviour required for compact spheroid formation may also contribute in the promotion of ovarian cancer progression [11, 12]. To study this mechanism *in vitro*, researchers developed the hanging drop culture system to monitor spheroid formation [12]. It has been reported that formation of tighter and more compact spheroids is associated with more aggressive EOC phenotypes [13].

MicroRNAs (miRNAs) are small non-coding RNAs that perform diverse functions within cells by regulating gene expression. miRNAs are typically 18-22 nucleotides in length and selectively target messenger RNA (mRNA) through complementary binding to the 3′ UTR of target mRNAs. Depending on the degree of the complementarity between miRNA and its

target mRNA sequence, miRNA with the help of AGO2-dependent slicer, a component of RISC complex, can cleave highly complementary target mRNAs, whereas miRNAs with lower complementarity to their target mRNAs reduce mRNA stability and inhibit translation [14]. Many studies have shown that miRNAs play an important role in determining cell fate, controlling cell proliferation [15, 16], migration, invasion, differentiation, as well as cell death [17, 18]. Moreover, aberrant miRNA expression has been implicated in the pathogenesis of human neurodegenerative disorders, viral and metabolic diseases, as well as cancer [19, 20].

MicroRNA-590-3p (miR-590-3p) has been reported to exert both oncogenic and anti-oncogenic effects in various types of cancer [21]. Recently, we have reported that miR-390-3p has tumor-promoting effects on EOC cells. We found that miR-590-3o levels were elevated in clinical samples collected from patients with high grade carcinoma, and miR-590-3p overexpression increased cell proliferation, migration, invasion and colony formation in several ECO cell lines, *in vitro*, and promoted tumor growth and metastasis *in vivo*. In addition, Forkhead box A2 (FOXA2) was identified as a direct target for miR-590-3p [21]. However, additional target genes that may be involved in ovarian cancer development remain to be identified.

Cyclin G2 (CCNG2), a protein encoded by *CCNG2* gene, belongs to a group of unconventional cyclins that play a role in maintaining the quiescent state and cell cycle arrest [11, 12], and has more recently been identified as a potential tumor suppressor [22]. It has been observed that CCNG2 levels are inversely correlated with cancer cell progression in breast [23], thyroid [24], oral [25], gastric cancers [26], and acute leukaemia [27]. Moreover, CCNG2 levels are increased during growth inhibition [28] and cell differentiation [29]. Previous studies from our lab have shown that CCNG2 reduces cell proliferation and is highly unstable in EOC cells [30]. More recently, we found that CCNG2 inhibits epithelial-to-mesenchymal transition, cell migration, invasion, and spheroid formation, *in vitro,* as well as tumor formation and

metastasis *in vivo*. We also identified a major mechanism by which CCNG2 exerts these anti-tumor effects is via disrupting Wnt/β-catenin signaling [22].

Canonical Wnt signaling pathway plays important roles in many developmental and physiological processes. Its dysregulation is highly associated with cancer development [31]. In the absence of Wnt signaling, β-catenin is localized in the cytoplasm, and is recruited to the destruction complex, which consists of Axin and APC that form a structural scaffold to bind β-catenin. β-catenin is subsequently phosphorylated by CK1 and glycogen synthase kinase-3β (GSK3β). In the destruction complex, GSK3β also phosphorylates APC, increasing its affinity for β-catenin binding, and causing dissociation from Axin. Phosphorylated cytosolic β-catenin is then ubiquitinated by β-transduction repeat-containing protein E3 ubiquitin protein ligase (β-TrCP) [32, 33].

In the presence of Wnt signalling, extracellular Wnt ligand binds the membrane receptor, Frizzled (FZ), which leads to phosphorylation of low-density lipoprotein receptor-related protein (LRP) co-receptor. When LRP is phosphorylated, it induces the translocation of the destruction complex closer to the membrane. At the new location, Dishevelled (DVL) interacts with LRP leading to the activation of DVL and inactivation of GSK3β, causing it to dissociate from Axin and hence, preventing β-catenin phosphorylation and degradation. Stabilized β-catenin accumulates in the cytoplasm and translocates into the nucleus where it functions as a coactivator. In the nucleus, β-catenin interacts with TCF/LEF transcription factors to regulate target gene expression [32, 33]. Several studies have reported that this pathway promotes ovarian cancer stem cell self-renewal [34, 35], chemoresistance [36], and metastasis [37]. In a previous study, we have shown that CCNG2 inhibits LRP6 and DVL2, leading to a decrease in total β-catenin and an increase in phosphorylated β-catenin, and suppression of β-catenin/TCF transcriptional activity [22].

In this study, we used bioinformatics tools to identify miR-590-3p binding sites on

CCNG2 3'UTR. Through reporter and functional assays, we found miR-590-3p targets CCNG2 and promotes β-catenin signaling.

MATERIALS AND METHODS

Cell culture

ES-2 was purchased from American Type Culture Collection (ATCC, Manassas, VA, USA), as previously reported [22], while SKOV3.ip1 cells were generously donated by Dr. Mien-Chie Hung (University of Texas M.D. Anderson Cancer Center, Huston, Texas). ES-2 and SKOV3.ip1 cells were maintained in McCoy 5A media (Sigma-Aldrich), supplemented with 10% Fetal Bovine Serum (FBS), 100 IU/ml penicillin and 100μg/ml streptomycin (all purchased from Life Technologies). Cells were incubated in a humidified atmosphere of 5% CO_2 at 37^0 C.

Transient transfection

Transient transfection of plasmids (0.25 to 1.5 μg), miRNA mimics, inhibitors or siRNA (150-200 nM) were carried out using Lipofectamine 2000 or Lipofectamine RNAiMAX (Life Technologies) following the manufacturer's suggested procedures. Non-targeting negative control (NC), hsa-miR-590-3p mimic [21], and siCCNG2 [22], were purchased from GenePharma Co. (Shanghai, China). Anti-miR-590-3p and its corresponding NC were purchased from RiboBio (Guangzhou, China).

Generation of mir-590 stable cell lines

ES-2 and SKOV3.ip1 cells stably overexpressing mir-590 precursor stem-loop sequence were cloned into the pRNAT-CMV3.2/Hygro expression Vector (GenScript). Control cells (EV), were transfected with pRNAT-CMV3.2/Hygro, without the mir-590 insert, as previously described [21].

Reagents and plasmids

CCNG2 was cloned into a retroviral vector, pBabe-puro [38]. The virus was produced by co-transfecting either pBabe-FLAG-CCNG2 or pBabe-empty vector**.** The plasmid was then packaged into pUMVC, and pCMV-VSVg envelope plasmid [39]. A mutant form of β-catenin (S33Y) [40], which is phosphorylation and degradation resistant, was cloned into a pcDNA plasmid. It was obtained from Addgene (Cambridge, MA, USA).

RNA extraction and real-time PCR

Total RNA was isolated using TRIzol reagent (Invitrogen) as previously described [41]. To determine mRNA levels, 1.5 μg of total RNA was used to synthesize first strand cDNA by M-MuLV Reverse Transcriptase (New England BioLabs Ltd, ON, Canada). Real-time PCR was carried out using gene-specific primers and EvaGreen qPCR Master Mix (Applied Biological Materials, ABM). The expression levels of mRNA were normalized to GAPDH. The relative expression levels of mRNAs were determined using the standard $2^{-\Delta\Delta ct}$ method.

Protein extraction and immunoblotting

Cells were lysed in RIPA buffer (20 mM Tris, pH 8.0, 150 mM NaCl, 10 mm NaF, 0.1% SDS, 1% Nonidet P-40 and 1 × protease inhibitor cocktail (Pierce, IL, USA). Cell lysates were then collected by centrifugation at 12,000g for 20 minutes at 4ºC. Bicinchoninic acid (BCA) assay was conducted to measure protein concentration. An equal amount of protein samples was subjected to 10% SDS-polyacrylamide gel electrophoresis and transferred onto polyvinylidene difluoride (PVDF, Bio-Rad) membranes. The membranes were then blocked with 5% milk for 1 hour at room temperature followed by incubation with primary antibodies in milk overnight at 4ºC. The membranes were washed with TBS-T and subsequently probed with an HRP-conjugated secondary antibody (1:5000) at room temperature for 2 hrs. Signals

were visualized using ECL (Millipore, ON, Canada) according to the manufacturer's protocol. CCNG2 antibody was obtained from Abcam (1:500). β-catenin and p-β-catenin antibodies were obtained from Cell Signaling (1:1000 and 1:500 respectively) and GAPDH antibody was purchased from Santa Cruz (1:10000).

Luciferase assay

Luciferase constructs fragments of the CCNG2 3′ UTR, containing the predicted miR-590-3p binding sites, were generated by PCR using forward primers 5′ - GCTGAAAGCTTGCAACTGCCGAC - 3′ and reverse primers 5′ - GGTATCGTTGGCAGCTCAGGAAC - 3′. The resulting cDNA fragments were cloned into pMIR-Report (Ambion, Austin, TX, USA) downstream of the luciferase coding sequence. Cells were seeded in 12-well plates at a density of $75x10^4$ cells/well and. pMIR-Report-CCNG2 3′ UTR plasmids and pRL-TK internal control (encoding Renilla luciferase) plasmids were co-transfected. Five hours after transfection, cells were recovered in media supplemented with 10% FBS. 24 hours after transfection, the cells were lysed and luciferase activities were measured using the Dual-Luciferase Reporter Assay System (Promega, WI, USA) according to the manufacturer's instructions as previously reported [42].

Spheroid formation assay (3D hanging drop)

Spheroid formation assays were performed as described in [22]. Briefly, at 24 hours after transfection, cells were collected and $2x10^4$ cells were re-suspended in 20 µl of culture media. 10-21 drops of cells were placed on the inside of a 100 mm culture dish cover for 3-4 days and spheroids were photographed.

Migration and invasion assays

Migration and invasion assays were performed as previously described in [21]. Briefly, for migration experiments, cells were seeded onto transwell membranes at a density of 12 $x10^3$ cells per well. To assess invasion, cells were seeded onto transwell membranes pre-coated with a thin layer of Matrigel, at a density of $15x10^3$. At 24 hr after seeding, cells were fixed and stained. Cells on the top of the transwell were removed by swabbing and filters were cut and mounted on a slide. Pictures were taken for the whole fields, and cells were counted using an automated quantification plugin for ImageJ [43].

TOPflash reporter assay

To assess β-catenin-TCF/LEF transcriptional activity, the TOPflash reporter assay was utilized. EOC cells were transiently co-transfected with TOPflash reporter construct and Renilla control plasmid. The Firefly and Renilla activities were then measured using the Dual-Luciferase Reporter Assay System (Promega, Fitchburg, WI, USA) according to the manufacturer's protocol.

Statistical analysis

All experiments were done at least three times with at least triplicates in each group. The results are expressed as mean ± SEM in bar graphs. GraphPad Prism 6 was used to perform all statistical analyses. Two groups comparison were analyzed using Student's t-test, while one-way ANOVA followed by Student-Newman-Keuls post hoc test was used to analyze multiple groups. Significance was defined as $p<0.05$.

RESULTS

CCNG2 is a target gene of miR-590-3p

The 3′ UTR of CCNG2 harbours three predicted targeting sites for miR-590-3p (Fig. 1A top). To determine if CCNG2 is a target gene of miR-590-3p, a CCNG2 3′ UTR fragment containing the predicted miR-590-3p target sites was cloned into the p-MIR-REPORT™ Expression Vector, downstream of the luciferase coding sequence. Cells were transfected with the reporter construct, together with miR-590-3p or a non-targeting control oligo (NC). Luciferase assays revealed that miR-590-3p decreased the luciferase activity when compared to NC (Fig. 3.1A bottom).

To determine if miR-590-3p regulates *CCNG2* expression, ES-2 and SKOV3.ip1 cells were transiently transfected with miR-590-3p or NC. Total RNA was extracted and reverse transcribed. As revealed by qRT-PCR, *CCNG2* mRNA levels were significantly lower in cells transfected with miR-590-3p than in the NC group (Fig. 3.1B). Similarly, in ES-2 cells stably transfected with mir-590, *CCNG2* mRNA levels were also significantly reduced when compared to cells expressing the control empty vector (EV) (Fig. 3.1C, left panel). In addition, Western blot analyses revealed that mir-590 downregulated CCNG2 protein levels (Fig. 3.1C, right).

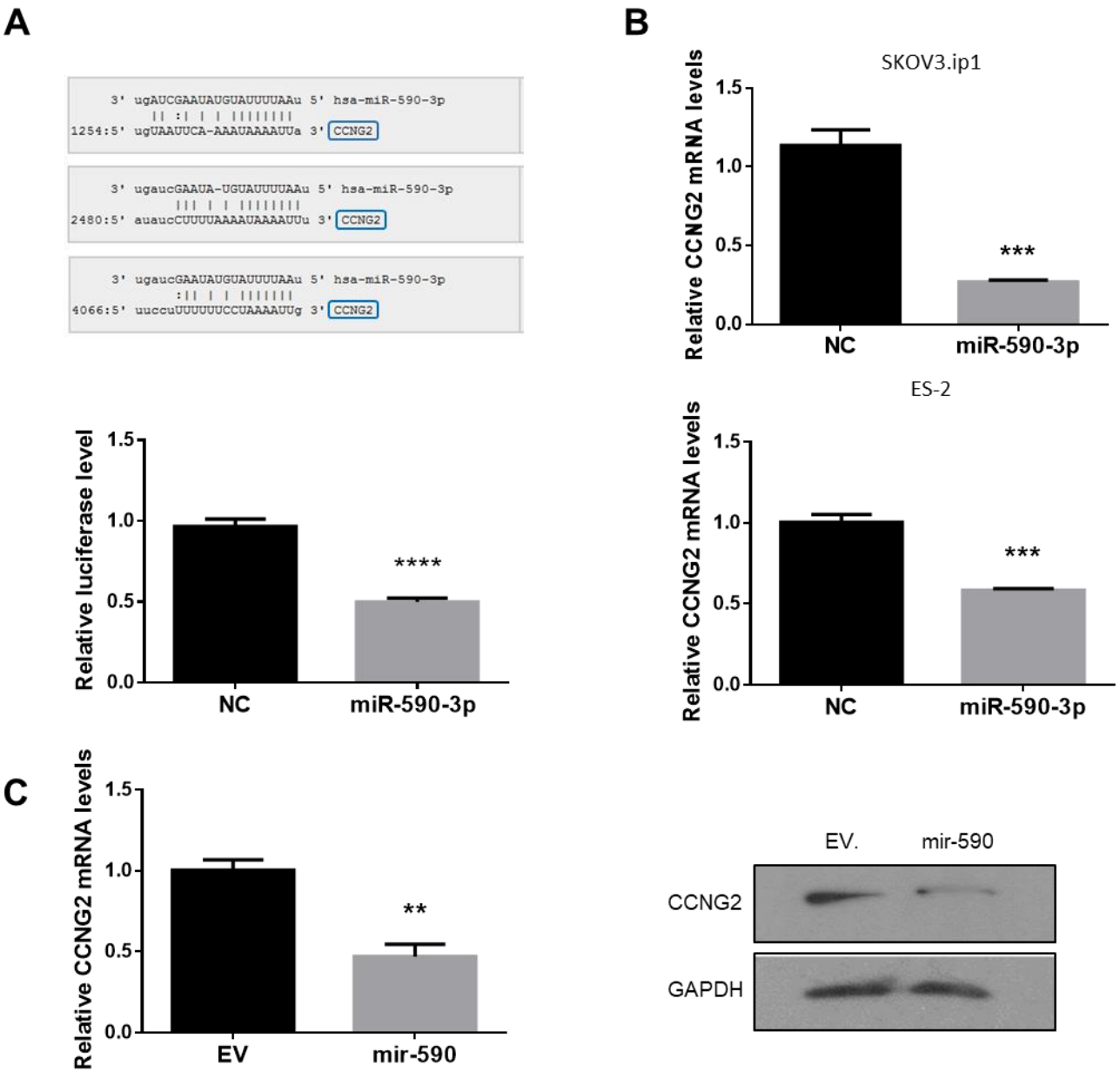
A
3' ugAUCGAAUAUGUAUUUUAAu 5' hsa-miR-590-3p
1254:5' ugUAAUUCA-AAAUAAAAUUa 3' CCNG2
3' ugaucGAAUA-UGUAUUUUAAu 5' hsa-miR-590-3p
2480:5' auaucCUUUUAAAAUAAAAUUu 3' CCNG2
3' ugaucGAAUAUGUAUUUUAAu 5' hsa-miR-590-3p
4066:5' uuccuUUUUUUCCUAAAAUUg 3' CCNG2
Relative luciferase level
1.5
1.0
0.5
0.0
****
NC
miR-590-3p
B
SKOV3.ip1
Relative CCNG2 mRNA levels
1.5
1.0
0.5
0.0
***
NC
miR-590-3p
ES-2
Relative CCNG2 mRNA levels
1.5
1.0
0.5
0.0
***
NC
miR-590-3p
C
Relative CCNG2 mRNA levels
1.5
1.0
0.5
0.0
**
EV
mir-590
EV.
mir-590
CCNG2
GAPDH

Figure 3.1. ***CCNG2*** **is a target gene of miR-590-3p**. **A)** miR-590-3p targets *CCNG2* 3'UTR. Three predicted miR-590-3p binding sites are found in *CCNG2* 3'UTR. A luciferase reporter construct containing these *CCNG2* 3'UTR was generated using the pMIR-REPORT vector. Transient transfection of miR-590-3p significantly decreased the luciferase activity in ES-2 cells. **B)** miR-590-3p downregulates *CCNG2* mRNA levels. In ES-2 and SKOV3.ip1 cells transiently transfected with miR-590-3p, *CCNG2* mRNA levels were significantly lower than in control cells transfected with a non-targeting oligo (NC). **C)** mir-590 inhibits CCNG2 expression. CCNG2 protein (left) and mRNA (right) levels were lower in ES-2 cells stably overexpressing mir-590 precursor then in control cells expressing the empty vector (EV). Data represents mean ± SEM (n=3). ** $p < 0.01$, *** $p < 0.001$, **** 0.0001 $p <$ vs controls.

Silencing of CCNG2 mimics the effect of miR-590-3p

To further investigate if miR-590-3p regulates cell growth by targeting CCNG2, ES-2 cells were transfected with siCCNG2 or NC. Western blotting and qRT-PCR confirmed that CCNG2 protein and mRNA levels were downregulated by siCCNG2 (Fig. 3.2A). Transient transfection of siCCNG2 and miR-590-3p significantly increased cell proliferation when compared to NC (Fig. 3.2B). Similarly, transient transfection with siCCNG2 or miR-590-3p significantly enhanced cell migration (Fig. 3.2C) and invasion (Fig. 3.2D).

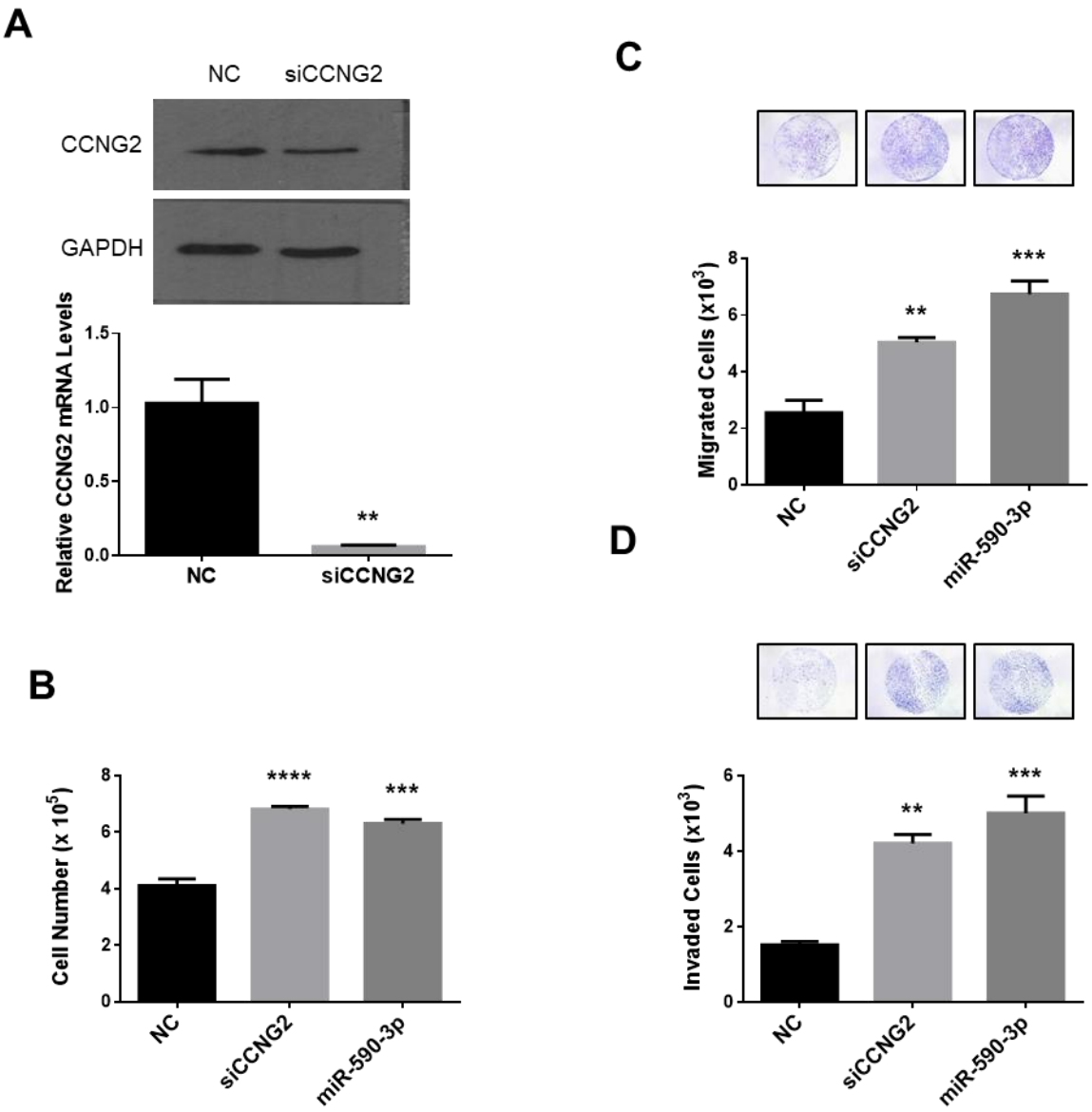
A
NC
siCCNG2
CCNG2
GAPDH
Relative CCNG2 mRNA Levels
1.5
1.0
0.5
0.0
**
NC
siCCNG2
B
Cell Number (x 10^5)
8
6
4
2
0
****
***
NC
siCCNG2
miR-590-3p
C
Migrated Cells (x10^3)
8
6
4
2
0
**
***
NC
siCCNG2
miR-590-3p
D
Invaded Cells (x10^3)
6
4
2
0
**
***
NC
siCCNG2
miR-590-3p

Figure 3.2. CCNG2 knockdown mimics the effect of miR-590-3p. A) Confirmation of *CCNG2* down-regulation after siRNA transfection. ES-2 cells were transfected with a siRNA targeting *CCNG2* or a non-targeting oligo (NC) and Western blotting (top) and qPCR (bottom) were performed. **B)** Silencing of *CCNG2* or overexpression of miR-590-3p increases cell proliferation**.** ES-2 cells were transfected with siCCNG2, miR590-3p, or NC and cell numbers were determined at 48h after transfection. **C)** Silencing of *CCNG2* or overexpression of miR-590-3p increases cell migration. SKOV3.ip1 cells transiently transfected with si*CCNG2* or miR-590-3p had a significantly higher number of migrated cells when compared to NC. **D)** Knockdown to *CCNG2* increases cell invasion. ES-2 cells transfected with si*CCNG2* or miR-590-3p had a significantly higher number of invaded cells when compared to NC. Data represent mean ± SEM (n=3). ** $p < 0.01$, *** $p < 0.001$, **** $p < 0.0001$ vs NC.

Overexpression of CCNG2 reversed the effect of miR-590-3p

A stable cell line overexpressing CCNG2 and a control cell line expressing the empty vector (EV) have been generated in our lab [22]. These stable cell lines were used to determine whether overexpression of CCNG2 can block the effect of miR-590-3p. Cells were transfected with miR-590-3p or NC. Overexpression of miR-590-3p significantly increased cell numbers in the control cells. However, in cells overexpressing CCNG2, the effect of miR-590-3p was strongly inhibited (Fig. 3.3A). Similarly, mir-590-stable cells transiently transfected with CCNG2 attenuated the effect of mir-590, and resulted in reduced numbers of invaded cells compared to the control (Fig. 3.3B).

We have previously reported that CCNG2 disrupts the formation of compact spheroids in 3D hanging drop culture [22]. To determine if miR-590-3p enhances spheroid formation, miR-590-3p or NC were transfected into SKOV3.ip1 cells and hanging drop spheroid assays were performed. Cells transfected with miR-590-3p formed smaller and more compact spheroids compared to the ones transfected with NC (Fig. 3.3C). On the other hand, transfection of anti-miR-590-3p into ES-2 cells disrupted this tight formation and lead to looser spheroid (Fig. 3.3D). To examine whether miR-590-3p enhances the spheroid formation by targeting CCNG2, we transfected SKOV3.ip1 stable cells expressing the control plasmid or CCNG2 with miR-590-3p or NC. Without CCNG2 overexpression, cells transfected with miR-590-3p formed very compact spheroids, when compared with cells transfected with NC. CCNG2 overexpression resulted in the formation of loose cell aggregates and also reduced the effect of miR-590-3p on promoting compact spheroid formation (Fig. 3.3E).

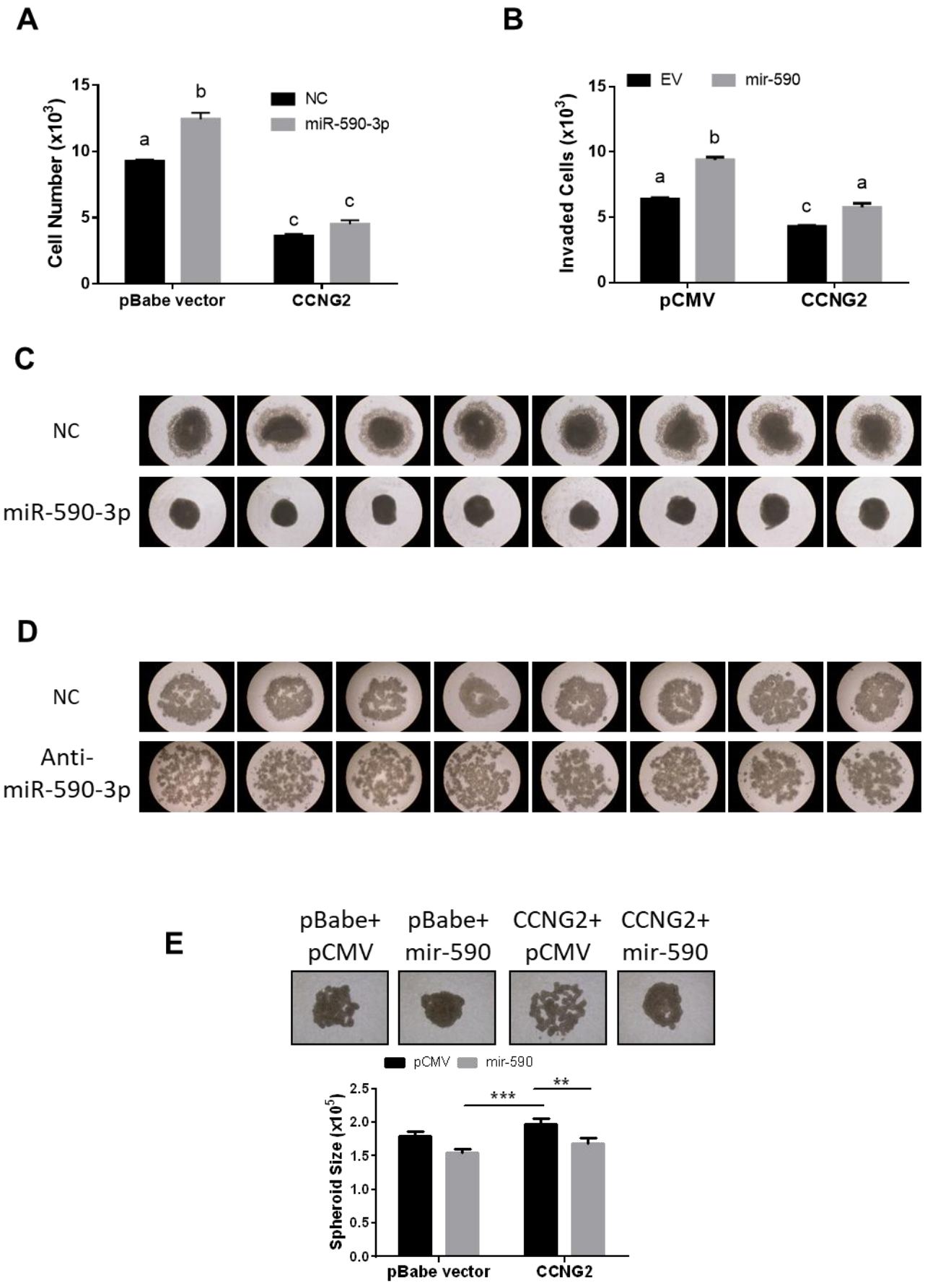
A
Cell Number (x10^3)
15
10
5
0
a
b
c
c
NC
miR-590-3p
pBabe vector
CCNG2
B
Invaded Cells (x10^3)
EV
mir-590
a
b
c
a
pCMV
CCNG2
C
NC
miR-590-3p
D
NC
Anti-
miR-590-3p
E
pBabe+
pCMV
pBabe+
mir-590
CCNG2+
pCMV
CCNG2+
mir-590
pCMV
mir-590
Spheroid Size (x10^5)
2.5
2.0
1.5
1.0
0.5
0.0
***
**
pBabe vector
CCNG2

Figure 3.3. CCNG2 overexpression reverses the effect of miR-590-3p. A) SKOV3.ip1 stably transfected with CCNG2 or its control vector, pBabe, were transiently transfected with miR-590-3p or a non-targeting control oligo. **B)** Overexpression of *CCNG2* reduces the effect of mir-590 on cell invasion. ES-2 cells stably expressing mir-590 or its empty vector (EV) were transiently transfected with *CCNG2* or its empty vector pCMV and cell invasion was determined. **C)** 3D spheroids were formed by the hanging drop culture method. Cells were transfected with miR-590-3p (n=12) or **D)** Anti-miR-590-3p (n=21) respectively. While spheres formed by cells transfected with miR-590-3p were smaller in size and more compact compared to the control ones, anti-miR-590-3p reversed this effect. **E)** Overexpression of *CCNG2* reverses the effect of miR-590-3p on the spheroid formation. Control or *CCNG2* stable cells were transiently transfected with miR-590-3p or NC and hanging drop cultures were performed. In control cells, miR-590-3p overexpression resulted in the formation of compact spheroids. *CCNG2* stable cells formed loose spheroids and also reduced the effect of miR-590-3p on spheroid formation (n=13). The circumferences of spheres were measured using ImageJ Software. Data represent mean ± SEM (A and B) n=3. Groups significantly different from each other are denoted by a different letter. ** $p < 0.01$, *** $p < 0.001$ vs controls.

mir-590 enhances β-catenin signaling by suppressing CCNG2

Since CCNG2 inhibits β-catenin activity [22], we investigated whether miR-590-3p promotes β-catenin signaling. TOPflash reporter assays were first performed to determine the transcriptional activity of β-catenin/TCF. In both SKOV3.ip1 and ES-2 cells, stable overexpression of mir-590 resulted in a significant increase in TOPflash activity (Fig. 3.4A). Transfection of CCNG2 significantly reduced basal luciferase levels while mir-590-induced luciferase activity (Fig. 3.4B). In mir-590 cells, higher total β-catenin and lower phosphor-β-catenin levels were observed (Fig. 3.4C). Finally, to determine if activation of the β-catenin pathway contributes to the tumor-promoting effects of miR-590-3p, we transfected control and mir-590 stable cells with a siRNA targeting β-catenin or a NC. As shown in Fig. 3.4C, silencing of β-catenin reversed the ability of mir-590 cells to form tight, compact spheroids (Fig. 3.4D).

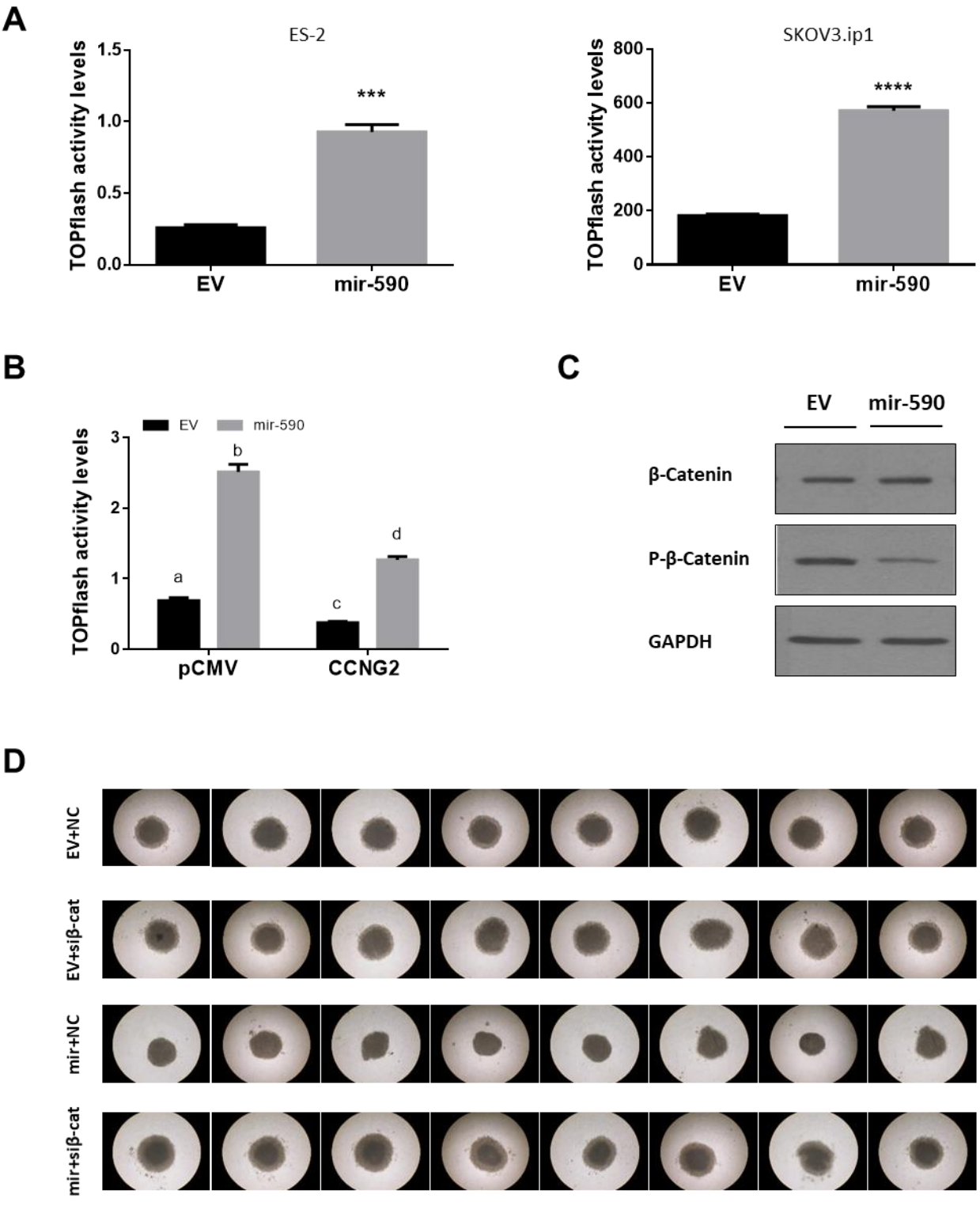
A
ES-2
TOPflash activity levels
1.5
1.0
0.5
0.0
***
EV
mir-590
SKOV3.ip1
TOPflash activity levels
800
600
400
200
0
****
EV
mir-590
B
EV
mir-590
TOPflash activity levels
3
2
1
0
a
b
c
d
pCMV
CCNG2
C
EV
mir-590
β-Catenin
P-β-Catenin
GAPDH
D
EV+NC
EV+siβ-cat
mir+NC
mir+siβ-cat

Figure 3.4. mir-590 enhances beta-catenin signaling by suppressing *CCNG2.* A) mir-590 overexpression increases β-catenin transcriptional activity. TOPflash reporter assays were performed in both ES-2 and SKOV3.ip1 cells stably transfected with mir-590 or its control empty vector (EV). **B)** Overexpression of *CCNG2* reduces the effect of mir-590 on β-catenin transcriptional activity. Control or mir-590 stable cells were transfected with CCNG2-expressing construct or its control vector. TOPflash reporter assays were performed in ES-2 cells. Data represent mean ± SEM (n=3). **C)** mir-590 overexpression slightly increases total β-catenin but decreases phospho-β-catenin when compared to its EV control. **D)** Knockdown of β-catenin blocks the effect of mir-590 on spheroid formation. Data represent mean ± SEM (n=10). *** $p < 0.001$, **** $p < 0.0001$ vs controls (A). Groups significantly different from each other are denoted by a different letter (B).

DISCUSSION

Recently, we have reported that miR-590-3p promotes EOC development via a novel FOXA2-VCAN pathway. In this study, we investigated additional target genes of miR-590-3p. Using bioinformatics tools, luciferase assays, and functional analyses, we identified *CCNG2* as a direct downstream target of miR-590-3p and demonstrate that down-regulation of CCNG2 is in part responsible for the tumor-promoting effects of miR-590-3p.

We have identified FOXA2 as a target gene for miR-590-3p. Since a miRNA can target many genes [44, 45], we investigated additional targets for miR-590-3p in this study. Analysis of CCNG2 3'UTR revealed that it has three predicted binding sites for miR-590-3p. When CCNG2 3'UTR was inserted downstream of the luciferase gene, miR-590-3p reduced the luciferase activity, suggesting that miR-590-3p can bind to the CCNG2 3'UTR to inhibit the luciferase expression. In addition, transient or stable transfection of miR-590-3p decreased mRNA and/or protein levels of CCNG2. Finally, silencing of CCNG2 mimicked, while overexpression of CCNG2 reduced, the effect of miR-590-3p on cell proliferation, migration, invasion, and spheroid formation. These findings strongly suggest that down-regulation of CCNG2 is also partially responsible for the tumor-promoting effects of miR-590-3p. While this study is the first in EOC cells to show that CCNG2 is targeted by a miRNA, several studies in other types of cancer have reported that miRNAs can target CCNG2 to promote cancer development. For example, miR-1246 induces cell proliferation and invasion, as well as drug resistance, by targeting CCNG2, in breast cancer [46] and pancreatic cancer [47]. miR-135b has also been reported to target CCNG2 and exert tumor promoting effects in lung cancer [48]. In addition, miR-340 promotes gastric cancer development by inhibiting CCNG2 [49]. Finally, miR-93 targets CCNG2 to exert tumor-promoting effects in laryngeal squamous cell carcinoma [50]. These findings suggest that CCNG2 is tightly regulated by miRNAs and down-regulation of CCNG2 by miRNAs is common to the development of many types of cancer.

Cancer cells possess varying capacities for spheroid formation [11, 12]. It has been demonstrated that more aggressive EOC cells form tighter and more compact spheroids [13]. In this study, we showed that cells overexpressing miR-590-3p were able to form more compact and much smaller spheroids than the control cells while anti-miR-590-3p disrupts this cell aggregation and compaction. On the other hand, overexpression of *CCNG2* reversed this effect. These findings, together with our previous studies, which show that miR-590-3p promote EOC cell proliferation, migration, and invasion *in vitro* and tumor growth and metastasis *in vivo*, strongly support the notion that miR-590-3p may exerts its tumor-promoting effects, at least in part, by targeting CCNG2 in EOC.

The Wnt/β-catenin signaling plays critical roles in carcinogenesis and the development of various types of cancers; including colorectal cancer [51], liver cancer [52], leukemia [53], melanoma [54], breast cancer [55] and ovarian cancer [56-58]. Although it was initially believed that aberrant β-catenin level is mainly reported in the endometrioid subtype of EOC, accumulating evidence suggests its role in the development of other subtypes, including serous ovarian cancer [22, 59]. In a previous study, we showed that CCNG2 overexpression decreased the levels of both DVL2 and LRP6 in EOC cells, and hence, indirectly promoted β-catenin phosphorylation and degradation [22]. In this study, we found that miR-590-3p reduced phosphorylated β-catenin levels and enhanced the transcriptional activity of β-catenin/TCF, as revealed by Western blotting and TOPflash Luciferase assays, respectively. Interestingly, overexpression of CCNG2 attenuated the stimulatory effects of miR-590-3p on TOPflash luciferase activity, suggesting that miR-590-3p enhances β-catenin signaling by down-regulating CCNG2. Furthermore, we found that in mir-590 stable cells, knock-down of β-catenin by siRNA reduced the ability of cells to form tight spheroids. These results suggest that activation of β-catenin contributes to the tumor-promoting effects of miR-590-3p. Recently, DKK1, an antagonist of the Wnt/ β-catenin

pathway, has been reported to be a miR-590-3p target gene [60]. In the mir-590 cells, we found that DKK1 levels were down-regulated [21]. It is possible that miR-590-3p also targets DKK1 to enhance β-catenin signaling. This will be investigated in the future.

In summary, we provide, for the first time to our knowledge, evidence to support that miR-590-3p promotes EOC progression, in part by inhibiting *CCNG2* expression and inducing β-catenin signaling. In addition, our results shed light on a new role for miR-590-3p in modulating β-catenin signaling in EOC tumorigenesis.

CHAPTER 4

SUMMARY AND FUTURE DIRECTIONS

SUMMARY

The objectives of my PhD were to investigate the function of miR-590-3p in human ovarian cancer cells and to determine the mechanisms of miR-590-3p actions.

Aim 1: To investigate the role of miR-590-3p in ovarian cancer cells

To understand the role of miR-590-3p in ovarian tumor development, we first investigated the level of miR-590-3p in human ovarian clinical samples. We found that miR-590-3p was significantly elevated in high-grade EOC tumors when compared with normal ovaries or lower grade tumors. In addition, miR-590-3p plasma level was higher in EOC patients than in subjects with benign gynecological disorders (Chapter 2). These findings suggest that increased expression of miR-590-3p in ovarian tumors is associated with a more aggressive phenotype.

To examine the function of miR-590-3p in ovarian cancer cells, gain- and loss-of function approaches were used. In EOC cell lines stably overexpressing mir-590, a precursor of miR-590-3p, we noticed a significant increase in cell proliferation, migration, invasion, and colony formation when compared to cells expressing a control vector (Chapter 2). Furthermore, we examined the ability of mir-590 stable cells to form spheroids using the hanging drop assay. A previous study showed that there is a direct relation between cell invasive behaviour and how compact the sphere is [1]. We found that mir-590-overexpressing cells formed tighter spheroids when compared to the control (Chapter 3). Similar results were obtained when cells were transiently transfected with miR-590-3p mimics. Conversely, cells transfected with anti-miR-590-3p decreased cell proliferation, migration, and invasion. Together, these in vitro assays provide evidence that miR-590-3p exerts a tumorigenic effect in ovarian cancer cells.

To further confirm that tumor-promoting effects of miR-590-3p on EOC, *in vivo* studies were carried out. To examine the effect of mir-590 on tumor formation, we injected mir-590-overexpressing cells or its control cells subcutaneously into nude mice. Results from this experiment showed that mice injected with mir-590 cells formed significantly larger tumors. To investigate the effects of mir-590 on tumor metastasis, mice were injected intraperitoneally with mir-590-overexpressing or control cells. Mice inoculated with mir-590 cells formed more nodules and disseminated more within the peritoneal cavity compared to those injected with control cells. These results support a tumor-promoting role of mir-590 in EOC development.

Aim 2: To determine the mechanisms by which miR-590-3p exerts its tumorigenic effects

To explain the mechanism of miR-590-3p action, we examined the molecular events altered in stable cells overexpressing miR-590-3p using cDNA microarray and bioinformatics tools. We identified two pathways, FOXA2/VCAN and CCNG2/β-catenin that mediate effects of miR-590-3p.

Firstly, using cDNA microarray, we identified FOXA2 as one of the most strongly down-regulated genes by mir-590. We further demonstrated, by luciferase reporter assays, real-time PCR and Western blotting, that miR-590-3p directly targets FOXA2. In addition, we found that FOXA2 level was greatly down-regulated in high-grade EOC tumors compared to low malignancy potential ones. Moreover, knockdown of FOXA2 by siRNAs or knockout of FOXA2 by CRISPR/Cas9 resulted in an increase in cell proliferation, migration and invasion. On the other hand, overexpressing FOXA2 in mir-590 stable cells reduced the tumor-promoting effects of mir-590. These findings demonstrate that the tumor-promoting effects of miR-590-3p is mediated, in part by inhibition of FOXA2.

We also identified a novel relationship between FOXA2 and VCAN. We showed that FOXA2 inhibition by either knockdown or knockout enhanced, while overexpression of FOXA2 reduced, VCAN expression. Moreover, we found that VCAN promoter and intragenic DNA has FOXA2 predicted binding sites. Results from ChIP-qPCR showed enrichments of VCAN DNA in the regions where FOXA2-binding sites were predicted when compared with the IgG group. This is in agreement with the expression patterns of FOXA2 and VCAN in EOC tumor samples from the TCGA database where we observed a negative correlation between FOXA2 and VCAN mRNA levels. These results strongly suggest that FOXA2 is a transcriptional repressor of VCAN.

Interestingly, in the same tumor samples, we found that low VCAN and high FOXA2 mRNA levels were associated with longer survival in ovarian cancer patients. In addition, knockdown of VCAN by siRNA led to inhibition of EOC cell proliferation, migration and invasion. These findings support the nation that VCAN has tumor-promoting effects in, while FOXA has a tumor suppressing effect in ovarian cancer.

Another miR-590-3p target genes identified in this study is CCNG2. Combined results from different miRNA target search engines revealed three potential target sites for miR-590-3p on the 3′UTR of CCNG2. Luciferase assay for cells co-transfected with miR-590-3p and a construct carrying the potential target sites showed a significant decrease in luciferase activity when compared to control cells. In addition, we noticed a decrease in CCNG2 mRNA and protein levels in the cells overexpressing miR-590-3p or its precursor.

Previous studies showed that CCNG2 inhibits cell proliferation, migration and invasion [2]. Silencing of CCNG2 using siRNA mimicked the effect of miR-590-3p and increased EOC cell proliferation, migration and invasion, while CCNG2 overexpression reduced the effect of miR-590-3p and decreased cell proliferation and invasion rates in EOC cells. In addition, hanging drop assays revealed that cells overexpressing CCNG2 formed much looser spheroids

compared to control cells, consistent with our previous findings that CCNG2 has anti-tumor function in EOC.

We previously showed that CCNG2 attenuates β-catenin transcriptional activity in EOC cells [2]. In this study, we examined the effect of miR-590-3p to on β-catenin signaling. We found that mir-590 reduced the phosphorylated level of β-catenin and significantly increased the transcriptional activity of β-catenin/TCF in luciferase reporter assays. Interestingly, overexpression of CCNG2 reduced the stimulatory effect of mir-590 on β-catenin/TCF transcriptional activity. Finally, in spheroid formation assays, we showed that when siRNA targeting β-catenin was transfected into mir-590 stable cells, the ability of mir-590 cells to form tight spheroids was reduced. These findings suggest that the CCNG2/ β-catenin pathway also mediates the effect of miR-590-3p on EOC development.

FUTURE DIRECTIONS

To further investigate the role of mir-590 in EOC

In the future, we would like to further investigate how miR-590-3p may regulate the *in vivo* progression of EOC tumors. Since our data suggest that miR-590-3p increase migration and invasion, it is likely that miR-590-3p may increase early dissemination of cancer cells. To better understand both primary and secondary tumor formation, we would like to pursue the *in vivo* study by implementing an orthotopic technique. Instead of injecting ovarian cancer cells subcutaneously or intraperitoneally, cells will be injected under the ovarian bursa. Using this assay will increase our understanding and assessment of how miR-590 overexpression regulates the formation of primary lesions, as well as ascites accumulation and cell spreading throughout the peritoneal cavity to mimic the disease in humans.

We would like to investigate the role of miR-590-5p in the malignant transformation of ovarian cancer. The tumor-promoting effects of mir-590 overexpression observed in our study could also be attributed to miR-590-5p overexpression. Our preliminary results showed that both anti-miR-590-3p and anti-miR-590-5p attenuated the effect of mir-590, suggesting that miR-590-5p is also playing a role in EOC development but further investigation is needed in the future.

The Wnt/β-catenin pathway is critical in maintaining cancer stem cells (CSCs) [3, 4]. Since mir-590 increases β-catenin signaling, it will be interesting to investigate if miR-590-3p and/or miR-590-5p play a role in CSC self-renewal. Previous studies suggested that both cancer and stem cells share common cellular mechanisms and characteristics [5, 6]. Some of these common characteristics are the ability of both cell types to proliferate continuously, to stay viable in suspension culture as well as the ability to form spheroids [7]. Many stem markers include: CD44, CD133, CD24, SOX2, NOTCH3 and ALP, have been utilized to measure the level of stemness in ovarian tumor-initiating cells, or ovarian cancer stem-like cells (CSLCs)

[8]. In the future, we will investigate whether mir-590 is contributing to the process of ovarian cancer development by promoting CSLCs stemness.

To further investigate the mechanisms of mir-590 actions in EOC

In our cDNA microarray, we found that a number of genes are up- or down-regulated by mir-590 overexpression. For example, we found that DKK1, which was reported to be targeted by miR-590-3p in colon cancer [9], was strongly downregulated in our mir-590 cells. In the future, we will investigate the role of miR-590-3p in promoting stemness and in regulating DKK1. Stemness-induced sphere formation assays will be performed in the mir-590 stable cells transfected with either DKK1 expression plasmid, or siDKK1 oligo. Results from these experiments will shed more light on the functional role of mir-590 in inducing stemness and regulating β-catenin during ovarian cancer development.

CONCLUSION

The present work provides evidence that miR-590-3p has a tumor-promoting effects by targeting FOXA2 and CCNG2 in ovarian cancer (Fig. 4.1). We also characterized a novel tumor-suppressive role of FOXA2 in EOC through the inhibition of VCAN expression. In addition, our microarray analysis has identified DKK-1, a known Wnt/β-catenin signal inhibitor, as one of the downregulated genes in cells overexpressing mir-590. All together, these targets affect several major downstream mediators that contribute to the development and progression of ovarian cancer disease.

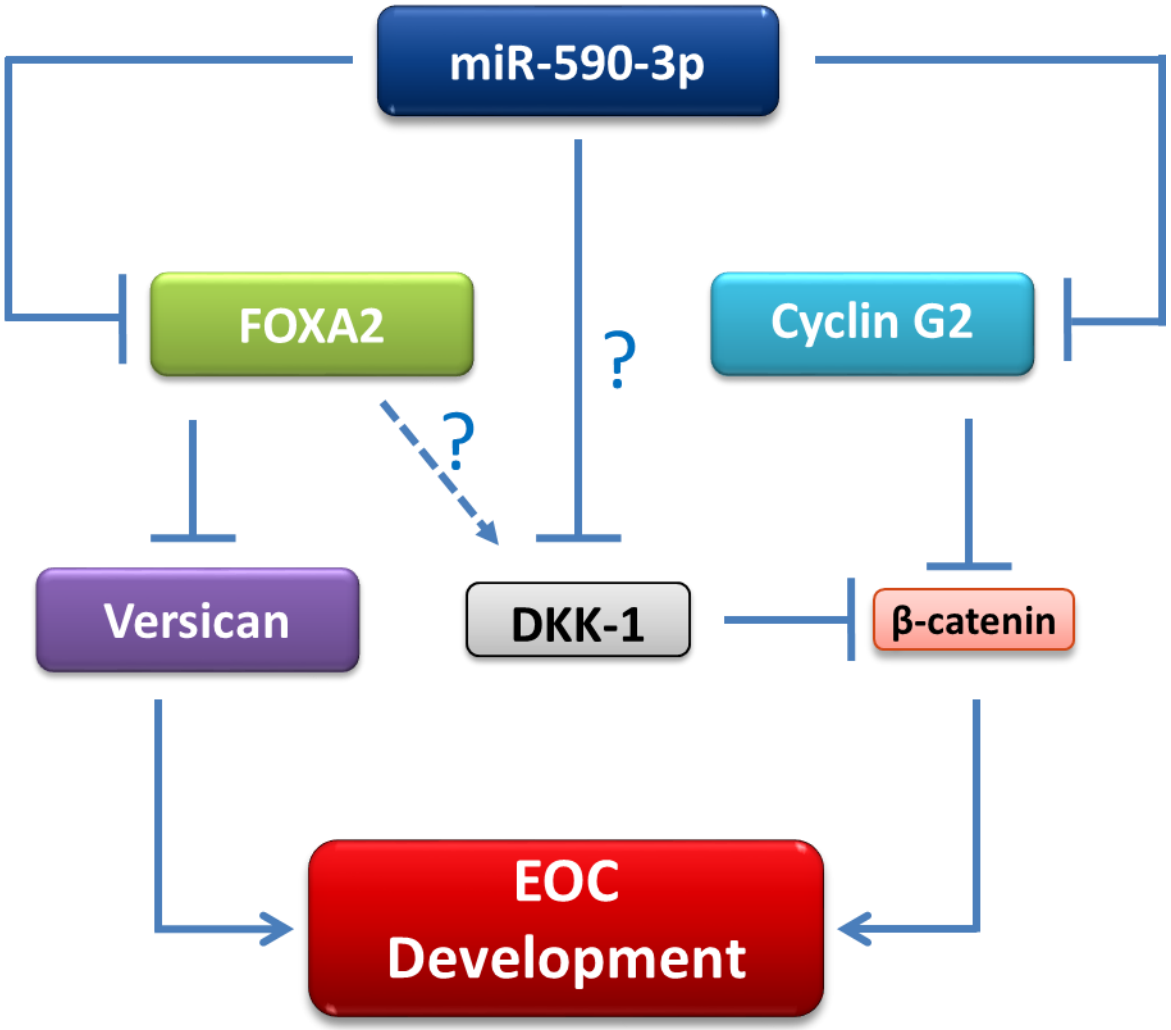

Figure. 4.1. Proposed summary model for the role of mir-590 in promoting EOC development. The levels of miR-590-3p were significantly elevated in high-grade EOC tumours and serum clinical samples. miR-590-3p targets the 3´UTR of *FOXA2* mRNA and inhibits its translation, while increasing *VCAN* levels. In addition, miR-590-3p targets the 3´UTR of *CCNG2* mRNA leading to an increase in β-catenin level. DKK-1, the Wnt/β-catenin suppressor, was also predicted to have a target site for miR-590-3p. These events cascade leads to a promotion of EOC cell proliferation, migration, invasion and metastasis.

REFERENCES

CHAPTER 1 REFERENCES

1. Gilks, C.B. and J. Prat, *Ovarian carcinoma pathology and genetics: recent advances.* Hum Pathol, 2009. **40**(9): p. 1213-23.
2. Goff, B.A., et al., *Frequency of symptoms of ovarian cancer in women presenting to primary care clinics.* JAMA, 2004. **291**(22): p. 2705-12.
3. *NIH: Surveillance, Epidemiology, and End Results Program*. 2015, National Cancer Institure: USA.
4. *Canadian Cancer Society's Advisory Committee on Cancer Statistics. Canadian Cancer Statistics 2018*. 2018: Toronto, ON.
5. Siegel, R.L., K.D. Miller, and A. Jemal, *Cancer statistics, 2017.* CA: A Cancer Journal for Clinicians, 2017. **67**(1): p. 7-30.
6. Committee on the State of the Science in Ovarian Cancer Research; Board on Health Care Services; Institute of Medicine; National Academies of Sciences, E., and Medicine., *Ovarian Cancers: Evolving Paradigms in Research and Care.* . 2016, Washington (DC), USA: National Academies Press
7. Goff, B.A., et al., *Ovarian carcinoma diagnosis.* Cancer, 2000. **89**(10): p. 2068-2075.
8. Smith, L.H., et al., *Ovarian cancer: can we make the clinical diagnosis earlier?* Cancer, 2005. **104**(7): p. 1398-1407.
9. Sun, C.C., P.T. Ramirez, and D.C. Bodurka, *Quality of life for patients with epithelial ovarian cancer.* Nat Clin Pract Oncol, 2007. **4**(1): p. 18-29.
10. Verheul, H.M., et al., *Targeting vascular endothelial growth factor blockade: ascites and pleural effusion formation.* Oncologist, 2000. **5 Suppl 1**: p. 45-50.
11. Kuk, C., et al., *Mining the ovarian cancer ascites proteome for potential ovarian cancer biomarkers.* Mol Cell Proteomics, 2009. **8**(4): p. 661-9.
12. Berchuck, A. and M. Carney, *Human ovarian cancer of the surface epithelium.* Biochem Pharmacol, 1997. **54**(5): p. 541-4.
13. Williams, T.I., et al., *Epithelial ovarian cancer: disease etiology, treatment, detection, and investigational gene, metabolite, and protein biomarkers.* J Proteome Res, 2007. **6**(8): p. 2936-62.
14. *American Cancer Society's* C.S. Center, Editor. 2016: USA.
15. Kurman, R.J., *Origin and molecular pathogenesis of ovarian high-grade serous carcinoma.* Annals of Oncology, 2013. **24**(suppl_10): p. x16-x21.
16. Braicu, E., et al., *Role of histological type on surgical outcome and survival following radical primary tumour debulking of epithelial ovarian, fallopian tube and peritoneal cancers.* British Journal of Cancer, 2011. **105**(12): p. 1818.
17. Seidman, J.D., et al., *The histologic type and stage distribution of ovarian carcinomas of surface epithelial origin.* International journal of gynecological pathology, 2004. **23**(1): p. 41-44.
18. Bell, D.A., *Low-grade serous tumors of ovary.* International journal of gynecological pathology, 2014. **33**(4): p. 348-356.
19. Bodurka, D.C., et al., *Reclassification of serous ovarian carcinoma by a 2-tier system.* Cancer, 2012. **118**(12): p. 3087-3094.
20. Malpica, A., et al., *Grading ovarian serous carcinoma using a two-tier system.* The American journal of surgical pathology, 2004. **28**(4): p. 496-504.
21. Gershenson, D.M., et al., *Recurrent low-grade serous ovarian carcinoma is relatively chemoresistant.* Gynecol Oncol, 2009. **114**(1): p. 48-52.
22. Tone, A.A., et al., *Intratumoral heterogeneity in a minority of ovarian low-grade serous carcinomas.* BMC cancer, 2014. **14**(1): p. 982.
23. Vang, R., I.-M. Shih, and R.J. Kurman, *Ovarian low-grade and high-grade serous carcinoma: pathogenesis, clinicopathologic and molecular biologic features, and diagnostic problems.* Advances in anatomic pathology, 2009. **16**(5): p. 267.
24. DePriest, P., et al., *Endometrioid carcinoma of the ovary and endometriosis: the association in postmenopausal women.* Gynecologic oncology, 1992. **47**(1): p. 71-75.
25. Eržen, M., et al., *Endometriosis-associated ovarian carcinoma (EAOC): an entity distinct from other ovarian carcinomas as suggested by a nested case-control study.* Gynecologic oncology, 2001. **83**(1): p. 100-108.
26. Yoshikawa, H., et al., *Prevalence of endometriosis in ovarian cancer.* Gynecologic and Obstetric Investigation, 2000. **50**(Suppl. 1): p. 11-17.

27. Gilks, C.B., et al., *Tumor cell type can be reproducibly diagnosed and is of independent prognostic significance in patients with maximally debulked ovarian carcinoma.* Human pathology, 2008. **39**(8): p. 1239-1251.
28. Storey, D.J., et al., *Endometrioid epithelial ovarian cancer.* Cancer, 2008. **112**(10): p. 2211-2220.
29. McConechy, M.K., et al., *Ovarian and endometrial endometrioid carcinomas have distinct CTNNB1 and PTEN mutation profiles.* Modern Pathology, 2014. **27**(1): p. 128.
30. Anglesio, M.S., et al., *Clear cell carcinoma of the ovary: a report from the first Ovarian Clear Cell Symposium, June 24th, 2010.* Gynecologic oncology, 2011. **121**(2): p. 407-415.
31. Jenison, E.L., et al., *Clear cell adenocarcinoma of the ovary: a clinical analysis and comparison with serous carcinoma.* Gynecologic oncology, 1989. **32**(1): p. 65-71.
32. Tammela, J., et al., *Clear cell carcinoma of the ovary: poor prognosis compared to serous carcinoma.* European journal of gynaecological oncology, 1998. **19**(5): p. 438-440.
33. Veras, E., et al., *Cystic and adenofibromatous clear cell carcinomas of the ovary: distinctive tumors that differ in their pathogenesis and behavior: a clinicopathologic analysis of 122 cases.* The American journal of surgical pathology, 2009. **33**(6): p. 844-853.
34. Jones, S., et al., *Frequent mutations of chromatin remodeling gene ARID1A in ovarian clear cell carcinoma.* Science, 2010. **330**(6001): p. 228-231.
35. Matsumoto, T., et al., *Distinct β-catenin and PIK3CA mutation profiles in endometriosis-associated ovarian endometrioid and clear cell carcinomas.* American journal of clinical pathology, 2015. **144**(3): p. 452-463.
36. Cho, K.R. and I.-M. Shih, *Ovarian cancer.* Annual Review of Pathological Mechanical Disease, 2009. **4**: p. 287-313.
37. McConechy, M.K., et al., *Subtype-specific mutation of PPP2R1A in endometrial and ovarian carcinomas.* The Journal of pathology, 2011. **223**(5): p. 567-573.
38. Shih, I.-M., et al., *Somatic mutations of PPP2R1A in ovarian and uterine carcinomas.* The American journal of pathology, 2011. **178**(4): p. 1442-1447.
39. Ledermann, J.A., et al., *Gynecologic Cancer InterGroup (GCIG) consensus review for mucinous ovarian carcinoma.* International Journal of Gynecological Cancer, 2014. **24**(9): p. S14-S19.
40. Zaino, R.J., et al., *Advanced stage mucinous adenocarcinoma of the ovary is both rare and highly lethal.* Cancer, 2011. **117**(3): p. 554-562.
41. Lee, K.R. and R.H. Young, *The distinction between primary and metastatic mucinous carcinomas of the ovary: gross and histologic findings in 50 cases.* The American journal of surgical pathology, 2003. **27**(3): p. 281-292.
42. Riopel, M.A., B.M. Ronnett, and R.J. Kurman, *Evaluation of diagnostic criteria and behavior of ovarian intestinal-type mucinous tumors: atypical proliferative (borderline) tumors and intraepithelial, microinvasive, invasive, and metastatic carcinomas.* The American journal of surgical pathology, 1999. **23**(6): p. 617-635.
43. Ronnett, B., et al., *Pseudomyxoma peritonei: new concepts in diagnosis, origin, nomenclature, and relationship to mucinous borderline (low malignant potential) tumors of the ovary.* Anatomic pathology (Chicago, Ill.: annual), 1997. **2**: p. 197-226.
44. Szych, C., et al., *Molecular genetic evidence supporting the clonality and appendiceal origin of pseudomyxoma peritonei in women.* The American journal of pathology, 1999. **154**(6): p. 1849-1855.
45. Vang, R., et al., *Cytokeratins 7 and 20 in primary and secondary mucinous tumors of the ovary: analysis of coordinate immunohistochemical expression profiles and staining distribution in 179 cases.* The American journal of surgical pathology, 2006. **30**(9): p. 1130-1139.
46. Hart, W.R., *Mucinous tumors of the ovary: a review.* International Journal of Gynecological Pathology, 2005. **24**(1): p. 4-25.
47. Rechsteiner, M., et al., *TP53 mutations are common in all subtypes of epithelial ovarian cancer and occur concomitantly with KRAS mutations in the mucinous type.* Experimental and molecular pathology, 2013. **95**(2): p. 235-241.
48. Anglesio, M.S., et al., *Molecular characterization of mucinous ovarian tumours supports a stratified treatment approach with HER2 targeting in 19% of carcinomas.* The Journal of pathology, 2013. **229**(1): p. 111-120.
49. Kurman, R.J. and I.-M. Shih, *The Origin and Pathogenesis of Epithelial Ovarian Cancer- a Proposed Unifying Theory.* The American journal of surgical pathology, 2010. **34**(3): p. 433-443.
50. Dubeau, L. and J. Teixeira, *Chapter 1 - Origins of Epithelial Ovarian Cancer*, in *Translational Advances in Gynecologic Cancers*, M.J. Birrer and L. Ceppi, Editors. 2017, Academic Press: Boston. p. 3-17.

51. Bell, D.A., *Origins and molecular pathology of ovarian cancer.* Mod Pathol, 2005. **18 Suppl 2**: p. S19-32.
52. Flesken-Nikitin, A., et al., *Ovarian surface epithelium at the junction area contains a cancer-prone stem cell niche.* Nature, 2013. **495**(7440): p. 241.
53. Ng, A. and N. Barker, *Ovary and fimbrial stem cells: biology, niche and cancer origins.* Nature reviews Molecular cell biology, 2015. **16**(10): p. 625.
54. Pavone, M.E. and B.M. Lyttle, *Endometriosis and ovarian cancer: links, risks, and challenges faced.* International journal of women's health, 2015. **7**: p. 663.
55. Sampson, J.A., *Metastatic or embolic endometriosis, due to the menstrual dissemination of endometrial tissue into the venous circulation.* The American journal of pathology, 1927. **3**(2): p. 93.
56. Brosens, I. and G. Benagiano, *Perinatal origin of endometriosis revisited*. 2015, Taylor & Francis.
57. Fukunaga, M., et al., *Ovarian atypical endometriosis: its close association with malignant epithelial tumours.* Histopathology, 1997. **30**(3): p. 249-255.
58. De La Cuesta, R.S., et al., *Histologic transformation of benign endometriosis to early epithelial ovarian cancer.* Gynecologic oncology, 1996. **60**(2): p. 238-244.
59. Fujii, K., et al., *Ovarian mucinous tumors arising from mature cystic teratomas—a molecular genetic approach for understanding the cellular origin.* Human pathology, 2014. **45**(4): p. 717-724.
60. Kerr, S.E., et al., *Matching maternal isodisomy in mucinous carcinomas and associated ovarian teratomas provides evidence of germ cell derivation for some mucinous ovarian tumors.* The American journal of surgical pathology, 2013. **37**(8): p. 1229-1235.
61. Wang, Y., et al., *Clonality analysis of combined Brenner and mucinous tumours of the ovary reveals their monoclonal origin.* The Journal of pathology, 2015. **237**(2): p. 146-151.
62. Kuhn, E., R.J. Kurman, and I.-M. Shih, *Ovarian cancer is an imported disease: fact or fiction?* Current obstetrics and gynecology reports, 2012. **1**(1): p. 1-9.
63. Rockhill, B., *Proteomic patterns in serum and identification of ovarian cancer.* Lancet, 2002. **360**(9327): p. 169.
64. Gehlenborg, N., et al., *Visualization of omics data for systems biology.* Nature methods, 2010. **7**(3s): p. S56.
65. Hanahan, D. and R.A. Weinberg, *Hallmarks of cancer: the next generation.* cell, 2011. **144**(5): p. 646-674.
66. Pal, T., et al., *BRCA1 and BRCA2 mutations account for a large proportion of ovarian carcinoma cases.* Cancer, 2005. **104**(12): p. 2807-2816.
67. King, M.-C., J.H. Marks, and J.B. Mandell, *Breast and ovarian cancer risks due to inherited mutations in BRCA1 and BRCA2.* Science, 2003. **302**(5645): p. 643-646.
68. Campeau, P.M., W.D. Foulkes, and M.D. Tischkowitz, *Hereditary breast cancer: new genetic developments, new therapeutic avenues.* Human genetics, 2008. **124**(1): p. 31-42.
69. Easton, D.F., *How many more breast cancer predisposition genes are there?* Breast Cancer Research, 1999. **1**(1): p. 14.
70. Kuchenbaecker, K.B., et al., *Identification of six new susceptibility loci for invasive epithelial ovarian cancer.* Nature genetics, 2015. **47**(2): p. 164.
71. Pharoah, P.D., et al., *Polygenic susceptibility to breast cancer and implications for prevention.* Nature genetics, 2002. **31**(1): p. 33.
72. Belanger, M.H., et al., *A targeted analysis identifies a high frequency of BRCA1 and BRCA2 mutation carriers in women with ovarian cancer from a founder population.* Journal of ovarian research, 2015. **8**(1): p. 1.
73. Network, C.G.A.R., *Integrated genomic analyses of ovarian carcinoma.* Nature, 2011. **474**(7353): p. 609.
74. Ahmed, A.A., et al., *Driver mutations in TP53 are ubiquitous in high grade serous carcinoma of the ovary.* The Journal of pathology, 2010. **221**(1): p. 49-56.
75. Dehari, R., et al., *The development of high-grade serous carcinoma from atypical proliferative (borderline) serous tumors and low-grade micropapillary serous carcinoma: a morphologic and molecular genetic analysis.* The American journal of surgical pathology, 2007. **31**(7): p. 1007-1012.
76. Vang, R., et al., *Molecular alterations of TP53 are a defining feature of ovarian high-grade serous carcinoma: a rereview of cases lacking TP53 mutations in the cancer genome atlas ovarian study.* International journal of gynecological pathology: official journal of the International Society of Gynecological Pathologists, 2016. **35**(1): p. 48.
77. Hennessy, B.T., et al., *Somatic mutations in BRCA1 and BRCA2 could expand the number of patients that benefit from poly (ADP ribose) polymerase inhibitors in ovarian cancer.* Journal of Clinical Oncology, 2010. **28**(22): p. 3570.

78. Pennington, K.P., et al., *Germline and somatic mutations in homologous recombination genes predict platinum response and survival in ovarian, fallopian tube, and peritoneal carcinomas.* Clinical Cancer Research, 2014. **20**(3): p. 764-775.
79. Martins, F.C., et al., *Combined image and genomic analysis of high-grade serous ovarian cancer reveals PTEN loss as a common driver event and prognostic classifier.* Genome biology, 2014. **15**(12): p. 526.
80. Lagos-Quintana, M., et al., *Identification of novel genes coding for small expressed RNAs.* Science, 2001. **294**(5543): p. 853-858.
81. Lujambio, A., et al., *A microRNA DNA methylation signature for human cancer metastasis.* Proceedings of the National Academy of Sciences, 2008. **105**(36): p. 13556-13561.
82. Hammond, S.M., A.A. Caudy, and G.J. Hannon, *Post-transcriptional gene silencing by double-stranded RNA.* Nature Reviews Genetics, 2001. **2**: p. 110.
83. Ambros, V., *microRNAs: Tiny Regulators with Great Potential.* Cell, 2001. **107**(7): p. 823-826.
84. Lee, R.C., R.L. Feinbaum, and V. Ambros, *The C. elegans heterochronic gene lin-4 encodes small RNAs with antisense complementarity to lin-14.* Cell, 1993. **75**(5): p. 843-854.
85. Wightman, B., I. Ha, and G. Ruvkun, *Posttranscriptional regulation of the heterochronic gene lin-14 by lin-4 mediates temporal pattern formation in C. elegans.* Cell, 1993. **75**(5): p. 855-862.
86. Reinhart, B.J., et al., *The 21-nucleotide let-7 RNA regulates developmental timing in Caenorhabditis elegans.* Nature, 2000. **403**: p. 901.
87. Vidigal, J.A. and A. Ventura, *The biological functions of miRNAs: lessons from in vivo studies.* Trends Cell Biol, 2015. **25**(3): p. 137-47.
88. Broderick, J.A. and P.D. Zamore, *MicroRNA therapeutics.* Gene Ther, 2011. **18**(12): p. 1104-10.
89. Ling, H., M. Fabbri, and G.A. Calin, *MicroRNAs and other non-coding RNAs as targets for anticancer drug development.* Nat Rev Drug Discov, 2013. **12**(11): p. 847-65.
90. Godnic, I., et al., *Genome-Wide and Species-Wide In Silico Screening for Intragenic MicroRNAs in Human, Mouse and Chicken.* PLOS ONE, 2013. **8**(6): p. e65165.
91. Ramalingam, P., et al., *Biogenesis of intronic miRNAs located in clusters by independent transcription and alternative splicing.* Rna, 2014. **20**(1): p. 76-87.
92. Kirigin, F.F., et al., *Dynamic MicroRNA Gene Transcription and Processing during T Cell Development.* The Journal of Immunology, 2012. **188**(7): p. 3257-3267.
93. Lee, Y., et al., *MicroRNA genes are transcribed by RNA polymerase II.* The EMBO journal, 2004. **23**(20): p. 4051-4060.
94. Kim, Y.-K., B. Kim, and V.N. Kim, *Re-evaluation of the roles of DROSHA, Exportin 5, and DICER in microRNA biogenesis.* Proceedings of the National Academy of Sciences, 2016. **113**(13): p. E1881-E1889.
95. Gregory, R.I., et al., *The Microprocessor complex mediates the genesis of microRNAs.* Nature, 2004. **432**(7014): p. 235.
96. Triboulet, R., et al., *Post-transcriptional control of DGCR8 expression by the Microprocessor.* RNA, 2009. **15**(6): p. 1005-1011.
97. Bohnsack, M.T., K. Czaplinski, and D. GÖRlich, *Exportin 5 is a RanGTP-dependent dsRNA-binding protein that mediates nuclear export of pre-miRNAs.* RNA, 2004. **10**(2): p. 185-191.
98. Lund, E. and J. Dahlberg. *Substrate selectivity of exportin 5 and Dicer in the biogenesis of microRNAs*. in *Cold Spring Harbor symposia on quantitative biology*. 2006. Cold Spring Harbor Laboratory Press.
99. Grishok, A., et al., *Genes and mechanisms related to RNA interference regulate expression of the small temporal RNAs that control C. elegans developmental timing.* Cell, 2001. **106**(1): p. 23-34.
100. Bernstein, E., et al., *Role for a bidentate ribonuclease in the initiation step of RNA interference.* Nature, 2001. **409**(6818): p. 363.
101. Knight, S.W. and B.L. Bass, *A role for the RNase III enzyme DCR-1 in RNA interference and germ line development in Caenorhabditis elegans.* Science, 2001. **293**(5538): p. 2269-2271.
102. Hammond, S.M., et al., *An RNA-directed nuclease mediates post-transcriptional gene silencing in Drosophila cells.* Nature, 2000. **404**: p. 293.
103. Gregory, R.I., et al., *Human RISC Couples MicroRNA Biogenesis and Posttranscriptional Gene Silencing.* Cell, 2005. **123**(4): p. 631-640.
104. Hammond, S.M., et al., *Argonaute2, a link between genetic and biochemical analyses of RNAi.* Science, 2001. **293**(5532): p. 1146-1150.
105. Kawamata, T. and Y. Tomari, *Making RISC.* Trends in Biochemical Sciences, 2010. **35**(7): p. 368-376.
106. Su, H., et al., *Essential and overlapping functions for mammalian Argonautes in microRNA silencing.* Genes Dev, 2009. **23**(3): p. 304-17.

107. Pfaff, J. and G. Meister, *Argonaute and GW182 proteins: an effective alliance in gene silencing.* Biochem Soc Trans, 2013. **41**(4): p. 855-60.
108. Moor, C.H.d., H. Meijer, and S. Lissenden, *Mechanisms of translational control by the 3′ UTR in development and differentiation.* Seminars in Cell & Developmental Biology, 2005. **16**(1): p. 49-58.
109. Watanabe, K., et al., *Genome structure-based screening identified epigenetically silenced microRNA associated with invasiveness in non-small-cell lung cancer.* International Journal of Cancer, 2012. **130**(11): p. 2580-2590.
110. Lai, E.C., *Micro RNAs are complementary to 3′ UTR sequence motifs that mediate negative post-transcriptional regulation.* Nature Genetics, 2002. **30**: p. 363.
111. Filipowicz, W., S.N. Bhattacharyya, and N. Sonenberg, *Mechanisms of post-transcriptional regulation by microRNAs: are the answers in sight?* Nat Rev Genet, 2008. **9**(2): p. 102-14.
112. Chiang, H.R., et al., *Mammalian microRNAs: experimental evaluation of novel and previously annotated genes.* Genes & development, 2010. **24**(10): p. 992-1009.
113. Kozomara, A. and S. Griffiths-Jones, *miRBase: annotating high confidence microRNAs using deep sequencing data.* Nucleic acids research, 2013. **42**(D1): p. D68-D73.
114. de Rie, D., et al., *An integrated expression atlas of miRNAs and their promoters in human and mouse.* Nature Biotechnology, 2017. **35**: p. 872.
115. Griffiths-Jones, S., et al., *MicroRNA evolution by arm switching.* EMBO Rep, 2011. **12**(2): p. 172-7.
116. Guo, L., et al., *Evolutionary and expression analysis of miR-#-5p and miR-#-3p at the miRNAs/isomiRs levels.* BioMed research international, 2015. **2015**.
117. Valencia-Sanchez, M.A., et al., *Control of translation and mRNA degradation by miRNAs and siRNAs.* Genes Dev, 2006. **20**(5): p. 515-24.
118. Huntzinger, E. and E. Izaurralde, *Gene silencing by microRNAs: contributions of translational repression and mRNA decay.* Nat Rev Genet, 2011. **12**(2): p. 99-110.
119. Xu, W., et al., *Identifying microRNA targets in different gene regions.* BMC Bioinformatics, 2014. **15 Suppl 7**: p. S4.
120. Dharap, A., et al., *MicroRNA miR-324-3p induces promoter-mediated expression of RelA gene.* PLoS One, 2013. **8**(11): p. e79467.
121. Forman, J.J., A. Legesse-Miller, and H.A. Coller, *A search for conserved sequences in coding regions reveals that the let-7 microRNA targets Dicer within its coding sequence.* Proc Natl Acad Sci U S A, 2008. **105**(39): p. 14879-84.
122. Zhang, J., et al., *Oncogenic role of microRNA-532-5p in human colorectal cancer via targeting of the 5'UTR of RUNX3.* Oncology letters, 2018. **15**(5): p. 7215-7220.
123. Kawamata, T. and Y. Tomari, *Making RISC.* Trends Biochem Sci, 2010. **35**(7): p. 368-76.
124. Jo, M.H., et al., *Human Argonaute 2 Has Diverse Reaction Pathways on Target RNAs.* Mol Cell, 2015. **59**(1): p. 117-24.
125. Ameres, S.L., et al., *Target RNA-directed trimming and tailing of small silencing RNAs.* Science, 2010. **328**(5985): p. 1534-9.
126. Jonas, S. and E. Izaurralde, *Towards a molecular understanding of microRNA-mediated gene silencing.* Nat Rev Genet, 2015. **16**(7): p. 421-33.
127. Meister, G., et al., *Human Argonaute2 mediates RNA cleavage targeted by miRNAs and siRNAs.* Mol Cell, 2004. **15**(2): p. 185-97.
128. Inada, T. and S. Makino, *Novel roles of the multi-functional CCR4-NOT complex in post-transcriptional regulation.* Frontiers in Genetics, 2014. **5**: p. 135.
129. Wilczynska, A. and M. Bushell, *The complexity of miRNA-mediated repression.* Cell Death Differ, 2015. **22**(1): p. 22-33.
130. Shivdasani, R.A., *MicroRNAs: regulators of gene expression and cell differentiation.* Blood, 2006. **108**(12): p. 3646-3653.
131. Calin, G.A., et al., *Human microRNA genes are frequently located at fragile sites and genomic regions involved in cancers.* Proc Natl Acad Sci U S A, 2004. **101**(9): p. 2999-3004.
132. Creighton, C.J., et al., *Integrated analyses of microRNAs demonstrate their widespread influence on gene expression in high-grade serous ovarian carcinoma.* PLoS One, 2012. **7**(3): p. e34546.
133. Bayani, J., et al., *Copy number and expression alterations of miRNAs in the ovarian cancer cell line OVCAR-3: impact on kallikrein 6 protein expression.* Clin Chem, 2013. **59**(1): p. 296-305.
134. Scott, G.K., et al., *Rapid alteration of microRNA levels by histone deacetylase inhibition.* Cancer Res, 2006. **66**(3): p. 1277-81.
135. Weber, B., et al., *Methylation of human microRNA genes in normal and neoplastic cells.* Cell Cycle, 2007.

6(9): p. 1001-5.
136. Suzuki, H., et al., *Methylation-associated silencing of microRNA-34b/c in gastric cancer and its involvement in an epigenetic field defect.* Carcinogenesis, 2010. **31**(12): p. 2066-73.
137. Ozsolak, F., et al., *Chromatin structure analyses identify miRNA promoters.* Genes Dev, 2008. **22**(22): p. 3172-83.
138. Wang, P., et al., *Methylation-mediated silencing of the miR-124 genes facilitates pancreatic cancer progression and metastasis by targeting Rac1.* Oncogene, 2014. **33**(4): p. 514-24.
139. Wong, K.Y., et al., *Epigenetic inactivation of the miR-124-1 in haematological malignancies.* PLoS One, 2011. **6**(4): p. e19027.
140. Kumar, M.S., et al., *Impaired microRNA processing enhances cellular transformation and tumorigenesis.* Nat Genet, 2007. **39**(5): p. 673-7.
141. Bernstein, E., et al., *Dicer is essential for mouse development.* Nature genetics, 2003. **35**(3): p. 215.
142. Kanellopoulou, C., et al., *Dicer-deficient mouse embryonic stem cells are defective in differentiation and centromeric silencing.* Genes & development, 2005. **19**(4): p. 489-501.
143. Murchison, E.P., et al., *Characterization of Dicer-deficient murine embryonic stem cells.* Proceedings of the National Academy of Sciences of the United States of America, 2005. **102**(34): p. 12135-12140.
144. Kumar, M.S., et al., *Dicer1 functions as a haploinsufficient tumor suppressor.* Genes Dev, 2009. **23**(23): p. 2700-4.
145. Melo, S.A., et al., *A genetic defect in exportin-5 traps precursor microRNAs in the nucleus of cancer cells.* Cancer Cell, 2010. **18**(4): p. 303-15.
146. Curtale, G., *MiRNAs at the Crossroads between Innate Immunity and Cancer: Focus on Macrophages.* Cells, 2018. **7**(2): p. 12.
147. Rogers, G.W., N.J. Richter, and W.C. Merrick, *Biochemical and Kinetic Characterization of the RNA Helicase Activity of Eukaryotic Initiation Factor 4A.* Journal of Biological Chemistry, 1999. **274**(18): p. 12236-12244.
148. Tomonaga, T., et al., *Identification of Altered Protein Expression and Post-Translational Modifications in Primary Colorectal Cancer by Using Agarose Two-Dimensional Gel Electrophoresis.* Clinical Cancer Research, 2004. **10**(6): p. 2007-2014.
149. Eulalio, A., et al., *Functional screening identifies miRNAs inducing cardiac regeneration.* Nature, 2012. **492**(7429): p. 376-381.
150. Salem, M., et al., *miR-590-3p Promotes Ovarian Cancer Growth and Metastasis via a Novel FOXA2-Versican Pathway.* Cancer Res, 2018. **78**(15): p. 4175-4190.
151. Miao, M.-h., et al., *miR-590 promotes cell proliferation and invasion in T-cell acute lymphoblastic leukaemia by inhibiting RB1.* Oncotarget, 2016. **7**(26): p. 39527-39534.
152. Sun, Z.Q., et al., *MiR-590-3p promotes proliferation and metastasis of colorectal cancer via Hippo pathway.* Oncotarget, 2017.
153. Chen, L., et al., *MicroRNA-590-3p enhances the radioresistance in glioblastoma cells by targeting LRIG1.* Exp Ther Med, 2017. **14**(2): p. 1818-1824.
154. Feng, Z., et al., *miR-590-3p promotes colon cancer cell proliferation via Wnt/β-catenin signaling pathway by inhibiting WIF1 and DKK1.* European review for medical and pharmacological sciences, 2017. **21**(21): p. 4844-4852.
155. Ge, X. and L. Gong, *MiR-590-3p suppresses hepatocellular carcinoma growth by targeting TEAD1.* Tumour Biol, 2017. **39**(3): p. 1010428317695947.
156. Mo, M., et al., *Roles of mitochondrial transcription factor A and microRNA-590-3p in the development of bladder cancer.* Oncol Lett, 2013. **6**(2): p. 617-623.
157. Myatt, S.S. and E.W. Lam, *The emerging roles of forkhead box (Fox) proteins in cancer.* Nat Rev Cancer, 2007. **7**(11): p. 847-59.
158. Jackson, B.C., et al., *Update of human and mouse forkhead box (FOX) gene families.* Human Genomics, 2010. **4**(5): p. 345.
159. Weigel, D., et al., *The homeotic gene fork head encodes a nuclear protein and is expressed in the terminal regions of the Drosophila embryo.* Cell, 1989. **57**(4): p. 645-658.
160. Lai, E., et al., *HNF-3A, a hepatocyte-enriched transcription factor of novel structure is regulated transcriptionally.* Genes & Development, 1990. **4**(8): p. 1427-1436.
161. Weigel, D. and H. Jäckle, *The fork head domain: A novel DNA binding motif of eukaryotic transcription factors?* Cell, 1990. **63**(3): p. 455-456.
162. Clark, K.L., et al., *Co-crystal structure of the HNF-3/fork head DNA-recognition motif resembles histone H5.* Nature, 1993. **364**(6436): p. 412.

163. Kaestner, K.H., W. Knöchel, and D.E. Martínez, *Unified nomenclature for the winged helix/forkhead transcription factors.* Genes & Development, 2000. **14**(2): p. 142-146.
164. Friedman, J. and K. Kaestner, *The Foxa family of transcription factors in development and metabolism.* Cellular and Molecular Life Sciences CMLS, 2006. **63**(19-20): p. 2317-2328.
165. Maruyama, R., et al., *Genome-wide analysis reveals a major role in cell fate maintenance and an unexpected role in endoreduplication for the Drosophila FoxA gene Fork head.* PloS one, 2011. **6**(6): p. e20901.
166. Wolfrum, C., et al., *Foxa2 regulates lipid metabolism and ketogenesis in the liver during fasting and in diabetes.* Nature, 2004. **432**(7020): p. 1027.
167. Weinstein, D.C., et al., *The winged-helix transcription factor HNF-3β is required for notochord development in the mouse embryo.* Cell, 1994. **78**(4): p. 575-588.
168. Lee, C.S., et al., *The initiation of liver development is dependent on Foxa transcription factors.* Nature, 2005. **435**(7044): p. 944.
169. Li, C.M.-C., et al., *Foxa2 and Cdx2 cooperate with Nkx2-1 to inhibit lung adenocarcinoma metastasis.* Genes & Development, 2015. **29**(17): p. 1850-1862.
170. Tang, Y., et al., *FOXA2 functions as a suppressor of tumor metastasis by inhibition of epithelial-to-mesenchymal transition in human lung cancers.* Cell research, 2011. **21**(2): p. 316.
171. Vorvis, C., et al., *Transcriptomic and CRISPR/Cas9 technologies reveal FOXA2 as a tumor suppressor gene in pancreatic cancer.* American Journal of Physiology-Gastrointestinal and Liver Physiology, 2016. **310**(11): p. G1124-G1137.
172. Zhu, C.-P., et al., *The Transcription Factor FOXA2 Suppresses Gastric Tumorigenesis In Vitro and In Vivo.* Digestive Diseases and Sciences, 2015. **60**(1): p. 109-117.
173. Li, Z., et al., *Foxa1 and Foxa2 are Essential for Sexual Dimorphism in Liver Cancer.* Cell, 2012. **148**(1-2): p. 72-83.
174. Zaret, K.S. and J.S. Carroll, *Pioneer transcription factors: establishing competence for gene expression.* Genes & Development, 2011. **25**(21): p. 2227-2241.
175. Sekiya, T., et al., *Nucleosome-binding affinity as a primary determinant of the nuclear mobility of the pioneer transcription factor FoxA.* Genes & Development, 2009. **23**(7): p. 804-809.
176. Romanelli, M.G., et al., *Nuclear localization domains in human thyroid transcription factor 2.* Biochimica et Biophysica Acta (BBA) - Molecular Cell Research, 2003. **1643**(1): p. 55-64.
177. Benayoun, B.A., S. Caburet, and R.A. Veitia, *Forkhead transcription factors: key players in health and disease.* Trends in Genetics, 2011. **27**(6): p. 224-232.
178. Sun, L., X.-J. Tang, and F.-M. Luo, *Forkhead box protein A2 and T helper type 2-mediated pulmonary inflammation.* World Journal of Methodology, 2015. **5**(4): p. 223-229.
179. Koon, H.B., et al., *FOXP1: a potential therapeutic target in cancer.* Expert Opin Ther Targets, 2007. **11**(7): p. 955-65.
180. Gartel, A.L., *A new target for proteasome inhibitors: FoxM1.* Expert Opin Investig Drugs, 2010. **19**(2): p. 235-42.
181. Nakshatri, H. and S. Badve, *FOXA1 as a therapeutic target for breast cancer.* Expert Opin Ther Targets, 2007. **11**(4): p. 507-14.
182. Carroll, J.S., et al., *Chromosome-Wide Mapping of Estrogen Receptor Binding Reveals Long-Range Regulation Requiring the Forkhead Protein FoxA1.* Cell, 2005. **122**(1): p. 33-43.
183. Gao, N., et al., *The Role of Hepatocyte Nuclear Factor-3α (Forkhead Box A1) and Androgen Receptor in Transcriptional Regulation of Prostatic Genes.* Molecular Endocrinology, 2003. **17**(8): p. 1484-1507.
184. Sorlie, T., et al., *Gene expression patterns of breast carcinomas distinguish tumor subclasses with clinical implications.* Proc Natl Acad Sci U S A, 2001. **98**(19): p. 10869-74.
185. Song, Y., M.K. Washington, and H.C. Crawford, *Loss of FOXA1/2 is essential for the epithelial-to-mesenchymal transition in pancreatic cancer.* Cancer research, 2010: p. 0008-5472. CAN-09-2979.
186. Liu, Y.-N., et al., *Regulatory mechanisms controlling human E-cadherin gene expression.* Oncogene, 2005. **24**(56): p. 8277-8290.
187. Rahmani, M., et al., *Versican: signaling to transcriptional control pathwaysThis paper is one of a selection of papers published in this Special Issue, entitled Young Investigator's Forum.* Canadian Journal of Physiology and Pharmacology, 2006. **84**(1): p. 77-92.
188. Ingber, D.E. and J. Folkman, *How does extracellular matrix control capillary morphogenesis?* Cell, 1989. **58**(5): p. 803-5.
189. Aruga, J., N. Yokota, and K. Mikoshiba, *Human SLITRK family genes: genomic organization and expression profiling in normal brain and brain tumor tissue.* Gene, 2003. **315**: p. 87-94.

190. Isogai, Z., et al., *2B1 antigen characteristically expressed on extracellular matrices of human malignant tumors is a large chondroitin sulfate proteoglycan, PG-M/versican.* Cancer Res, 1996. **56**(17): p. 3902-8.
191. Lebaron, R.G., *Versican.* Perspect Dev Neurobiol, 1996. **3**(4): p. 261-71.
192. Dours-Zimmermann, M.T. and D.R. Zimmermann, *A novel glycosaminoglycan attachment domain identified in two alternative splice variants of human versican.* Journal of Biological Chemistry, 1994. **269**(52): p. 32992-32998.
193. Naso, M.F., D.R. Zimmermann, and R.V. Iozzo, *Characterization of the complete genomic structure of the human versican gene and functional analysis of its promoter.* Journal of Biological Chemistry, 1994. **269**(52): p. 32999-33008.
194. Kischel, P., et al., *Versican overexpression in human breast cancer lesions: known and new isoforms for stromal tumor targeting.* International Journal of Cancer, 2010. **126**(3): p. 640-650.
195. Arslan, F., et al., *The role of versican isoforms V0/V1 in glioma migration mediated by transforming growth factor-beta2.* Br J Cancer, 2007. **96**(10): p. 1560-8.
196. Wight, T.N., *Versican: a versatile extracellular matrix proteoglycan in cell biology.* Current Opinion in Cell Biology, 2002. **14**(5): p. 617-623.
197. Perissinotto, D., et al., *Avian neural crest cell migration is diversely regulated by the two major hyaluronan-binding proteoglycans PG-M/versican and aggrecan.* Development, 2000. **127**(13): p. 2823-42.
198. Sakko, A.J., et al., *Versican accumulation in human prostatic fibroblast cultures is enhanced by prostate cancer cell-derived transforming growth factor beta1.* Cancer Res, 2001. **61**(3): p. 926-30.
199. Sheng, W., et al., *The roles of versican V1 and V2 isoforms in cell proliferation and apoptosis.* Mol Biol Cell, 2005. **16**(3): p. 1330-40.
200. Lemire, J.M., et al., *Overexpression of the V3 variant of versican alters arterial smooth muscle cell adhesion, migration, and proliferation in vitro.* J Cell Physiol, 2002. **190**(1): p. 38-45.
201. Serra, M., et al., *V3 versican isoform expression alters the phenotype of melanoma cells and their tumorigenic potential.* Int J Cancer, 2005. **114**(6): p. 879-86.
202. Miquel-Serra, L., et al., *V3 versican isoform expression has a dual role in human melanoma tumor growth and metastasis.* Lab Invest, 2006. **86**(9): p. 889-901.
203. Voutilainen, K., et al., *Versican in epithelial ovarian cancer: relation to hyaluronan, clinicopathologic factors and prognosis.* International Journal of Cancer, 2003. **107**(3): p. 359-364.
204. Casey, R.C., et al., *Cell membrane glycosylation mediates the adhesion, migration, and invasion of ovarian carcinoma cells.* Clinical & experimental metastasis, 2003. **20**(2): p. 143-152.
205. Lancaster, J., et al., *Identification of genes associated with ovarian cancer metastasis using microarray expression analysis.* International Journal of Gynecological Cancer, 2006. **16**(5): p. 1733-1745.
206. Zagorianakou, N., et al., *CD44s expression, in benign, borderline and malignant tumors of ovarian surface epithelium. Correlation with p53, steroid receptor status, proliferative indices (PCNA, MIB1) and survival.* Anticancer research, 2004. **24**(3A): p. 1665-1670.
207. Sakko, A.J., et al., *Versican accumulation in human prostatic fibroblast cultures is enhanced by prostate cancer cell-derived transforming growth factor β1.* Cancer Research, 2000. **61**(3): p. 926-930.
208. Casey, R.C., et al., *Establishment of an in vitro assay to measure the invasion of ovarian carcinoma cells through mesothelial cell monolayers.* Clinical & experimental metastasis, 2003. **20**(4): p. 343-356.
209. Ricciardelli, C., et al., *Formation of hyaluronan-and versican-rich pericellular matrix by prostate cancer cells promotes cell motility.* Journal of Biological Chemistry, 2007. **282**(14): p. 10814-10825.
210. Ween, M.P., et al., *Versican induces a pro-metastatic ovarian cancer cell behavior which can be inhibited by small hyaluronan oligosaccharides.* Clin Exp Metastasis, 2011. **28**(2): p. 113-25.
211. Russell, D.L., et al., *Hormone-regulated expression and localization of versican in the rodent ovary.* Endocrinology, 2003. **144**(3): p. 1020-31.
212. Ricciardelli, C., et al., *The biological role and regulation of versican levels in cancer.* Cancer Metastasis Rev, 2009. **28**(1-2): p. 233-45.
213. Cattaruzza, S., et al., *Distribution of PG-M/versican variants in human tissues and de novo expression of isoform V3 upon endothelial cell activation, migration, and neoangiogenesis in vitro.* J Biol Chem, 2002. **277**(49): p. 47626-35.
214. Hakkinen, L., et al., *Human granulation-tissue fibroblasts show enhanced proteoglycan gene expression and altered response to TGF-beta 1.* J Dent Res, 1996. **75**(10): p. 1767-78.
215. Anttila, M.A., et al., *High levels of stromal hyaluronan predict poor disease outcome in epithelial ovarian cancer.* Cancer Res, 2000. **60**(1): p. 150-5.
216. Bernaudo, S., et al., *Cyclin G2 inhibits epithelial-to-mesenchymal transition by disrupting Wnt/β-catenin*

signaling. Oncogene, 2016. **35**(36): p. 4816-4827.
217. Johnson, D.G. and C.L. Walker, *Cyclins and cell cycle checkpoints.* Annu Rev Pharmacol Toxicol, 1999. **39**: p. 295-312.
218. Morgan, D.O., *Cyclin-dependent kinases: engines, clocks, and microprocessors.* Annu Rev Cell Dev Biol, 1997. **13**: p. 261-91.
219. Pines, J., *Cyclins and cyclin-dependent kinases: theme and variations.* Adv Cancer Res, 1995. **66**: p. 181-212.
220. Bates, S., S. Rowan, and K.H. Vousden, *Characterisation of human cyclin G1 and G2: DNA damage inducible genes.* Oncogene, 1996. **13**(5): p. 1103-9.
221. Horne, M.C., et al., *Cyclin G1 and Cyclin G2 Comprise a New Family of Cyclins with Contrasting Tissue-specific and Cell Cycle-regulated Expression.* Journal of Biological Chemistry, 1996. **271**(11): p. 6050-6061.
222. Adorno, M., et al., *A Mutant-p53/Smad complex opposes p63 to empower TGFbeta-induced metastasis.* Cell, 2009. **137**(1): p. 87-98.
223. Choi, M.G., et al., *Expression levels of cyclin G2, but not cyclin E, correlate with gastric cancer progression.* J Surg Res, 2009. **157**(2): p. 168-74.
224. Kim, Y., et al., *Cyclin G2 dysregulation in human oral cancer.* Cancer Res, 2004. **64**(24): p. 8980-6.
225. Ito, Y., et al., *Decreased expression of cyclin G2 is significantly linked to the malignant transformation of papillary carcinoma of the thyroid.* Anticancer Res, 2003. **23**(3b): p. 2335-8.
226. Jia, J.S., et al., *[Expression of cyclin g2 mRNA in patients with acute leukemia and its clinical significance.].* Zhongguo Shi Yan Xue Ye Xue Za Zhi, 2005. **13**(2): p. 254-9.
227. Xu, G., et al., *Cyclin G2 Is Degraded through the Ubiquitin-Proteasome Pathway and Mediates the Antiproliferative Effect of Activin Receptor-like Kinase 7.* Molecular Biology of the Cell, 2008. **19**(11): p. 4968-4979.
228. Fu, G. and C. Peng, *Nodal enhances the activity of FoxO3a and its synergistic interaction with Smads to regulate cyclin G2 transcription in ovarian cancer cells.* Oncogene, 2011. **30**(37): p. 3953.
229. Bernaudo, S., et al., *Cyclin G2 inhibits epithelial-to-mesenchymal transition by disrupting Wnt/β-catenin signaling.* Oncogene, 2016. **35**: p. 4816.
230. Martinez-Gac, L., et al., *Control of cyclin G2 mRNA expression by forkhead transcription factors: novel mechanism for cell cycle control by phosphoinositide 3-kinase and forkhead.* Mol Cell Biol, 2004. **24**(5): p. 2181-9.
231. Le, X.F., et al., *Roles of human epidermal growth factor receptor 2, c-jun NH2-terminal kinase, phosphoinositide 3-kinase, and p70 S6 kinase pathways in regulation of cyclin G2 expression in human breast cancer cells.* Mol Cancer Ther, 2007. **6**(11): p. 2843-57.
232. Bennin, D.A., et al., *Cyclin G2 associates with protein phosphatase 2A catalytic and regulatory B' subunits in active complexes and induces nuclear aberrations and a G1/S phase cell cycle arrest.* J Biol Chem, 2002. **277**(30): p. 27449-67.
233. Li, J.M. and G. Brooks, *Cell cycle regulatory molecules (cyclins, cyclin-dependent kinases and cyclin-dependent kinase inhibitors) and the cardiovascular system; potential targets for therapy?* Eur Heart J, 1999. **20**(6): p. 406-20.
234. Horne, M.C., et al., *Cyclin G2 is up-regulated during growth inhibition and B cell antigen receptor-mediated cell cycle arrest.* J Biol Chem, 1997. **272**(19): p. 12650-61.
235. Jensen, M.R., et al., *Gene structure and chromosomal localization of mouse cyclin G2 (Ccng2).* Gene, 1999. **230**(2): p. 171-80.
236. Horne, M.C., et al., *Cyclin G1 and cyclin G2 comprise a new family of cyclins with contrasting tissue-specific and cell cycle-regulated expression.* J Biol Chem, 1996. **271**(11): p. 6050-61.
237. Yue, L., et al., *Cyclin G1 and cyclin G2 are expressed in the periimplantation mouse uterus in a cell-specific and progesterone-dependent manner: evidence for aberrant regulation with Hoxa-10 deficiency.* Endocrinology, 2005. **146**(5): p. 2424-33.
238. Kasukabe, T., et al., *Effects of combined treatment with rapamycin and cotylenin A, a novel differentiation-inducing agent, on human breast carcinoma MCF-7 cells and xenografts.* Breast Cancer Res, 2005. **7**(6): p. R1097-110.
239. Gajate, C., F. An, and F. Mollinedo, *Differential cytostatic and apoptotic effects of ecteinascidin-743 in cancer cells. Transcription-dependent cell cycle arrest and transcription-independent JNK and mitochondrial mediated apoptosis.* J Biol Chem, 2002. **277**(44): p. 41580-9.
240. Olivier, S., et al., *Raloxifene-induced myeloma cell apoptosis: a study of nuclear factor-kappaB inhibition and gene expression signature.* Mol Pharmacol, 2006. **69**(5): p. 1615-23.

241. Liu, J., et al., *Effect of cyclin G2 on proliferative ability of SGC-7901 cell.* World J Gastroenterol, 2004. **10**(9): p. 1357-60.
242. Logan, C.Y. and R. Nusse, *The Wnt signaling pathway in development and disease.* Annu Rev Cell Dev Biol, 2004. **20**: p. 781-810.
243. Clevers, H., *Wnt/β-Catenin Signaling in Development and Disease.* Cell, 2006. **127**(3): p. 469-480.
244. Polakis, P., *The many ways of Wnt in cancer.* Current Opinion in Genetics & Development, 2007. **17**(1): p. 45-51.
245. Tetsu, O. and F. McCormick, *Beta-catenin regulates expression of cyclin D1 in colon carcinoma cells.* Nature, 1999. **398**(6726): p. 422-6.
246. Shtutman, M., et al., *The cyclin D1 gene is a target of the beta-catenin/LEF-1 pathway.* Proc Natl Acad Sci U S A, 1999. **96**(10): p. 5522-7.
247. Howe, L.R., et al., *Twist Is Up-Regulated in Response to Wnt1 and Inhibits Mouse Mammary Cell Differentiation.* Cancer Research, 2003. **63**(8): p. 1906-1913.
248. DiMeo, T.A., et al., *A novel lung metastasis signature links Wnt signaling with cancer cell self-renewal and epithelial-mesenchymal transition in basal-like breast cancer.* Cancer Res, 2009. **69**(13): p. 5364-73.
249. Nusse, R. and H.E. Varmus, *Wnt genes.* Cell, 1992. **69**(7): p. 1073-87.
250. Banziger, C., et al., *Wntless, a conserved membrane protein dedicated to the secretion of Wnt proteins from signaling cells.* Cell, 2006. **125**(3): p. 509-22.
251. Bartscherer, K., et al., *Secretion of Wnt ligands requires Evi, a conserved transmembrane protein.* Cell, 2006. **125**(3): p. 523-33.
252. Hsieh, J.C., et al., *Biochemical characterization of Wnt-frizzled interactions using a soluble, biologically active vertebrate Wnt protein.* Proc Natl Acad Sci U S A, 1999. **96**(7): p. 3546-51.
253. Mikels, A.J. and R. Nusse, *Wnts as ligands: processing, secretion and reception.* Oncogene, 2006. **25**(57): p. 7461-8.
254. He, X., et al., *LDL receptor-related proteins 5 and 6 in Wnt/beta-catenin signaling: arrows point the way.* Development, 2004. **131**(8): p. 1663-77.
255. Tamai, K., et al., *LDL-receptor-related proteins in Wnt signal transduction.* Nature, 2000. **407**(6803): p. 530-5.
256. Frame, S. and P. Cohen, *GSK3 takes centre stage more than 20 years after its discovery.* Biochem J, 2001. **359**(Pt 1): p. 1-16.
257. Yamamoto, H., et al., *Phosphorylation of axin, a Wnt signal negative regulator, by glycogen synthase kinase-3beta regulates its stability.* J Biol Chem, 1999. **274**(16): p. 10681-4.
258. Rubinfeld, B., D.A. Tice, and P. Polakis, *Axin-dependent phosphorylation of the adenomatous polyposis coli protein mediated by casein kinase 1epsilon.* J Biol Chem, 2001. **276**(42): p. 39037-45.
259. Zeng, X., et al., *A dual-kinase mechanism for Wnt co-receptor phosphorylation and activation.* Nature, 2005. **438**(7069): p. 873-7.
260. Cadigan, K.M. and M. Peifer, *Wnt signaling from development to disease: insights from model systems.* Cold Spring Harb Perspect Biol, 2009. **1**(2): p. a002881.
261. Cavallo, R.A., et al., *Drosophila Tcf and Groucho interact to repress Wingless signalling activity.* Nature, 1998. **395**(6702): p. 604-8.
262. Roose, J., et al., *The Xenopus Wnt effector XTcf-3 interacts with Groucho-related transcriptional repressors.* Nature, 1998. **395**(6702): p. 608-12.
263. Daniels, D.L. and W.I. Weis, *Beta-catenin directly displaces Groucho/TLE repressors from Tcf/Lef in Wnt-mediated transcription activation.* Nat Struct Mol Biol, 2005. **12**(4): p. 364-71.
264. Arce, L., N.N. Yokoyama, and M.L. Waterman, *Diversity of LEF/TCF action in development and disease.* Oncogene, 2006. **25**(57): p. 7492-504.
265. Hoppler, S. and C.L. Kavanagh, *Wnt signalling: variety at the core.* J Cell Sci, 2007. **120**(Pt 3): p. 385-93.
266. Li, F.Q., et al., *Chibby cooperates with 14-3-3 to regulate beta-catenin subcellular distribution and signaling activity.* J Cell Biol, 2008. **181**(7): p. 1141-54.
267. Tago, K., et al., *Inhibition of Wnt signaling by ICAT, a novel beta-catenin-interacting protein.* Genes Dev, 2000. **14**(14): p. 1741-9.
268. Voronkov, A. and S. Krauss, *Wnt/beta-catenin signaling and small molecule inhibitors.* Curr Pharm Des. **19**(4): p. 634-64.
269. Huber, A.H., W.J. Nelson, and W.I. Weis, *Three-dimensional structure of the armadillo repeat region of beta-catenin.* Cell, 1997. **90**(5): p. 871-82.
270. Bienz, M. and H. Clevers, *Armadillo/beta-catenin signals in the nucleus--proof beyond a reasonable doubt?* Nat Cell Biol, 2003. **5**(3): p. 179-82.

271. Robles-Frias, A., et al., *Robinson cytologic grading in invasive ductal carcinoma of the breast: correlation with E-cadherin and alpha-, beta- and gamma-catenin expression and regional lymph node metastasis.* Acta Cytol, 2006. **50**(2): p. 151-7.
272. Cai, C. and X. Zhu, *The Wnt/beta-catenin pathway regulates self-renewal of cancer stem-like cells in human gastric cancer.* Mol Med Rep. **5**(5): p. 1191-6.
273. Gaujoux, S., et al., *Silencing mutated beta-catenin inhibits cell proliferation and stimulates apoptosis in the adrenocortical cancer cell line H295R.* PLoS One. **8**(2): p. e55743.
274. Reya, T. and H. Clevers, *Wnt signalling in stem cells and cancer.* Nature, 2005. **434**(7035): p. 843-50.
275. Gamallo, C., et al., *β-catenin expression pattern in stage I and II ovarian carcinomas: relationship with β-catenin gene mutations, clinicopathological features, and clinical outcome.* The American journal of pathology, 1999. **155**(2): p. 527-536.
276. Palacios, J. and C. Gamallo, *Mutations in the beta-catenin gene (CTNNB1) in endometrioid ovarian carcinomas.* Cancer Res, 1998. **58**(7): p. 1344-7.
277. Gatcliffe, T.A., et al., *Wnt signaling in ovarian tumorigenesis.* International journal of gynecological cancer : official journal of the International Gynecological Cancer Society, 2008. **18**(5): p. 954-962.
278. Mohammed, M.K., et al., *Wnt/β-catenin signaling plays an ever-expanding role in stem cell self-renewal, tumorigenesis and cancer chemoresistance.* Genes & Diseases, 2016. **3**(1): p. 11-40.
279. Schindler, A.J., A. Watanabe, and S.B. Howell, *LGR5 and LGR6 in stem cell biology and ovarian cancer.* Oncotarget, 2018. **9**(1): p. 1346-1355.
280. Nagaraj, A.B., et al., *Critical role of Wnt/β-catenin signaling in driving epithelial ovarian cancer platinum resistance.* Oncotarget, 2015. **6**(27): p. 23720-23734.
281. Lee, E., et al., *The roles of APC and Axin derived from experimental and theoretical analysis of the Wnt pathway.* PLoS Biol, 2003. **1**(1): p. E10.
282. Cheng, H., et al., *Nuclear beta-catenin overexpression in metastatic sentinel lymph node is associated with synchronous liver metastasis in colorectal cancer.* Diagn Pathol. **6**: p. 109.
283. Wang, L., et al., *Prognostic value of nuclear beta-catenin overexpression at invasive front in colorectal cancer for synchronous liver metastasis.* Ann Surg Oncol. **18**(6): p. 1553-9.
284. Hou, J., et al., *Cytoplasmic HDPR1 is involved in regional lymph node metastasis and tumor development via beta-catenin accumulation in esophageal squamous cell carcinoma.* J Histochem Cytochem. **59**(7): p. 711-8.
285. Noordhuis, M.G., et al., *Involvement of the TGF-beta and beta-catenin pathways in pelvic lymph node metastasis in early-stage cervical cancer.* Clin Cancer Res. **17**(6): p. 1317-30.
286. Cheng, C.W., et al., *Prognostic significance of cyclin D1, beta-catenin, and MTA1 in patients with invasive ductal carcinoma of the breast.* Ann Surg Oncol. **19**(13): p. 4129-39.
287. Lee, J.M., et al., *The epithelial-mesenchymal transition: new insights in signaling, development, and disease.* J Cell Biol, 2006. **172**(7): p. 973-81.
288. Takahashi-Yanaga, F. and M. Kahn, *Targeting Wnt signaling: can we safely eradicate cancer stem cells?* Clin Cancer Res. **16**(12): p. 3153-62.
289. Ozols, R.F., *Systemic therapy for ovarian cancer: current status and new treatments.* Semin Oncol, 2006. **33**(2 Suppl 6): p. S3-11.
290. Lee, R.C. and V. Ambros, *An extensive class of small RNAs in Caenorhabditis elegans.* Science, 2001. **294**(5543): p. 862-4.
291. Kong, W., et al., *Strategies for profiling microRNA expression.* J Cell Physiol, 2009. **218**(1): p. 22-5.
292. Saini, H.K., S. Griffiths-Jones, and A.J. Enright, *Genomic analysis of human microRNA transcripts.* Proc Natl Acad Sci U S A, 2007. **104**(45): p. 17719-24.
293. Yang, H., et al., *Roles of miR-590-5p and miR-590-3p in the development of hepatocellular carcinoma.* Nan fang yi ke da xue xue bao= Journal of Southern Medical University, 2013. **33**(6): p. 804-811.
294. Keller, A., et al., *Next-generation sequencing identifies novel microRNAs in peripheral blood of lung cancer patients.* Molecular bioSystems, 2011. **7**(12): p. 3187-3199.

CHAPTER 2 REFERENCES

1. Coleman, R.L., et al., *Latest research and treatment of advanced-stage epithelial ovarian cancer.* Nature reviews Clinical oncology, 2013. **10**(4): p. 211-224.
2. Lengyel, E., *Ovarian cancer development and metastasis.* Am J Pathol, 2010. **177**(3): p. 1053-64.
3. Pradeep, S., et al., *Hematogenous metastasis of ovarian cancer: rethinking mode of spread.* Cancer Cell, 2014. **26**(1): p. 77-91.
4. Lin, S. and R.I. Gregory, *MicroRNA biogenesis pathways in cancer.* Nature reviews cancer, 2015. **15**(6): p. 321-333.
5. Eulalio, A., et al., *Functional screening identifies miRNAs inducing cardiac regeneration.* Nature, 2012. **492**(7429): p. 376-381.
6. Miao, M.-h., et al., *miR-590 promotes cell proliferation and invasion in T-cell acute lymphoblastic leukaemia by inhibiting RB1.* Oncotarget, 2016. **7**(26): p. 39527-39534.
7. Sun, Z.Q., et al., *MiR-590-3p promotes proliferation and metastasis of colorectal cancer via Hippo pathway.* Oncotarget, 2017.
8. Pang, H., et al., *miR-590-3p suppresses cancer cell migration, invasion and epithelial–mesenchymal transition in glioblastoma multiforme by targeting ZEB1 and ZEB2.* Biochemical and Biophysical Research Communications, 2015. **468**(4): p. 739-745.
9. Keller, A., et al., *Next-generation sequencing identifies novel microRNAs in peripheral blood of lung cancer patients.* Molecular bioSystems, 2011. **7**(12): p. 3187-3199.
10. Friedman, J.R. and K.H. Kaestner, *The Foxa family of transcription factors in development and metabolism.* Cellular and Molecular Life Sciences CMLS, 2006. **63**(19): p. 2317-2328.
11. Vorvis, C., et al., *Transcriptomic and CRISPR/Cas9 technologies reveal FOXA2 as a tumor suppressor gene in pancreatic cancer.* American Journal of Physiology - Gastrointestinal and Liver Physiology, 2016. **310**(11): p. G1124-G1137.
12. Li, C.M.-C., et al., *Foxa2 and Cdx2 cooperate with Nkx2-1 to inhibit lung adenocarcinoma metastasis.* Genes & Development, 2015. **29**(17): p. 1850-1862.
13. Tang, Y., et al., *FOXA2 functions as a suppressor of tumor metastasis by inhibition of epithelial-to-mesenchymal transition in human lung cancers.* Cell research, 2011. **21**(2): p. 316.
14. Zhu, C.-P., et al., *The Transcription Factor FOXA2 Suppresses Gastric Tumorigenesis In Vitro and In Vivo.* Digestive Diseases and Sciences, 2015. **60**(1): p. 109-117.
15. Zhang, Z., et al., *FOXA2 attenuates the epithelial to mesenchymal transition by regulating the transcription of E-cadherin and ZEB2 in human breast cancer.* Cancer Letters, 2015. **361**(2): p. 240-250.
16. Perez-Balaguer, A., et al., *FOXA2 mRNA expression is associated with relapse in patients with triple-negative/basal-like breast carcinoma.* Breast cancer research and treatment, 2015. **153**(2): p. 465-474.
17. Li, Z., et al., *Foxa1 and Foxa2 are Essential for Sexual Dimorphism in Liver Cancer.* Cell, 2012. **148**(1-2): p. 72-83.
18. Wight, T.N., *Provisional matrix: A role for versican and hyaluronan.* Matrix Biology, 2017. **60–61**: p. 38-56.
19. Ghosh, S., et al., *Up-regulation of stromal versican expression in advanced stage serous ovarian cancer.* Gynecologic oncology, 2010. **119**(1): p. 114-120.
20. Yeung, T.-L., et al., *TGF-β modulates ovarian cancer invasion by upregulating CAF-derived versican in the tumor microenvironment.* Cancer Research, 2013. **73**(16): p. 5016-5028.
21. Bernaudo, S., et al., *Cyclin G2 inhibits epithelial-to-mesenchymal transition by disrupting Wnt/β-catenin signaling.* Oncogene, 2016. **35**(36): p. 4816.
22. Ye, G., et al., *MicroRNA 376c enhances ovarian cancer cell survival by targeting activin receptor-like kinase 7: implications for chemoresistance.* J Cell Sci, 2011. **124**(Pt 3): p. 359-68.
23. Fu, G., et al., *MicroRNA-376c impairs transforming growth factor-beta and nodal signaling to promote trophoblast cell proliferation and invasion.* Hypertension, 2013. **61**(4): p. 864-72.
24. O'Brien, J., H. Hayder, and C. Peng, *Automated Quantification and Analysis of Cell Counting Procedures Using ImageJ Plugins.* J Vis Exp, 2016(117).
25. Fu, G. and C. Peng, *Nodal enhances the activity of FoxO3a and its synergistic interaction with Smads to regulate cyclin G2 transcription in ovarian cancer cells.* Oncogene, 2011. **30**(37): p. 3953-66.
26. Pundir, S., M.J. Martin, and C. O'Donovan, *UniProt Protein Knowledgebase.* Methods Mol Biol, 2017. **1558**: p. 41-55.
27. Kent, W.J., et al., *The human genome browser at UCSC.* Genome research, 2002. **12**(6): p. 996-1006.
28. Sanjana, N.E., O. Shalem, and F. Zhang, *Improved vectors and genome-wide libraries for CRISPR screening.* Nature methods, 2014. **11**(8): p. 783-784.
29. Gao, J., et al., *Integrative analysis of complex cancer genomics and clinical profiles using the cBioPortal.*

Sci Signal, 2013. **6**(269): p. 1-20.
30. Metzakopian, E., et al., *Genome-wide characterization of Foxa2 targets reveals upregulation of floor plate genes and repression of ventrolateral genes in midbrain dopaminergic progenitors.* Development, 2012. **139**(14): p. 2625-2634.
31. Adorno, M., et al., *A Mutant-p53/Smad complex opposes p63 to empower TGFbeta-induced metastasis.* Cell, 2009. **137**(1): p. 87-98.
32. Feng, Z., et al., *miR-590-3p promotes colon cancer cell proliferation via Wnt/β-catenin signaling pathway by inhibiting WIF1 and DKK1.* European review for medical and pharmacological sciences, 2017. **21**(21): p. 4844-4852.
33. Chen, L., et al., *MicroRNA-590-3p enhances the radioresistance in glioblastoma cells by targeting LRIG1.* Exp Ther Med, 2017. **14**(2): p. 1818-1824.
34. Ge, X. and L. Gong, *MiR-590-3p suppresses hepatocellular carcinoma growth by targeting TEAD1.* Tumor Biol, 2017. **39**(3): p. 1010428317695947.
35. Mo, M., et al., *Roles of mitochondrial transcription factor A and microRNA-590-3p in the development of bladder cancer.* Oncol Lett, 2013. **6**(2): p. 617-623.
36. Schwede, M., et al., *Stem cell-like gene expression in ovarian cancer predicts type II subtype and prognosis.* PLoS One, 2013. **8**(3): p. e57799.
37. Desjardins, M., et al., *Versican regulates metastasis of epithelial ovarian carcinoma cells and spheroids.* J Ovarian Res, 2014. **7**: p. 70.
38. Sheng, W., et al., *The roles of versican V1 and V2 isoforms in cell proliferation and apoptosis.* Mol Biol Cell, 2005. **16**(3): p. 1330-40.
39. Du, W.W., W. Yang, and A.J. Yee, *Roles of versican in cancer biology--tumorigenesis, progression and metastasis.* Histol Histopathol, 2013. **28**(6): p. 701-13.
40. Foulcer, S.J., et al., *Determinants of versican-V1 proteoglycan processing by the metalloproteinase ADAMTS5.* J Biol Chem, 2014. **289**(40): p. 27859-73.
41. Committee on the State of the Science in Ovarian Cancer, R., et al., in *Ovarian Cancers: Evolving Paradigms in Research and Care*. 2016, National Academies Press (US) Copyright 2016 by the National Academy of Sciences. All rights reserved.: Washington (DC).
42. Kim, C.W., et al., *Hypoxia-induced microRNA-590-5p promotes colorectal cancer progression by modulating matrix metalloproteinase activity.* Cancer Lett, 2018. **416**: p. 31-41.
43. Yu, D., et al., *Enhanced c-erbB-2/neu expression in human ovarian cancer cells correlates with more severe malignancy that can be suppressed by E1A.* Cancer Res, 1993. **53**(4): p. 891-8.
44. Li, B., et al., *HOXA10 is overexpressed in human ovarian clear cell adenocarcinoma and correlates with poor survival.* International Journal of Gynecological Cancer, 2009. **19**(8): p. 1347-1352.
45. Domcke, S., et al., *Evaluating cell lines as tumor models by comparison of genomic profiles.* Nat Commun, 2013. **4**: p. 2126.
46. Lengyel, E., et al., *Epithelial Ovarian Cancer Experimental Models.* Oncogene, 2014. **33**(28): p. 3619-3633.

CHAPTER 3 REFERENCES

1. Coleman, R.L., et al., *Latest research and treatment of advanced-stage epithelial ovarian cancer.* Nature reviews Clinical oncology, 2013. **10**(4): p. 211-224.
2. Ozols, R.F., *Systemic therapy for ovarian cancer: current status and new treatments.* Semin Oncol, 2006. **33**(2 Suppl 6): p. S3-11.
3. Mesiano, S., N. Ferrara, and R.B. Jaffe, *Role of Vascular Endothelial Growth Factor in Ovarian Cancer: Inhibition of Ascites Formation by Immunoneutralization.* The American Journal of Pathology, 1998. **153**(4): p. 1249-1256.
4. Goff, B.A., et al., *Ovarian carcinoma diagnosis.* Cancer, 2000. **89**(10): p. 2068-2075.
5. Smith, L.H., et al., *Ovarian cancer: can we make the clinical diagnosis earlier?* Cancer, 2005. **104**(7): p. 1398-1407.
6. Gotlieb, W.H., et al., *Intravenous aflibercept for treatment of recurrent symptomatic malignant ascites in patients with advanced ovarian cancer: a phase 2, randomised, double-blind, placebo-controlled study.* The Lancet Oncology, 2012. **13**(2): p. 154-162.
7. Desoize, B. and J. Jardillier, *Multicellular resistance: a paradigm for clinical resistance?* Crit Rev Oncol Hematol, 2000. **36**(2-3): p. 193-207.
8. Verheul, H.M., et al., *Targeting vascular endothelial growth factor blockade: ascites and pleural effusion formation.* Oncologist, 2000. **5 Suppl 1**: p. 45-50.
9. Kuk, C., et al., *Mining the ovarian cancer ascites proteome for potential ovarian cancer biomarkers.* Mol Cell Proteomics, 2009. **8**(4): p. 661-9.
10. Berchuck, A. and M. Carney, *Human ovarian cancer of the surface epithelium.* Biochem Pharmacol, 1997. **54**(5): p. 541-4.
11. Casey, R.C., et al., *β1-Integrins Regulate the Formation and Adhesion of Ovarian Carcinoma Multicellular Spheroids.* The American Journal of Pathology, 2001. **159**(6): p. 2071-2080.
12. Kelm, J.M., et al., *Method for generation of homogeneous multicellular tumor spheroids applicable to a wide variety of cell types.* Biotechnology and Bioengineering, 2003. **83**(2): p. 173-180.
13. Sodek, K.L., M.J. Ringuette, and T.J. Brown, *Compact spheroid formation by ovarian cancer cells is associated with contractile behavior and an invasive phenotype.* International Journal of Cancer, 2009. **124**(9): p. 2060-2070.
14. Jo, M.H., et al., *Human Argonaute 2 Has Diverse Reaction Pathways on Target RNAs.* Mol Cell, 2015. **59**(1): p. 117-24.
15. Cheng, A.M., et al., *Antisense inhibition of human miRNAs and indications for an involvement of miRNA in cell growth and apoptosis.* Nucleic Acids Research, 2005. **33**(4): p. 1290-1297.
16. Chen, J., et al., *Overexpression of miR-429 induces mesenchymal-to-epithelial transition (MET) in metastatic ovarian cancer cells.* Gynecologic Oncology, 2011. **121**(1): p. 200-205.
17. Miska, E.A., *How microRNAs control cell division, differentiation and death.* Curr Opin Genet Dev, 2005. **15**(5): p. 563-8.
18. Nakahara, K. and R.W. Carthew, *Expanding roles for miRNAs and siRNAs in cell regulation.* Curr Opin Cell Biol, 2004. **16**(2): p. 127-33.
19. Scaria, V., et al., *microRNA: an emerging therapeutic.* ChemMedChem, 2007. **2**(6): p. 789-92.
20. Scaria, V., et al., *Host-virus genome interactions: macro roles for microRNAs.* Cell Microbiol, 2007. **9**(12): p. 2784-94.
21. Salem, M., et al., *miR-590-3p Promotes Ovarian Cancer Growth and Metastasis via a Novel FOXA2-Versican Pathway.* Cancer Res, 2018. **78**(15): p. 4175-4190.
22. Bernaudo, S., et al., *Cyclin G2 inhibits epithelial-to-mesenchymal transition by disrupting Wnt/β-catenin signaling.* Oncogene, 2016. **35**(36): p. 4816.
23. Adorno, M., et al., *A Mutant-p53/Smad complex opposes p63 to empower TGFbeta-induced metastasis.* Cell, 2009. **137**(1): p. 87-98.
24. Ito, Y., et al., *Decreased expression of cyclin G2 is significantly linked to the malignant transformation of papillary carcinoma of the thyroid.* Anticancer Res, 2003. **23**(3b): p. 2335-8.
25. Kim, Y., et al., *Cyclin G2 dysregulation in human oral cancer.* Cancer Res, 2004. **64**(24): p. 8980-6.
26. Choi, M.G., et al., *Expression levels of cyclin G2, but not cyclin E, correlate with gastric cancer progression.* J Surg Res, 2009. **157**(2): p. 168-74.
27. Jia, J.S., et al., *[Expression of cyclin g2 mRNA in patients with acute leukemia and its clinical significance].*

Zhongguo Shi Yan Xue Ye Xue Za Zhi, 2005. **13**(2): p. 254-9.
28. Horne, M.C., et al., *Cyclin G2 is up-regulated during growth inhibition and B cell antigen receptor-mediated cell cycle arrest.* J Biol Chem, 1997. **272**(19): p. 12650-61.
29. Aguilar, V., et al., *Cyclin G2 regulates adipogenesis through PPAR gamma coactivation.* Endocrinology, 2010. **151**(11): p. 5247-54.
30. Fu, G. and C. Peng, *Nodal enhances the activity of FoxO3a and its synergistic interaction with Smads to regulate cyclin G2 transcription in ovarian cancer cells.* Oncogene, 2011. **30**: p. 3953.
31. Logan, C.Y. and R. Nusse, *The Wnt signaling pathway in development and disease.* Annu Rev Cell Dev Biol, 2004. **20**: p. 781-810.
32. Palacios, J. and C. Gamallo, *Mutations in the beta-catenin gene (CTNNB1) in endometrioid ovarian carcinomas.* Cancer Res, 1998. **58**(7): p. 1344-7.
33. Li, Vivian S.W., et al., *Wnt Signaling through Inhibition of β-Catenin Degradation in an Intact Axin1 Complex.* Cell, 2012. **149**(6): p. 1245-1256.
34. Mohammed, M.K., et al., *Wnt/β-catenin signaling plays an ever-expanding role in stem cell self-renewal, tumorigenesis and cancer chemoresistance.* Genes & Diseases, 2016. **3**(1): p. 11-40.
35. Schindler, A.J., A. Watanabe, and S.B. Howell, *LGR5 and LGR6 in stem cell biology and ovarian cancer.* Oncotarget, 2018. **9**(1): p. 1346-1355.
36. Nagaraj, A.B., et al., *Critical role of Wnt/β-catenin signaling in driving epithelial ovarian cancer platinum resistance.* Oncotarget, 2015. **6**(27): p. 23720-23734.
37. Gatcliffe, T.A., et al., *Wnt signaling in ovarian tumorigenesis.* International journal of gynecological cancer : official journal of the International Gynecological Cancer Society, 2008. **18**(5): p. 954-962.
38. Morgenstern, J.P. and H. Land, *Advanced mammalian gene transfer: high titre retroviral vectors with multiple drug selection markers and a complementary helper-free packaging cell line.* Nucleic acids research, 1990. **18**(12): p. 3587-3596.
39. Stewart, S.A., et al., *Lentivirus-delivered stable gene silencing by RNAi in primary cells.* Rna, 2003. **9**(4): p. 493-501.
40. Kolligs, F.T., et al., *Neoplastic transformation of RK3E by mutant beta-catenin requires deregulation of Tcf/Lef transcription but not activation of c-myc expression.* Mol Cell Biol, 1999. **19**(8): p. 5696-706.
41. Ye, G., et al., *MicroRNA 376c enhances ovarian cancer cell survival by targeting activin receptor-like kinase 7: implications for chemoresistance.* J Cell Sci, 2011. **124**(Pt 3): p. 359-68.
42. Fu, G., et al., *MicroRNA-376c impairs transforming growth factor-beta and nodal signaling to promote trophoblast cell proliferation and invasion.* Hypertension, 2013. **61**(4): p. 864-72.
43. O'Brien, J., H. Hayder, and C. Peng, *Automated Quantification and Analysis of Cell Counting Procedures Using ImageJ Plugins.* JoVE (Journal of Visualized Experiments), 2016(117): p. e54719-e54719.
44. van Rooij, E., *The art of microRNA research.* Circ Res, 2011. **108**(2): p. 219-34.
45. Baek, D., et al., *The impact of microRNAs on protein output.* Nature, 2008. **455**: p. 64.
46. Li, X.J., et al., *Exosomal MicroRNA MiR-1246 Promotes Cell Proliferation, Invasion and Drug Resistance by Targeting CCNG2 in Breast Cancer.* Cell Physiol Biochem, 2017. **44**(5): p. 1741-1748.
47. Hasegawa, S., et al., *MicroRNA-1246 expression associated with CCNG2-mediated chemoresistance and stemness in pancreatic cancer.* Br J Cancer, 2014. **111**(8): p. 1572-80.
48. Yao, D., et al., *Morin inhibited lung cancer cells viability, growth, and migration by suppressing miR-135b and inducing its target CCNG2.* Tumour Biol, 2017. **39**(10): p. 1010428317712443.
49. Yin, G., et al., *MicroRNA-340 promotes the tumor growth of human gastric cancer by inhibiting cyclin G2.* Oncol Rep, 2016. **36**(2): p. 1111-8.
50. Xiao, X., et al., *MicroRNA-93 regulates cyclin G2 expression and plays an oncogenic role in laryngeal squamous cell carcinoma.* Int J Oncol, 2015. **46**(1): p. 161-74.
51. YOSHIDA, N., et al., *Analysis of Wnt and β-catenin Expression in Advanced Colorectal Cancer.* Anticancer Research, 2015. **35**(8): p. 4403-4410.
52. Takigawa, Y. and A.M. Brown, *Wnt signaling in liver cancer.* Curr Drug Targets, 2008. **9**(11): p. 1013-24.
53. Ashihara, E., T. Takada, and T. Maekawa, *Targeting the canonical Wnt/β-catenin pathway in hematological malignancies.* Cancer Science, 2015. **106**(6): p. 665-671.
54. Kovacs, D., et al., *The role of WNT/β-catenin signaling pathway in melanoma epithelial-to-mesenchymal-like switching: evidences from patients-derived cell lines.* Oncotarget, 2016. **7**(28): p. 43295-43314.
55. Pohl, S.-G., et al., *Wnt signaling in triple-negative breast cancer.* Oncogenesis, 2017. **6**: p. e310.
56. Boone, J.D., et al., *Targeting the Wnt/beta-catenin pathway in primary ovarian cancer with the porcupine inhibitor WNT974.* Lab Invest, 2016. **96**(2): p. 249-59.
57. Wu, R., et al., *Diverse mechanisms of beta-catenin deregulation in ovarian endometrioid*

adenocarcinomas. Cancer Res, 2001. **61**(22): p. 8247-55.
58. Wright, K., et al., *beta-catenin mutation and expression analysis in ovarian cancer: exon 3 mutations and nuclear translocation in 16% of endometrioid tumours.* Int J Cancer, 1999. **82**(5): p. 625-9.
59. Saegusa, M. and I. Okayasu, *Frequent nuclear beta-catenin accumulation and associated mutations in endometrioid-type endometrial and ovarian carcinomas with squamous differentiation.* J Pathol, 2001. **194**(1): p. 59-67.
60. Feng, Z.Y., et al., *miR-590-3p promotes colon cancer cell proliferation via Wnt/beta-catenin signaling pathway by inhibiting WIF1 and DKK1.* Eur Rev Med Pharmacol Sci, 2017. **21**(21): p. 4844-4852.

CHAPTER 4 REFERENCES

1. Sodek, K.L., M.J. Ringuette, and T.J. Brown, *Compact spheroid formation by ovarian cancer cells is associated with contractile behavior and an invasive phenotype.* Int J Cancer, 2009. **124**(9): p. 2060-70.
2. Bernaudo, S., et al., *Cyclin G2 inhibits epithelial-to-mesenchymal transition by disrupting Wnt/β-catenin signaling.* Oncogene, 2016. **35**(36): p. 4816-4827.
3. Mohammed, M.K., et al., *Wnt/β-catenin signaling plays an ever-expanding role in stem cell self-renewal, tumorigenesis and cancer chemoresistance.* Genes & Diseases, 2016. **3**(1): p. 11-40.
4. Schindler, A.J., A. Watanabe, and S.B. Howell, *LGR5 and LGR6 in stem cell biology and ovarian cancer.* Oncotarget, 2018. **9**(1): p. 1346-1355.
5. Frank, N.Y., T. Schatton, and M.H. Frank, *The therapeutic promise of the cancer stem cell concept.* The Journal of Clinical Investigation, 2010. **120**(1): p. 41-50.
6. Valent, P., et al., *Cancer stem cell definitions and terminology: the devil is in the details.* Nat Rev Cancer, 2012. **12**(11): p. 767-775.
7. Pastrana, E., V. Silva-Vargas, and F. Doetsch, *Eyes Wide Open: A Critical Review of Sphere-Formation as an Assay for Stem Cells.* Cell Stem Cell, 2011. **8**(5): p. 486-498.
8. Bapat, S.A., et al., *Stem and Progenitor-Like Cells Contribute to the Aggressive Behavior of Human Epithelial Ovarian Cancer.* Cancer Research, 2005. **65**(8): p. 3025-3029.
9. Feng, Z., et al., *miR-590-3p promotes colon cancer cell proliferation via Wnt/β-catenin signaling pathway by inhibiting WIF1 and DKK1.* European review for medical and pharmacological sciences, 2017. **21**(21): p. 4844-4852.

APPENDIX

ADDITIONAL PUBLICATIONS

I. mir-590-3p Promotes Ovarian Cancer Growth and Metastasis via Novel FOXA2 Versican Pathway

Salem M[1], O'Brien JA[1], Peng C[1, 2].

[1]Department of Biology, York University, Toronto, Canada
[2]Centre for Research on Molecular Interactions, York University, Toronto, Canada

The article was selected for a highlight

Matrix Biology Highlights, 2018. (In Press)

I contributed to this paper by Designing the figure and writing the summary and captions. JO assisted in designing the figure.

II. Cyclin G2 Inhibits Epithelial-To-Mesenchymal Transition by Disrupting Wnt/β-Catenin Signaling

Bernaudo S [1], **Salem M [1]**, Qi X [1], Zhou W [1], Zhang C [1], Yang W [1], Rosman D [1], Deng Z [2,5], Ye G [1], Yang B [2], Vanderhyden B [3], Wu Z [1,4] and Peng C [1.]

[1]Department of Biology, York University, 4700 Keel Street, Toronto, ON M3J 1P3, Canada
[2]Sunnybrook Research Institute, Sunnybrook Health Sciences Centre, Toronto, Ontario, Canada
[3]Department of Cellular and Molecular Medicine, University of Ottawa, Ottawa, Ontario, Canada
[4]Division of Life Science, Hong Kong University of Science and Technology, Hong Kong, China
[5]Current address: People's Hospital of Jiangsu University, Zhenjiang, Jiangsu, China.

Oncogene, 2016. 35(36): 4816-4827

I contributed to this paper by processing clinical tumor samples, preforming and optimizing several RT-qPCR assays. I also, helped in the *in vivo* studies that was performed in the York University animal facility, and processed tumors extracted from mice. In addition, I also provided editing for the final draft of the paper.

III. Neurokinin B Exerts Direct Effects on the Ovary to Stimulate Estradiol Production

Qi X [1], **Salem M [1]**, Zhou W [1], Sato-Shimizu M [2], Ye G [1], Smitz J [2] and Peng C [1]

[1]Department of Biology, York University, 4700 Keel Street, Toronto, ON M3J 1P3, Canada [2]Free University of Brussels Vrije Universiteit Brussel, 1090 Brussel, Belgium

Endocrinology, 2016. 157(9): 3355-3365.

I contributed to this paper by processing ovarian follicles of PCOS patients and isolating RNA from these samples. In addition, I performed the corresponding RT-qPCR and run agarose gels. I was also involved in the final revision of the manuscript.

IV. microRNA-378a-5p Targets Cyclin G2 to Inhibit Fusion and Differentiation in BeWo Cells

Nadeem U, Ye G, **Salem M**, Peng C

Department of Biology, York University, 4700 Keel Street, Toronto, ON M3J 1P3, Canada

Biology of Reproduction, 2014. 91(3): 76, 1-10-76, 1-10

I contributed to this paper by performing the cloning of the 3'UTR of CCNG2, which was used for luciferase assays in figure 4. Also, I helped in the final revision of the manuscript.

V. MicroRNA-218-5p Promotes Endovascular Trophoblast Differentiation and Spiral Artery Remodeling

Brkić J[1], Dunk C[2], O'Brien J[1], Fu G[3], Nadeem L[3], Wang YL[4], Rosman D[5], **Salem M[1]**, Shynlova O[6], Yougbaré I[7], Ni H[8], Lye SJ[6], Peng C[9].

[1]Department of Biology, York University, Toronto, ON M3J 1P3, Canada.
[2]Lunenfeld-Tanenbaum Research Institute, Mount Sinai Hospital, Toronto, ON M5T 3H7, Canada.
[3]Department of Biology, York University, Toronto, ON M3J 1P3, Canada; Lunenfeld-Tanenbaum Research Institute, Mount Sinai Hospital, Toronto, ON M5T 3H7, Canada.
[4]State Key Laboratory of Stem Cell and Reproductive Biology, Institute of Zoology, Chinese Academy of Sciences, Beijing 100101, China.
[5]Obstetrics and Gynaecology, Mackenzie Richmond Hill Hospital, Richmond Hill, ON L4C 4Z3, Canada.
[6]Lunenfeld-Tanenbaum Research Institute, Mount Sinai Hospital, Toronto, ON M5T 3H7, Canada; Department of Obstetrics and Gynecology, University of Toronto, Toronto, ON M5G 1E2, Canada; Department of Physiology, University of Toronto, Toronto, ON M5S 1A8, Canada.
[7]Toronto Platelet Immunobiology Group and Department of Laboratory Medicine, Keenan Research Centre for Biomedical Science, St. Michael's Hospital, Toronto, ON, Canada, M5B 1W8; Canadian Blood Services, Toronto, ON K1G 4J5, Canada.
[8]Toronto Platelet Immunobiology Group and Department of Laboratory Medicine, Keenan Research Centre for Biomedical Science, St. Michael's Hospital, Toronto, ON, Canada, M5B 1W8; Canadian Blood Services, Toronto, ON K1G 4J5, Canada; Department of Physiology, University of Toronto, Toronto, ON M5S 1A8, Canada; Department of Laboratory Medicine and Pathobiology, University of Toronto, Toronto, ON M5S 1A8, Canada; Department of Medicine, University of Toronto, Toronto, ON M5S 1A8, Canada.
[9]Department of Biology, York University, Toronto, ON M3J 1P3, Canada; Centre for Research in Biomolecular Interactions, York University, Toronto, ON M3J 1P3, Canada. Electronic address: cpeng@yorku.ca.

Molecular Therapy, 2018. 26(9): 2189-2205.

I contributed to this paper by preparing and depositing the microarray raw data to the GEO repository.